เอทิลีนพอลิเมอร์ไรเซชันบนตัวเร่งปฏิกิริยาเซอร์โคโนซีนกับเมทิลอะลูมินอกเซนซึ่งปรับปรุงที่ถูกยึดเกาะบนเซลลูโลส

นางสาวนัฐฎาพร ธนรัตนทรัพย์

วิทยานิพนธ์นี้เป็นส่วนหนึ่งของการศึกษาตามหลักสูตรปริญญาวิศวกรรมศาสตรมหาบัณฑิต
สาขาวิชาวิศวกรรมเคมี ภาควิชาวิศวกรรมเคมี
คณะวิศวกรรมศาสตร์ จุฬาลงกรณ์มหาวิทยาลัย
ปีการศึกษา 2560

ETHYLENE POLYMERIZATION OVER CELLULOSE-SUPPORTED MODIFIED METHYLALUMINOXANE/ZIRCONOCENE CATALYST

Miss Natthadabhorn Thanarattanasap

A Thesis Submitted in Partial Fulfillment of the Requirements
for the Degree of Master of Engineering Program in Chemical Engineering
Department of Chemical Engineering
Faculty of Engineering
Chulalongkorn University
Academic Year 2017

Thesis Title	ETHYLENE POLYMERIZATION OVER CELLULOSE-SUPPORTED MODIFIED METHYLALUMINOXANE/ZIRCONOCENE CATALYST
By	Miss Natthadabhorn Thanarattanasap
Field of Study	Chemical Engineering
Thesis Advisor	Professor Bunjerd Jongsomjit, Ph.D.

Accepted by the Faculty of Engineering, Chulalongkorn University in Partial Fulfillment of the Requirements for the Master's Degree

.....Dean of the Faculty of Engineering

(Associate Professor Supot Teachavorasinskun, D.Eng.)

THESIS COMMITTEE

.....Chairman

(Assistant Professor Suphot Phatanasri, D.Eng.)

.....Thesis Advisor

(Professor Bunjerd Jongsomjit, Ph.D.)

.....Examiner

(Chutimon Satirapipathkul, D.Eng.)

.....External Examiner

(Assistant Professor Ekrachan Chaichana, D.Eng.)

นัฐฎาพร ธนรัตนทรัพย์ : เอทิลีนพอลิเมอร์ไรเซชันบนตัวเร่งปฏิกิริยาเซอร์โคโนซีนกับเมทิลอะลูมินอกเซนซึ่งปรับปรุงที่ถูกยึดเกาะบนเซลลูโลส (ETHYLENE POLYMERIZATION OVER CELLULOSE-SUPPORTED MODIFIED METHYLALUMINOXANE/ZIRCONOCENE CATALYST) อ.ที่ปรึกษาวิทยานิพนธ์หลัก: ศ. ดร.บรรเจิด จงสมจิตร, 111 หน้า.

ปัจจุบันเอทิลีนถูกนำไปใช้ในหลากหลายอุตสาหกรรม เช่น การผลิตท่อน้ำ ฟิล์ม และถุงพลาสติก ซึ่งตัวเร่งปฏิกิริยาที่ใช้ในการผลิตพอลิเอทิลีนมีด้วยกัน 2 ชนิด ได้แก่ ซีเกลอร์-นัตตาและเมทัลโลซีนสำหรับตัวเร่งปฏิกิริยาเมทัลโลซีนนั้นตัวเร่งปฏิกิริยาจะถูกตรึงไว้บนตัวรองรับ และใช้ตัวเร่งปฏิกิริยาร่วมเพื่อกระตุ้นให้ตัวเร่งปฏิกิริยาทำงาน งานวิจัยนี้ศึกษาทั้งตัวรองรับที่เป็นอนินทรีย์ และอินทรีย์ โดยที่ตัวรองรับประเภทอินทรีย์ที่ใช้คือเซลลูโลส เนื่องจากเป็นพอลิเมอร์ชีวภาพที่ใช้อย่างแพร่หลาย และสามารถผลิตได้เป็นจำนวนมาก ทั้งยังเป็นวัสดุธรรมชาติที่นำมาใช้งานทดแทนวัสดุสังเคราะห์เพื่อลดปัญหาสิ่งแวดล้อม แต่ว่าปัจจุบันยังไม่มีการศึกษาเกี่ยวกับการใช้เซลลูโลสเป็นตัวรองรับอย่างแพร่หลายนัก จึงเป็นที่มาในการศึกษาตัวรองรับที่ผลิตจากเซลลูโลสที่ได้จากชีวมวล และแบคทีเรีย โดยแคลไซน์เซลลูโลสทุกชนิดที่อุณหภูมิ 150 องศาเซลเซียสภายใต้ระบบสุญญากาศเป็นเวลา 4 ชั่วโมง จากนั้นจึงตรึงตัวเร่งปฏิกิริยาร่วมเมทิลอะลูมินอกเซน (MMAO) ลงบนตัวรองรับ ก่อนนำไปใช้สังเคราะห์พอลิเอทิลีนผ่านปฏิกิริยาพอลิเมอไรเซชันด้วยตัวเร่งปฏิกิริยาเมทัลโลซีน/เมทิลอะลูมินอกเซน (metallocene/MMAO) ซึ่งผลได้ของผลิตภัณฑ์ และความสามารถในการเร่งปฏิกิริยาจากการทดลองจะถูกนำไปเปรียบเทียบกับผลที่ได้จากการใช้ตัวรองรับเชิงพาณิชย์ที่มีโครงสร้างเป็นผลึกจากผลการทดลองพบว่าการใช้เซลลูโลสเป็นตัวรองรับสำหรับตัวเร่งปฏิกิริยาเมทัลโลซีน/เมทิลอะลูมินอกเซนทำให้ความเป็นผลึกของผลิตภัณฑ์มีแนวโน้มเพิ่มขึ้น เมื่อเปรียบเทียบกับระบบที่เป็นเอกพันธุ์

ภาควิชา วิศวกรรมเคมี ลายมือชื่อนิสิต .....

สาขาวิชา วิศวกรรมเคมี ลายมือชื่อ อ.ที่ปรึกษาหลัก .....

ปีการศึกษา 2560

5970219921 : MAJOR CHEMICAL ENGINEERING

KEYWORDS: POLYMERIZATION, POLYETHYLENE, METALLOCENE CATALYST, CELLULOSE

NATTHADABHORN THANARATTANASAP: ETHYLENE POLYMERIZATION OVER CELLULOSE-SUPPORTED MODIFIED METHYLALUMINOXANE/ZIRCONOCENE CATALYST. ADVISOR: PROF. BUNJERD JONGSOMJIT, Ph.D., 111 pp.

Presently, the polyethylene has been profusely applied in the several industries, for instance manufacturing of pipe, film and plastic bags. In polyethylene production, there are two catalysts which are used in production, including Ziegler-Natta catalyst and metallocene catalyst. The metallocene catalyst is immobilized by support and activated by cocatalyst. For the support of metallocene catalysts, both of inorganic and organic supports are applied and in this research study, cellulose which is organic support for metallocene catalyst, was used. Since, cellulose is extensively used biopolymer representing a great deal of total annual biomass production. Due to environmental issues, natural materials have been widely used instead of synthetic material. However, cellulose, which has played the role as a support for catalytic application is not well explored.

In this present study, several types of cellulose were used as support for metallocene catalyst by varying cellulose from different biomass, including bacteria cellulose. All types of cellulose were calcined under vacuum at 150°C for 4 h, and then the cocatalyst (modified methylaluminoxane, MMAO) was *ex situ* immobilized on these various supports. Polyethylene was synthesized by *in situ* polymerization using zirconocene/MMAO catalytic system. These cellulose-supported catalysts were compared with the commercial microcrystalline cellulose (MCC) supported catalyst in terms of yield and catalytic activity. It was found that the addition of cellulose as a support for metallocene/MMAO catalyst for *in situ* ethylene polymerization tended to increase crystallinity when compared with homogeneous catalytic system.

Department:	Chemical Engineering	Student's Signature	.....
Field of Study:	Chemical Engineering	Advisor's Signature	.....
Academic Year:	2017		

ACKNOWLEDGEMENTS

Firstly, I would like to extend my sincere gratitude and appreciation to my thesis advisor, Professor Dr. Bunjerd Jongsomjit for his generosity in providing continuously encouraging guidance, greatest support, and useful suggestions and discussion throughout this thesis. His advices are always worthwhile and without him this research thesis could not be possible. I sincerely appreciate his essential help.

Furthermore, I would also like to thank Assistance Professor Dr. Suphot Patthanasi as the chairman, Dr. Chutimon Satirapipathkul as the examiner, and Assistance Professor Dr. Ekrachan Chaichana as the external examiner of this thesis for their valuable guidance and revision throughout my thesis.

My most sincere thanks to Department of Chemical Engineering, Chulalongkorn University, Department of Chemistry, Faculty of Science, Kasetsart University, Department of Chemistry, Faculty of Science, Ubon Ratchathani University, and Department of Chemistry, Faculty of Science, Nakhon Pathom Rajabhat University.

I wish to special thanks to whole members in ZM group and students of Center of Excellence on Catalysis and Catalytic Reaction Engineering for the good spirit shared, encouragement, support and wonderful time.

Finally, this thesis would not be complete without my family for their monstrous support, excessive inspiration and encouragement and unconditional love all the times. I would like extremely my highest gratitude to my aunt and my mom for their continuous support throughout my study. This achievement of graduation is dedicated to them.

CONTENTS

Page

Page

Page

Page

Page

Page

LIST OF TABLES

LIST OF FIGURES

CHAPTER 1
INTRODUCTION

1.1 General Introduction

There are several materials produced from polyethylene. Due to the development of plastic industry, polyethylene production is widely expanding in each day around the world. The application of polyethylene is used to produce water pipe, plastic bag, plastic films, packaging of food, toys, foam, geomembranes, bulletproof vests, bottle, and etc. Generally, polyethylene has been classified by its density, for instance, low density polyethylene (LDPE), high density polyethylene (HDPE), and linear low density polyethylene (LLDPE). The use of polyethylene in each types depends on the application for materials [1, 2]. Normally, polyethylene has been produced from ethylene monomer reacted over the catalyst, which is classified by 2 main catalyst types, namely Ziegler-Natta and metallocene catalysts. The polymer, which is produced from Ziegler-Natta catalysts, is broad molecular weight distribution (MWD) and chemical composite distribution (CCD), while the one produced by metallocene catalysts is narrow molecular weight distribution (MWD) and chemical composite distribution (CCD). This is because metallocene catalyst is single-site catalyst, which has only one type of an active site. For homogeneous system, Ziegler-Natta catalysts exhibit lower catalytic activity than metallocene catalysts [3]. So, that is the reason for supporting continuous development of ethylene polymerization by using metallocene catalysts.

Cellulose is extensively used biopolymer representing a great deal of total annual biomass production. Due to environmental issues, natural materials have been widely used instead of synthetic material. There are many interesting features in biopolymers. For instance, they have high sorption capacity, high stability of metal anions, metal binding capacity and physical and chemical versatility, which make them attractive to use as supports for catalyst. Especially, the hydroxyl groups on cellulose is easily enable chemical modifications, such as carboxymethylation, silylationandperiodate oxidation. It can be used to improve the physical and chemical properties of polymer. However, cellulose, which has played the role as a support for catalytic application is not well explored [4, 5].

In this present study, several types of cellulose were used as support for metallocene catalyst by varying cellulose from different sources of biomass, including

celluloses from pineapple leaves, sugarcane, water hyacinth, rice straw, leaf sheaf of banana tree and bacteria cellulose. All types of cellulose were calcined under vacuum at 150°C for 4 h, and then the cocatalyst (Modified Methylaluminoxane, MMAO) was *ex situ* immobilized on these various supports. Then, all cellulosed-supported MMAO obtained from different celluloses, were characterized by various techniques including, scanning energy dispersive X-ray spectroscopy (SEM-EDX) in order to determine the morphology and the quantity of elements, which were distributed on these modified support. Inductively coupled plasma (ICP) was used to determine the amount of aluminium (Al) from MMAO, which was distributed on the cellulose supports. The bulk crystalline phases were investigated by X-ray diffraction (XRD) and differential scanning calorimetry (DSC). Fourier transform infrared spectroscopy (FT-IR) was used to determine the functional group of cellulose and X-ray photoelectron spectroscopy (XPS) was used to measure the interaction between MMAO and cellulose. Polyethylene was synthesized by *in situ* polymerization using zirconocene/MMAO catalytic system. These supports were compared to the commercial microcrystalline cellulose (MCC) one in terms of yield and catalytic activity. The obtained polymers were further investigated by several techniques, including scanning electron microscope (SEM) for their size and morphology, X-ray diffraction (XRD) for their order and crystallinity, and differential scanning calorimetry (DSC) for their crystallinity and thermal properties. The catalytic activity of polymerization reaction was also determined at different cellulose supports.

1.2 Research Objective

1.2.1) To synthesize polyethylene by in situ polymerization with different cellulose-supported MMAO with a zirconocene catalyst

1.2.2) To investigate cellulose material from biomass which plays the role as a support for metallocene catalyst in in situ polymerization

1.2.3) To compare different cellulose materials obtained from different sources, including commercial cellulose, bacteria cellulose, and cellulose from biomass

1.3 Research Scopes

1.3.1) Cellulose from different sources, including commercial cellulose, bacteria cellulose, and cellulose from biomass (sugarcane, rice straw, water hyacinth, leaf sheaf of banana tree, and pineapple leaf) are used as support for MMAO in *in situ* ethylene polymerization reaction.

1.3.2) Cellulose-supported MMAO was prepared by *ex situ* immobilization compared with homogeneous system.

1.3.3) Cellulose and Cellulose-supported MMAO are characterized by SEM, EDX, XRD, TGA, DSC, ICP, and FT-IR method.

1.3.4) Ethylene polymerization was carried out to measure the catalytic activity and it was performed in a 100 mL of stainless steels reactor equipped with a mechanical stirrer.

1.3.5) Polymerization temperature is 70 ^{o}C, while stirring at 600 rpm under 3.5 bar of ethylene pressure in slurry process.

1.3.6) Polyethylene obtained is characterized by XRD, SEM, TGA, and DSC.

1.4 Research Benefits

1.4.1) To understand the effects of the different cellulose-supported MMAO on the catalytic activity of metallocene catalyst for *in situ* ethylene polymerization and polyethylene properties.

1.4.2) To obtain cellulose from biomass in each type and find suitable cellulose from biomass as a support for metallocene catalyst in *in situ* ethylene polymerization reaction.

1.5 Research Methodology

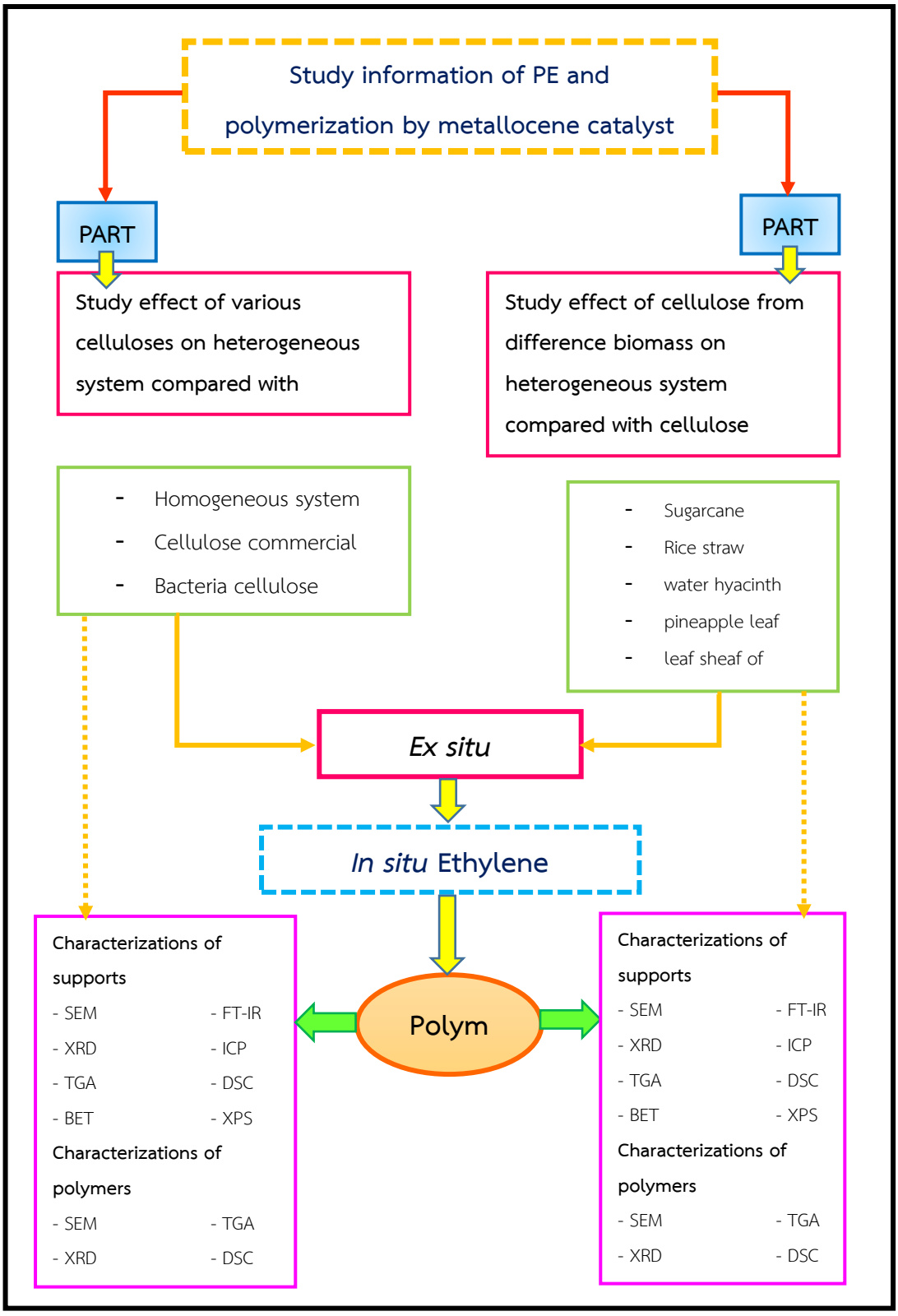

CHAPTER 2
THEORY AND LITERATURE REVIEWS

This chapter is described about the theoretical background and literature reviews relevant to this research. The metallocene catalyst, cocatalyst for metallocene catalyst namely modified methylaluminoxanes (MMAO), heterogeneous system, polyethylene, polymerization reaction, and mechanism of polymerization with single site, are provided in this chapter 2.

2.1 Metallocene Catalyst

Metallocene catalysts are organometallic compound which were discovered from ferrocene. Ferrocene could be considered as the positive charge of metal ion, that was having sandwiched structure between two cyclopentadienyl anions through pi-bonding.

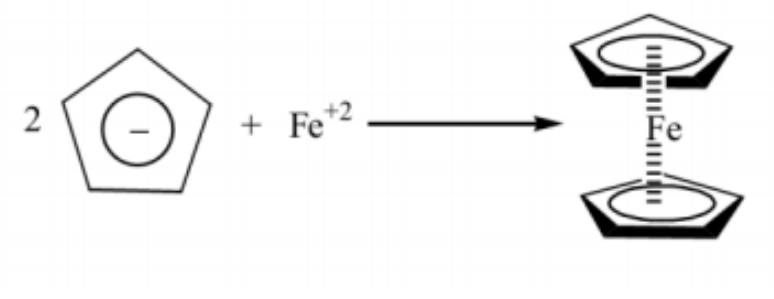

Figure 2.1 The first metallocene to be synthesized, namely ferrocene

Generally, metallocene is having one or two cyclopentadienyl rings or substituted cyclopentadienyl rings, those are bonded to the central transition metal atom (**Figure 2.2**). The cyclopentadienyl ring of a metallocene, is singly bonded to the central metal atom by n-bond. Accordingly, the formation of valence, which is the ring metal bond, is not centered on any five carbon atoms in the ring. It is still equally on all of them. The nature and number of the rings and substituents (S); the type of transition metal (M) and its substituents (R); the type of the bridge determine the catalytic behavior of these organometallic compounds towards the polymerization [6].

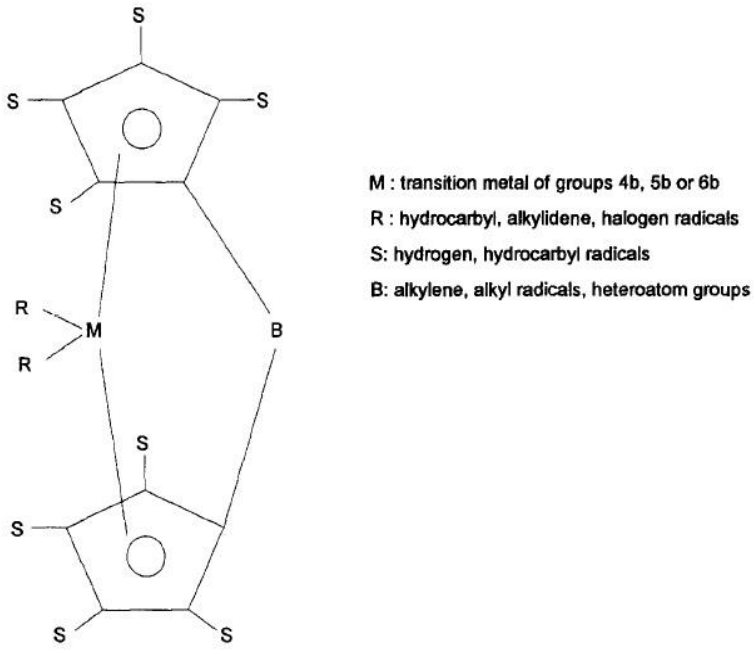

Figure 2.2 Generic structure of a metallocene catalyst [6]

Seeing that, metallocene catalysts have metal transition atom, including zirconocene (Zr), titanium (Ti), and hafnium (Hf) which especially are in group IV-B, following periodic table of elements. Metal atom and cyclopentadienyl rings, which are in coordinated form, can be in a bent form or parallel form (**Figure 2.3**). There are substituting hydrogen atom, such as methyl-, phenyl-, and pentamethyl group on the modified cyclopentadienyl ring. Moreover, there are hydrogen substitution through anellated rings, including indenyl ring (Ind) and fluorenyl ring (Flu) on the modification of cyclopentadienyl ring. Additionally, the C-H group on cyclopentadienyl ring can be also modified by replacing with phosphorus atom or an isoelectric nitrogen like phosphoryl ring and pyrrolyl ring (**Figure 2.4**) [7].

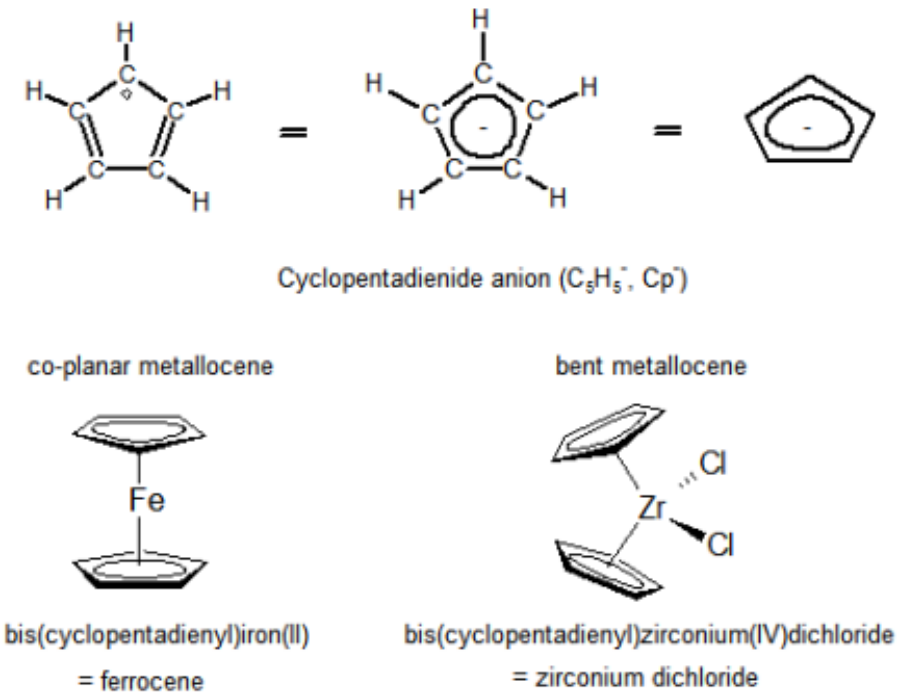

Figure 2.3 Structure of metallocene and nomenclature [7]

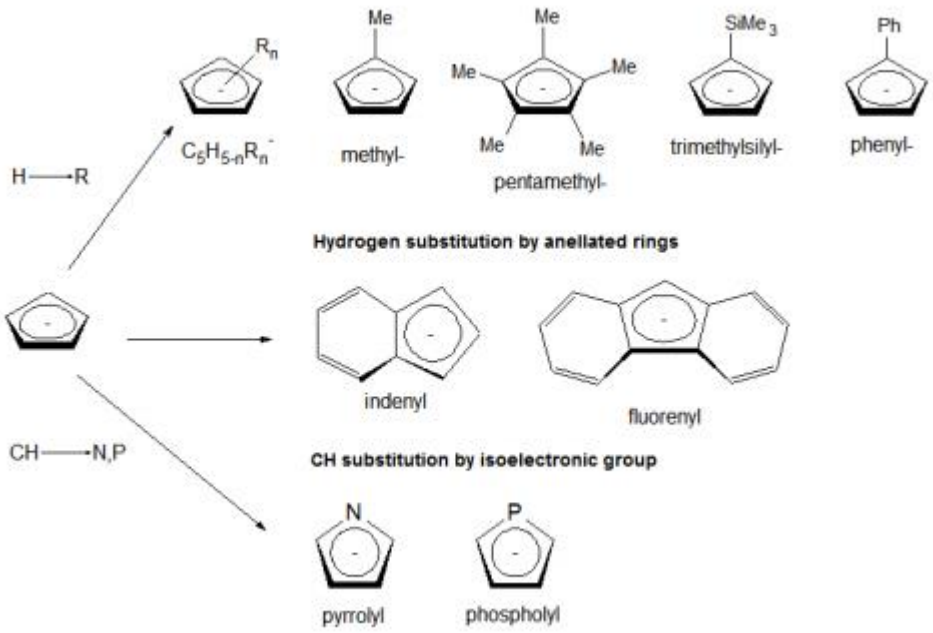

Figure 2.4 Examples of modifications of the cyclopentadienyl ring [7]

Subsequently, metallocene catalysts in that higher charged metal ion for instance zirconium (Zr, oxidation state is +4) would been bonded with two chlorine atoms for observe a stable system (**Figure 2.5**) [8]. The complexes consist of group IV metal which can be encapsulated by two ligands. Active center of these catalysts, is having largely shielded. It can be influence of immediate surroundings of the catalysts complex. The bridged ligand can give forward control over the characteristic of the result of polymer in polymerization control with the presence of suitable cocatalyst.

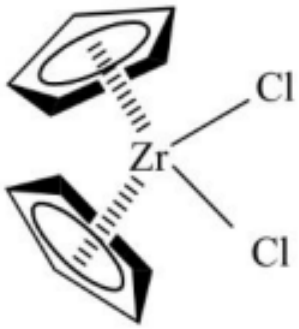

Figure 2.5 Zirconocene dichloride (inactive metallocene catalyst form) [9]

2.2 Cocatalyst for metallocene

Since, metallocene catalyst was discovered, there had been several ways to enhance the catalytic activity by converting the catalyst structure and polymerization condition. To activate metallocene catalyst, methylaluminoxane (MAO) cocatalyst is probably the best activator to activate and enhance the catalytic activity of metallocene catalyst for ethylene polymerization.

2.2.1 Modified Methylaluminoxanes (MMAO) cocatalyst

Mostly, cocatalyst is used for support application of catalysts in each reaction. Since, there is discovery of metallocene catalyst, its application have not been applied in polymerization reaction due to low activity. Subsequently, cocatalyst which is named methylaluminoxane (MAO) was found. It had been attempted to improve the catalytic activity by using metallocene catalyst throughout the changing of catalyst structure and condition for polymerization reaction. Thus, the plenty of researchers still have interested in cocatalyst and mentioned it as the one of key in polymerization reaction.

Especially, the discovering and application of methylaluminoxane (MAO) were possible to supply the catalytic activity. MAO is absolutely soluble in aromatic solvents for instance toluene and benzene, but it exactly has constrained solubility in aliphatic hydrocarbon. To improve this limitation, isobutyl group was substituted methyl group in MAO structure, this new cocatalyst is named modified methylaluminoxane (MMAO). MMAO is synthesized by hydrolyzing the mixture of $AlMe_3$ and $Al^{i}\text{-}Bu_3$. The comparison of efficiency between MMAO and MAO, it identified their efficiency was similar, however the solubility of MMAO in aliphatic hydrocarbon was more attractive in polyolefin. The structure of MMAO is shown in (**Figure 2.6**).

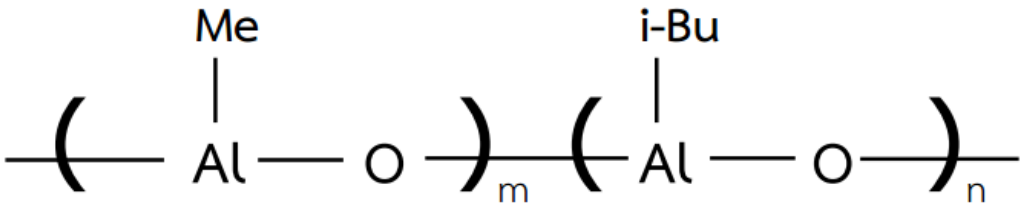

Figure 2.6 Structure of cocatalyst, namely modified methylaluminoxane (MMAO)

Almost MMAO are prepared from reaction with water, which is shown as **equation 2.1**. There are various formulations of MMAO, for instance commercial MMAO is produced by non –hydrolytic. All of MMAO contain ≥ 65% methyl group and remain predominantly MAO. Absolutely, there are 95% of methyl groups contain on MMAO formulation and MMAO presents more improve storage stability, and its solubility are highly in aliphatic hydrocarbon. MMAO has been submitted commercially and the most ordinarily used as modifier are isobutyl and n-octyl groups. MMAO provides higher yield and less cost than MAO. Although MMAO creates another types of alkylaluminoxane in several single site catalyst system and it ought to be also determined as cocatalyst for single site catalysts [7].

$$xR_3Al + xH_2O \rightarrow -(RAlO)_x- + 2xRH \qquad (2.1)$$

As mentioned earlier, MMAO is applied as interesting activator for metallocene catalyst due to highly catalytic activity compared to another types of cocatalyst. Accordingly, MMAO is employed in this present research.

2.3 Heterogeneous system

Generally, the production of polyethylene using metallocene catalyst can be divided into two systems; one is homogeneous system and other is heterogeneous system. For comparison between homogeneous system and heterogeneous system in term of cost, it is found that the homogeneous one is more expensive. This is because the plenty of cocatalyst, including MAO and MMAO cocatalysts is required for the homogeneous system. The ratio between metallocene catalyst and MAO or MMAO cocatalyst is defined as zirconocene/MMAO (Zr/Al). For some heterogeneous system, the ratio of zirconocene/MMAO is as low as 1:40, nevertheless in homogeneous system is estimated as 1:1000 or higher. In addition, the comparison in term of morphology, it is found that in the homogeneous system, it is less controllable of morphology than that of the heterogeneous one, which has support for promoting morphology. Therefore, it shows that the support structure is the key control the morphology of polymer. Finally, for comparison in term of catalytic activity, it reveals that the catalytic activity obtained heterogeneous system is lower than that from the homogeneous one.

As mentioned earlier, there are many researches which aim to improve the activity of heterogeneous system including controlling of morphology and ability to produce polymer. Furthermore, the researchers pay attention in the supported catalysts which are in heterogeneous system for application in slurry polymerization process.

Kaminsky and Renner [10] has explored the high melting polypropenes by silica-supported zirconocene catalysts. There was comparison between homogeneous system and heterogeneous system using metallocene as a catalyst and silica as support for metallocene catalyst in ethylene polymerization under the same condition. Using silica supported zirconocene displayed the higher molecular weight of polyethylene than homogeneous system. It is known that the immobilization of zirconocene catalyst on silica support protects bimolecular processes, which are the cause of deactivation. Thus, the molecular weight of polyethylene apparently increases.

Desharun *et al.* [11] has studied the LLDPE/alumina nanocomposites synthesized by *in situ* polymerization with zirconocene/d-MMAO catalyst. The ratios between zirconocene and MMAO were varied and alumina was used as support for metallocene catalyst. They were 1135, 2270 and 3405 (Al/Zr) and it was found that at ratio $[Al]_{d\text{-}MMAO}/[Zr]_{cat}$ equal to 1135, it presented the highest catalytic activity via *in situ* polymerization of ethylene/1-hexene.

Wannaborworn *et al.* [12] has explored the LLDPE synthesis via SiO_2-Ga-supported zirconocene/MMAO catalyst. The various sizes of silica supported metallocene catalyst using gallium as modifier for silica support in heterogeneous system were compared to homogeneous system. The polymerization under heterogeneous system showed the higher catalytic activity than homogeneous system.

2.3.1 Crystalline cellulose (AVICEL®)

Microcrystalline cellulose (MCC) is generally used as an additive for direct compression due to its good compressibility, compatibility and flow ability. MCC has been commonly manufactured with following process; wood pulp made of needle-leaf trees or return pulp made of cotton-seed fiber is partially hydrolyzed and washed then eliminating the amorphous region and impurity to get purify of the MCC. Thus, it is presented the different properties of MCC in manufacturers because of pulp, which is used as raw material and manufacturing condition. The different properties can be affected in the compressibility and compatibility of MCC [13, 14].However, purified MCC which is partially depolymerized cellulose is prepared by treating alpha cellulose achieved as pulp from fibrous plant material with mineral acid. This cellulose consists of linear chains of β-1,4-D anhydroglucopyranosyl units [15, 16] and its structure is shown in (**Figure 2.7**). For commercial MCC which is name Avicel®, was discovered by Battista and Smith in 1955, and first of commercial MCC was recorded in the supplement to the National Formulary, twelfth edition, in 1966 [17, 18].

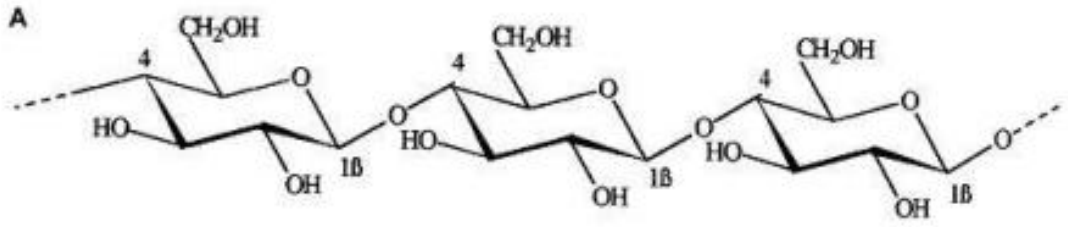

Figure 2.7 Chemical structure of microcrystalline cellulose (MCC) [13]

Microcrystalline cellulose (MCC) in polymer industries is used as composite polymer for instance polyethylene, polypropylene, polybutadiene, etc. due to its special properties including, eco-friendly and it can be decreased waste plastic and renewable nature. For polyethylene-cellulose composite had expanded to enhance tensile properties and compatibility in hydrophilic of cellulose and hydrophobic of thermoplastic material [19, 20].

In this present research, the cellulose was used as support for metallocene catalyst. It focused on organic material as supported metallocene catalyst. Generally, commercial cellulose which is named Avicel PH101, consists of hemicellulose sugar and lignin. Its property is white powder, porous, odorless, tasteless, fine, and insoluble with organic solvent and water.

2.3.2 Bacteria cellulose

Ordinarily, Bacteria Cellulose (BC) is one of cellulose forms synthesized by bacteria. As mentioned in previous part cellulose structure is organic compound which is having formula in this form $(C_6H_{10}O_5)_n$ and the repeating unit of D-glucose joined by β-1,4-glycosidic linkages as polysaccharides (**Figure 2.8**). There are several producing of BC for instance *Rhizobium*, *Sarcina*, *Agrobacterium*, and *Acetobacter*. There is overview of BC production as shown in (**Table 2.1**) [21, 22]. The production of BC which is the most efficient, is *Acetobacter xylinium*. Its property is rod shaped, simple gram-negative, and stickily aerobic bacteria that has potentiality to synthesize a plenty of high quality cellulose established as twisting ribbon of microfiber bundles [22].

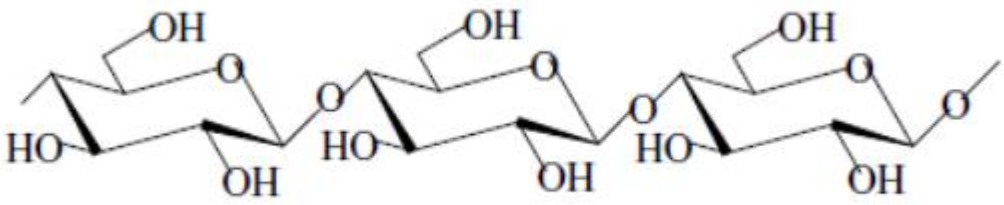

Figure 2.8 Chemical structure of general cellulose [23]

Table 2.1 The microbe producing BC [21]

Genus	Cellulose structure
Acetobacter	Extracellulare pellicle composed of ribbons
Achromobacter	fibrils
Aerobacter	Fibrils
Agrobacterium	Short fibrils
Alcligenes	Fibrils
Pseudomonas	No distinct
Rhizobium	Fibrils
Sarcina	Short fibrils
Zoogloea	Amorphous cellulose
	Not well defined

The synthesis of nanocellulose fiber which is well-known as named bacteria cellulose (BC), is the production of *Acetobacterxylinium* that is the most several applied bacterium. Accordingly, the properties of BC are ultra-fine network structure, high water holding capacity, high crystallinity, high purity, high tensile strength, and hydrophilicity [24]. However BC has been widely in several application for example using BC as fibers in industrial paper and viscosity modifiers in the food industry [21, 25].

2.4 Polyethylene

Nowadays, polyethylene (PE) is commonly used in plastic application for several industries. Due to its various advantage for example, polyethylene which has been used for shopping bags, food wrap, pipe, toys, pipe film, bottles and fuel tank for chemical industry, it has been tended to growing up in each day around the world. Normally, monomer for polyethylene is ethylene which is having chemical formulation as C_2H_4. There are a long backbone of covalently linked carbon atoms with pair atoms of hydrogen attached to each atom of carbon, and methyl group which is its terminated chain ends. Polyethylene structure is shown in (**Figure 2.9**). Polyethylene has been produced from diverse polymerization processes, including cationic addition polymerization or ion coordination polymerization, anionic addition polymerization, and radical polymerization [26, 27].

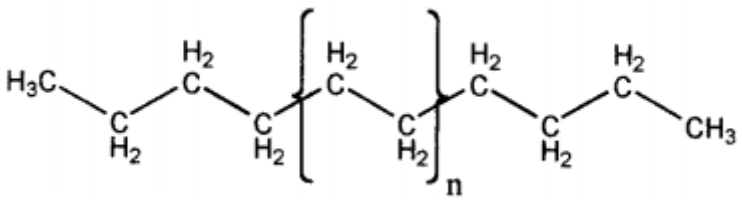

Figure 2.9 Simple polyethylene structure [26]

Accordingly, the classification of polyethylene has been many types. Because of the differences of catalyst, temperature, and pressure in polymerization process, there are harsh effects with molecule of polyethylene branching, which is the simplest side chain off the polymer backbone and when carbon-hydrogen bond was broken between polymerization processes this side chain is form. For significantly branching of polyethylene molecules, its structure has been become to uninformed chain and amorphous [28]. Therefore, polyethylene is classified into various types based on density and its branching which is shown as (**Table 2.2**). For this research, focuses on High-Density Polyethylene (HDPE) and Low-Density Polyethylene (LDPE), respectively. And their structures are shown in (**Figure 2.10**).

Table 2.2 Classification of polyethylene following various density

Types of PE	General named	Density (g/cm^3)
Very Low Density Polyethylene	VLDPE	0.860-0.900
Low Density Polyethylene	LDPE	0.910-0.925
Linear Low Density Polyethylene	LLDPE	0.919-0.925
Medium Density Polyethylene	MDPE	0.926-0.940
Linear Medium Density Polyethylene	LMDPE	0.926-0.940
High Density Polyethylene	HDPE	>0.941

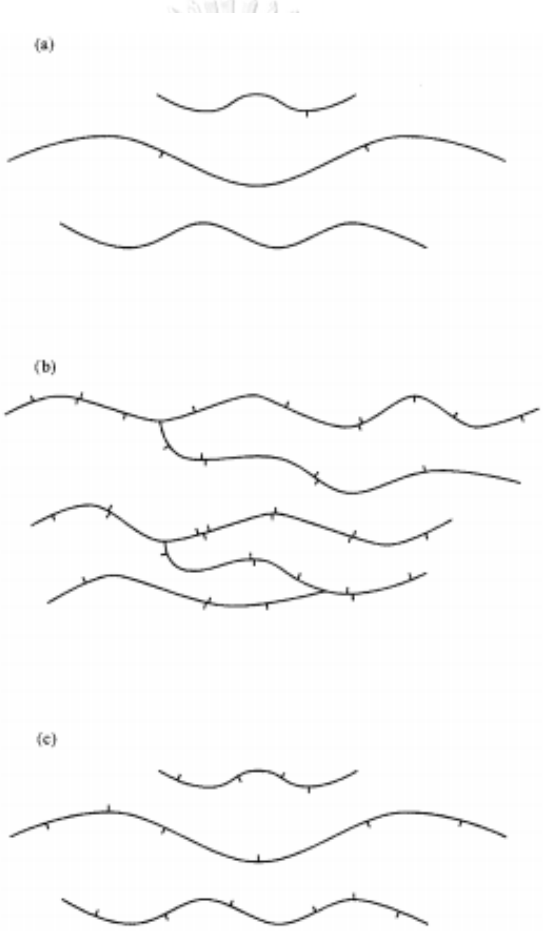

Figure 2.10 Different structure of polyethylene (a) High Density Polyethylene; (b) Low Density Polyethylene; (c) Linear Low Density Polyethylene [26]

2.4.1 High-Density Polyethylene (HDPE)

The one type of polyethylene which is mostly used in widely industries, is High Density Polyethylene (HDPE). It is classified by density and having value of density greater than 0.941 g/cm^3. Its properties include lower degree of polymer branch, strong intermolecular force and high tensile strength. HDPE products are from polymerization of ethylene which has produced at low temperature under low pressure. And free radical polymerization could not been applied to produce HDPE. HDPE can be conducted as several products in daily life for instance bottle caps, food storage containers, electrical and plumbing boxes, plastic bag, plastic bottles, piping for water or sewer and more.

2.4.2 Low-Density Polyethylene (LDPE)

For present industries, High Density Polyethylene (HDPE) is not only extensively used, but Low Density Polyethylene (LDPE) are also used for corrosion-resistant work surfaces, plastic wraps, canned goods, six pack rings, computer hardware package including hard disk drives, screen cards, and optical disc drives. Low Density Polyethylene (LDPE) is having density value range 0.910-0.925 g/cm^3. Its properties is different from High Density Polyethylene (HDPE) including high degree of short and long chain branching, that can determine the chain of LDPE structure could not be packed as well. It means LDPE structure is amorphous. LDPE can be produced under high pressure process via free radical polymerization and get interesting application including good impact resistance, extreme flexibility, no moisture absorption, lightweight, and chemical resistant.

2.5 Polymerization reaction

Polymerization process is the process which chemically related small molecule (it is called monomer) combined to form large network molecule (it is called polymer).Monomer molecules can be produced the product which definitely unique physical properties for example elasticity, and high tensile strength. The stable covalent chemical bond between the plenty of monomers establish polymerization apart from other processes for instance crystallization, in respect of a large number of molecules aggregate under weak intermolecular force influences.

Bergstra [29] identified that in 1935 there is discovering of ethylene which could be used for polymerization process at high pressure into semi crystalline solid by Perrin. Commercial Low Density Polyethylene (LDPE) was discovered by supercritical ethylene

at high temperature under high pressure at ICI laboratories in 1938. In 1950 the researchers which work at the Phillips Petroleum Company, their name are Hogan and Banks discovered highly crystalline polyethylene. And it could be produced at moderate temperature under moderate pressure with using chromium oxide catalyst on silica support. Accordingly, in 1953 there is discovering of highly crystalline polyethylene which had been synthesized at temperature range 50-100 ^{o}C under atmospheric pressure by using Ziegler-Natta catalyst including titanium chloride ($TiCl_4$) and alkylaluminium compound.

Chatuma Suttivutnarubet [30] has explored the synthesized polyethylene/coir dust hybrid filler with zirconocene/MAO catalyst by using *in situ* polymerization. The concentration of zirconocene($Et(Ind)_2ZrCl_2$) was 0.0083 grams in 20 ml of toluene solution ($1.98x10^{-5}$ moles), thus stirred at room temperature under inert atmosphere. The operation of polymerization process was using 100 ml semi-batch stainless steel autoclave reactor with a magnetic stirrer. The ratio of catalyst (zirconocene catalyst) and cocatalyst (methylaluminoxane, MAO) was 1135, then volume of MMAO was equal to 1.1 ml, was mixed and stirred for 30 minutes at room temperature. The condition of polymerization was initiated under pressure 6 psi at 70^{o}C. The reaction was deactivated by acidic methanol (0.1% HCl in methanol) and stirred overnight. Therefore, polymer was filtrated by vacuum filter system, washed by using methanol, and dried at room temperature. The obtained polymer was white powder. The results and discussion identified that the catalytic activity was decreased while the number coir dust was increased, that was due to effect of support.

Sineenart Jamnongphol [31] has studied the preparation of silica coated with polyethylene by using zirconocene/MMAO catalyst in *in situ* polymerization. The concentration of zirconocene ($Et(Ind)_2ZrCl_2$) was 0.0083 grams in 20 ml of toluene solution (1.98x10-5 moles), thus stirred at room temperature under inert atmosphere. The operation of polymerization process was using 100 ml semi-batch stainless steel autoclave reactor with a magnetic stirrer. The ratio of catalyst (zirconocene catalyst) and cocatalyst (modified methylaluminoxane, MMAO) was 1135, then silica (SiO_2) which played the role as support for metallocene catalyst, was immobilized using *ex situ* immobilization. Thus, 10 ml of MMAO was mixed and stirred with 0.3 grams silica for 30 minutes. The silica/MMAO was dried by vacuum system. The condition of polymerization was initiated under pressure 6 psi at 70^{o}C. The reaction was deactivated by acidic methanol (0.1% HCl in methanol) and stirred overnight. Therefore, polymer was filtrated by vacuum filter system, washed by using methanol, and dried at room temperature. The obtained polymer was white powder. The results and discussion

identified that the highly catalytic activity was polymerization process which using temperature equal to 70°C, and its catalytic activity was compared following polymerization temperature, the using temperature was 60°C and 70°C, respectively.

There were many researches, identified that immobilization of catalyst supplied highly catalytic activity but that was not widely used. Consequently, production of polyethylene using *in situ* polymerization has been studied, due to this procedure could be approximate morphology and catalytic activity [32, 33].

2.6 Mechanism of Polymerization

Generally, polymerization mechanism, which is used metallocene catalyst, consists of three steps including initiation, propagation and termination, respectively. To control production of polymer properties, kinetics and mechanism are the important factors. And these factors also depend on properties of catalyst. Mostly, the active centers of catalyst is identified to be cationic. Cocatalyst is the one of polymerization keys which can affect to simple mechanism.

2.6.1 Initiation

At the first step of polymerization mechanism is named initiation. The cation in metallocene catalyst has been produced by cocatalyst which inferences methyl group from metal atom for metallocene catalyst. This mechanism for this step is shown in (**Figure 2.11**).

2.6.2 Propagation

The insertion of monomer in cationic site is defined as propagation step of polymerization mechanism. Polymer chain is connected by free radical as shown in (**Figure 2.11**).

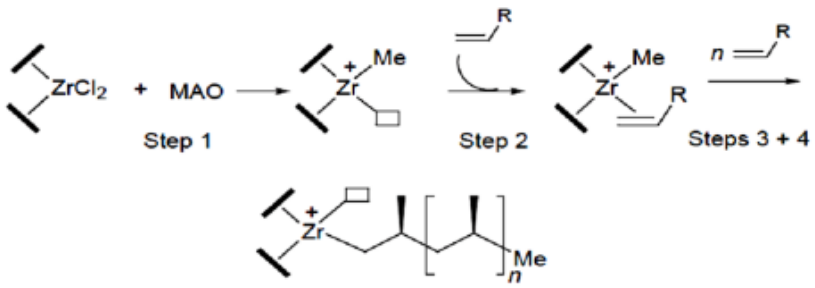

Figure 2.11 Mechanism of initiation and propagation step in polymerization by using zirconocene catalysts [34]

2.6.3 Termination

In the final step of polymerization mechanism, namely termination is having 3 ways of termination polymerization including β-H elimination with hydride transfer to transition metal, chain transfer to the cocatalyst, and hydrogen transfer to monomer, respectively. The mechanism as mention is shown in (**Figure 2.12**).

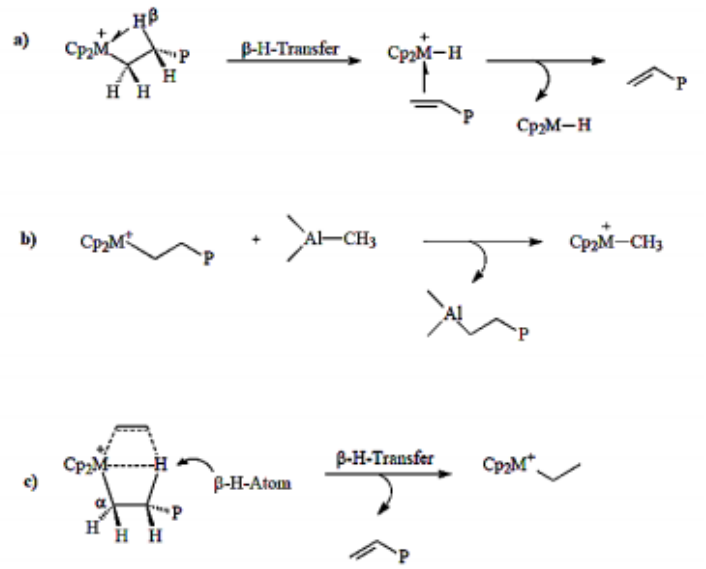

Figure 2.12 Mechanism of termination step in polymerization a) β-H elimination; b) chain transfer to the cocatalyst; c) hydrogen transfer to monomer [35]

CHAPTER 3
EXPERIMENTAL

This present chapter is described about the experiment and method relevant to this research. There are chemicals and equipment, which are used in each method. The experiment includes preparation of all supports, which are used for metallocene catalyst, condition of calcination and immobilization for all supports, and characterization of supports and polymers. All contents as mentioned earlier are explained in this chapter.

3.1 Chemicals

Table 3.1 The chemicals used in the preparation of support for metallocene catalyst and the polymerization reaction

Chemicals	Formulation	Supplier	Purification
rac-ethylenebis(indenyl) zirconiumdichloride	$[Et(Ind)_2ZrCl_2]$	Aldrich Chemical Company, Inc	Used as received
Modified methylaluminoxane (MMAO)	$(Al(CH_3)O)_m(Al(i\text{-}Bu)O)_n$	Tosoh Finechem Co.Ltd.	6.5% in toluene
Microcrystalline cellulose (Avicel PH101)	$(C_6H_{10}O_5)_n$		Used as received
Ethylene gas	C_2H_4	National Petrochemical Co., Ltd.	99.99%
Toluene	$C_6H_5\text{-}CH_3$	Quality Reagent Chemical	99.5% Soaked in molecular sieve
Hydrochloric acid	HCl	Aldrich Chemical Company	Fuming 36.7%
Methanol	CH_3OH	S.R. lab	Used as received
Ultra high purity argon gas	Ar	Thai Industrial Gas Co., Ltd.	99.999%

3.2 Equipment

Generally, the metallocene catalyst has to be used without moisture and oxygen. Thus, there are a lot of equipments, which are used for ethylene polymerization. They are as follows;

3.2.1 Glove box

MRBAUN LABstar Glove box was used to control moisture and oxygen in atmosphere. This provided an inert surrounding for handling high moisture and oxygen sensitive materials. There are 2 parts to produce inert atmosphere; gas purification system, and closed loop gas recirculation to eliminate water (H_2O) and oxygen (O_2). In addition, moisture and oxygen analyzer, including MB-MO-SE1 and MB-OX-SE1, respectively, were also applied for investigating moisture and oxygen concentration in Glove box system.

3.2.2 Schlenk line

To eliminate moisture and oxygen in all operation within this research, Schlenk line was applied. It is composed of vacuum line and nitrogen gas line with several stopcocks. This operation was operated under vacuum. Gas and solvent vapors from evacuation were trapped by liquid nitrogen cold trap for preventing the vacuum pump contamination. The Schlenk line is shown in (**Figure 3.1**).

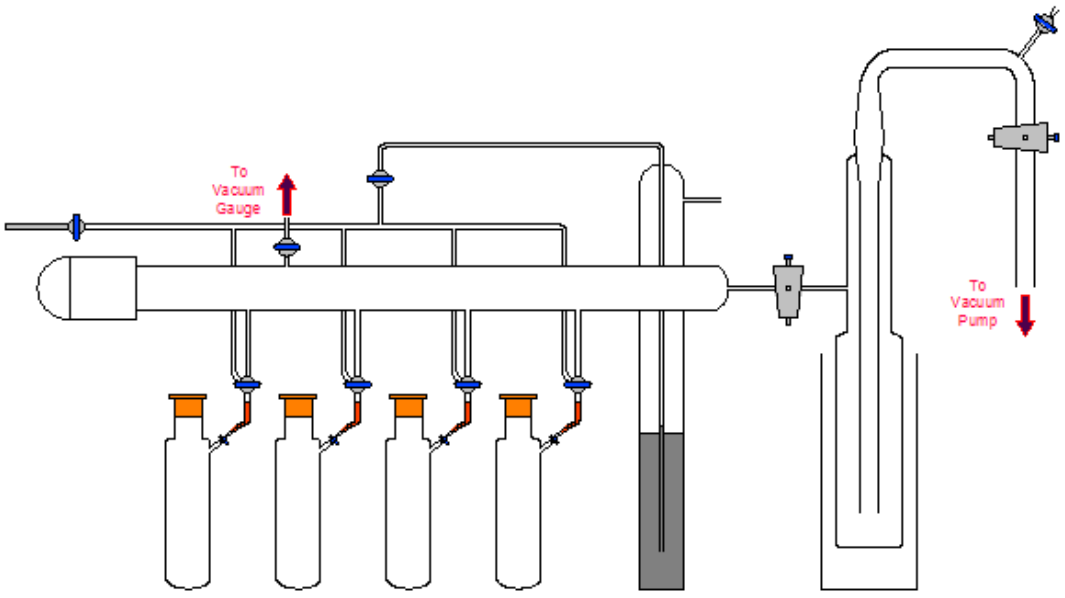

Figure 3.1 Schlenk line

3.2.3 Schlenk tube

The tube with a ground glass joint and side arm having three-way glass valve is shown in (**Figure 3.2**). There are 50, 100 and 200 ml. of Schlenk tubes. These were used to prepare the immobilized cellulose and store cellulose materials, which were sensitive to moisture and oxygen.

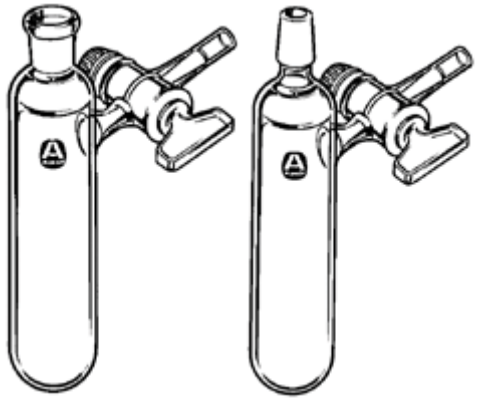

Figure 3.2 Schlenk tubes

3.2.4 Cooling system

Cooling system was in a solvent distillation to condense the newly evaporated solvent.

3.2.5 Vacuum pump

Vacuum pump model 195, supplied from Labconco Corporation was used to eliminate oxygen from the system. The pressure of 10^{-1} to 10^{-3} mmHg was enough for the vacuum supply to the vacuum line in the Schlenk line.

3.2.6 Polymerization reactor

Polymerization reactor was 100 ml of stainless steel autoclave with a magnetic stirrer.

3.2.7 Magnetic stirrer and heater

To control heat of reaction and mix solution during polymerization, the magnetic stirrer and heater model RTC basis from IKA Labortechnik were used.

3.2.8 Polymerization line

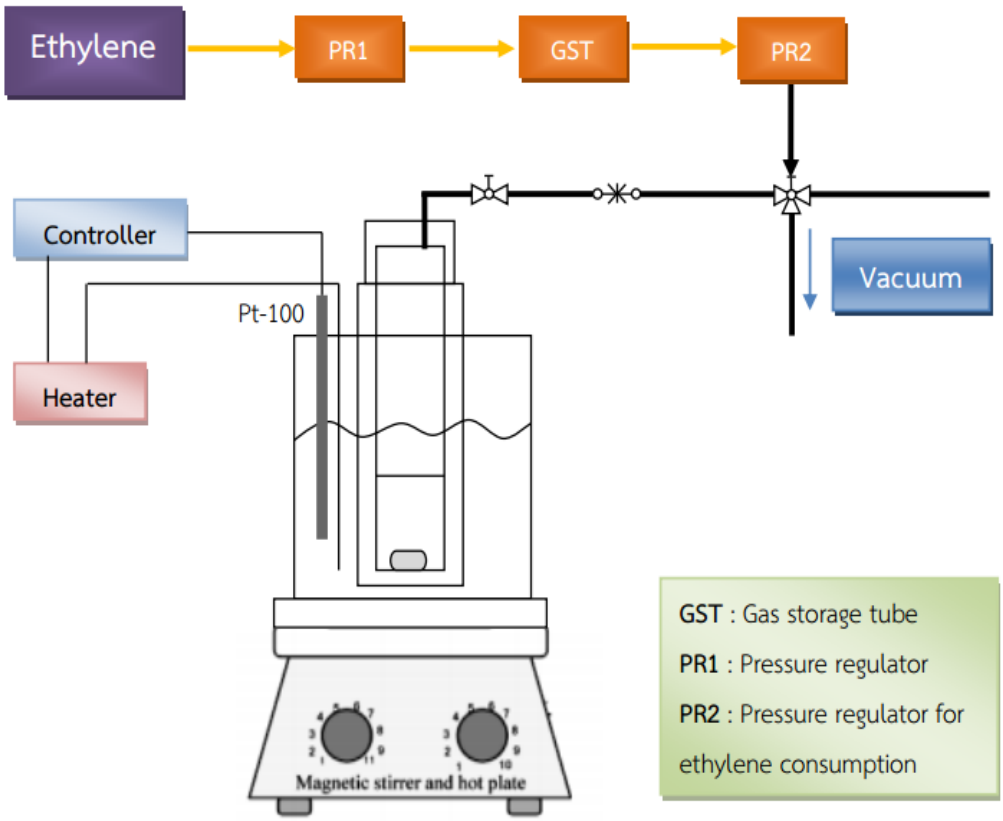

Figure 3.3 Diagram of polymerization system in slurry phase

3.3 Experimental

This content consists of 4 steps before it was used in polymerization reaction. There are preparation of supports, calcination, *ex situ* immobilization and *in situ* ethylene polymerization, as mentioned below;

3.3.1 Preparation of supports

3.3.1.1 Bacteria cellulose (BC)

There are 2 types of bacteria cellulose, which were used in this research. One is bacteria cellulose from natural pineapple juice fed by using *A. xylinium* AGR60. This BC type I used in this study was supplied by Research Center of Agricultural Residue Products and Biomaterials, Nakhon Pathom Rajabhat University, Bangkok, Thailand. The bacteria cellulose material was treated by ammonium sulphate ($(NH_4)_2SO_4$) solution and acetic acid. Then, the incubation for 7 days at room temperature had been applied. After that it was washed with deionized water, dried at room temperature. And the other is bacteria cellulose from coconut fed by using *A. xylinium* AGR60. This

BC type II used in this study was supplied by a local BC processing from Kasetsart University, Bangkok, Thailand. The material was treated with NaOH solution (1% w/v) for 24 hours, and then it was washed with deionized water until pH 7, dried at 110°C for 24 hrs.

3.3.1.2 Cellulose from biomass

Sugarcane, rice straw, water hyacinth, pineapple leaf, and leaf sheaf of banana tree are celluloses obtained from biomass. The first preparation is from drying all materials by using sunlight. Then, drying materials were blended using moulinex machine. The selected size of cellulose powder was collected for further studies.

3.3.2 Calcination

Commercial cellulose, named Avicel PH101, bacteria cellulose and cellulose from biomass, including cellulose from sugarcane, rice straw, water hyacinth, pineapple leaf, and leaf sheaf of banana tree, were calcined under vacuum at 150°C with heating rate 10°C/min for 4 hours. Then, they were cooled down at room temperature and stored in bottle under argon atmosphere.

3.3.3 *Ex situ* immobilization

The modified methylaluminoxane (MMAO) supported on different celluloses were prepared by *ex situ* immobilization. The ratio of cellulose materials and MMAO in toluene was 1:10 with the magnetic stirrer at room temperature. Then, cellulose-supported MMAO was dried followed by vacuum system at room temperature. The solid powder of cellulose-supported MMAO was achieved.

3.3.4 *In situ* ethylene polymerization

Ethylene polymerization reaction was operated in 100 ml semi-batch stainless steel autoclave reactor with magnetic stirrer. Approximately, 0.2 g of cellulose-supported MMAO was added into reactor corresponding to $[Al]_{MMAO}/[Zr]_{cat}$ = 1135. After that, rac-Et$[Ind]_2ZrCl_2$, which was controlled concentration as $5x10^{-5}$M was added. The solvent (toluene) that plays to role as heat releasing, was added into the reactor to fulfill a total volume of reactor as 30 ml at room temperature. Polymerization reaction was started while ethylene gas was fed. It was performed under 3.5 bar under vacuum. Ethylene consumption rate was observed by mass flow meter. After 15 minutes of polymerization time, it was terminated with acidic methanol and stirred around 15 minutes. The polymer obtained was filtrated and dried at room temperature.

3.4 Characterization of supports and polymers

The characterization in this current research consists of 3 parts; for the first, all cellulose supports before immobilization were investigated for fundamental properties. Secondly, all supports after immobilization were investigated for structure and properties. Eventually, polymers were characterized for investigating of polymer properties.

3.4.1 Characterization of supports before immobilization

3.4.1.1 Scanning electron microscopy (SEM)

The morphology of cellulose material was investigated by using JEOL mode JSM-6400 model of SEM at Center of Excellence on Catalysis and Catalytic Reaction Engineering, Chulalongkorn University.

3.4.1.2 X-ray diffraction (XRD)

To investigate bulk crystalline phases of cellulose materials, the SIEMENS D-5000 X-ray diffractometer with CuK_{α} radiation (λ = 1.54439×10^{-10} m) with Ni filter was used in the 2θ range of 10 to 80 degrees. The spectrum rate was scanned at 2.4 degree/min.

3.4.1.3 Thermal gravimetric analysis-differential scanning calorimetry (TGA-DSC)

Thermal stability of cellulose materials were determined using TGA instrument. It was produced using TA Instruments SDT Q600 analyzer. For DSC, it was used to analyze melting temperature (T_m), and crystallinity (X_c), following DSC *204 F1 phoenix*. Approximately, 10-20 mg of sample was used. Carrier gas was nitrogen UHP. The temperature ramp was operated from 25 to 700 °C at 10 °C/min.

3.4.1.4 Fourier transform infrared spectrophotometer (FTIR)

To determine functional group of cellulose materials, FTIR were used. The powder samples of IR were casted as thin film on NaCl plate under argon gas protection from oxygen and moisture. The analyzed samples were investigated by Nicolet 6700 FTIR spectrometer with ATR mode. The collected spectra were in the scanning range from 400-4000 cm^{-1} with 100 numbers of scan at resolution as 4 cm^{-1}. The spectra of FTIR were noted on ATI Mattson Infinity Series spectrometer.

3.4.2 Characterization of supports after immobilization

3.4.2.1 Scanning electron microscopy (SEM) and energy dispersive X-ray spectroscopy (EDX)

The morphology of cellulose material was investigated using JEOL mode JSM-6400 model of SEM. The elemental distribution of Al was observed by EDX using Link Isis series 300 program to confirm the modification of cellulose by MMAO.

3.4.2.2 X-ray diffraction (XRD)

For this session, the cellulose-supported MMAO was operated as identical as cellulose materials before immobilization as mentioned in 3.4.1.2.

3.4.2.3 Fourier transform infrared spectrophotometer (FTIR)

In this session, the cellulose-supported MMAO was operated as identical as cellulose materials before immobilization as mentioned in 3.4.1.4.

3.4.2.4 X-ray photoelectron spectroscopy (XPS)

The interaction force on the cellulose-supported MMAO, was investigated using XPS study. It was evaluated by the AMICUS photoelectron spectrometer and a KRATOS VISION 2 software. The experimental condition was carried out at 0.1 eV/step of resolution, 75 eV pass energy and the operating pressure approximately $1x10^{-6}$ Pa. Analyzed samples were prepared in glove box and transferred to the XPS under argon atmosphere.

3.4.2.5 Inductively coupled plasma (ICP)

The metal composition in the cellulose-supported MMAO, named Al was investigated using inductively coupled plasma optical emission spectrometer (ICP-OES optima 2100 DV from Perkin Elmer). The powder samples were dissolved with hydrochloric acid (HCl) and diluted for controlled volume by deionized water.

3.4.3 Characterization of polymer

3.4.3.1 Scanning electron microscopy (SEM)

In this session, polyethylene was operated as identical as cellulose materials before immobilization as mentioned in 3.4.1.1.

3.4.3.2 X-ray diffraction (XRD)

In this session, polyethylene was operated as identical as cellulose materials before immobilization as mentioned in 3.4.2.1.

3.4.3.3 Thermal gravimetric analysis-differential scanning calorimetry (TGA-DSC)

In this session, polyethylene was operated as identical as cellulose materials before immobilization as mentioned in 3.4.1.3.

CHAPTER 4
RESULTS AND DISCUSSION

This present chapter is described about the results and discussion relevant to this research. There are divided into two parts in this research; part 1 focuses on the effect of various celluloses on heterogeneous system compared with homogeneous system and part 2 describes the effect of cellulose from different biomass on heterogeneous system compared with commercial cellulose. All contents as mentioned are provided in this chapter.

There are 8 samples of cellulose materials, which are used as organic supports for metallocene catalyst in both part 1 and part 2. They are denoted as shown in (**Table 4.1**);

Table 4.1 Abbreviation of cellulose samples

Section	Full name of sample	Abbreviation of sample
PART 1	Microcrystalline cellulose	MCC
	Bacteria cellulose from pineapple	BAC-P
	Bacteria cellulose from coconut	BAC-C
PART 2	Biomass cellulose from sugarcane	SC
	Biomass cellulose from leaf sheath of banana tree	BS
	Biomass cellulose from rice straw	RS
	Biomass cellulose from water hyacinth	WH
	Biomass cellulose from pineapple leaf	PA
Other	Modified methylaluminoxane	MMAO

4.1 Effect of various celluloses on heterogeneous system compared with homogeneous system (part 1)

In part 1, the characteristics and activity of catalyst using various celluloses as supports were investigated. This part is divided into 3 portions. First, various celluloses are characterized using different techniques. Then, the effect of MMAO immobilization on various cellulose supports is presented in second portion. Finally, the obtained polyethylene was characterized in terms of morphology, crystallization and thermal properties.

4.1.1 Characterization of support

4.1.1.1 Characterization of support with scanning electron microscopy (SEM)

The morphology of various cellulose supports was characterized using scanning electron microscopy (SEM) as shown in (**Figure 4.1**). It was found that the particle sizes of various celluloses presented were in the range from 200-100 μm for MCC and 300-100 μm for bacteria celluloses including BAC-P and BAC-C. The particle size of bacterial cellulose appeared to be larger when compared to microcrystalline cellulose. The MCC exhibited mixture between pellet shape and rough layer surface, whereas both bacteria celluloses presented slightly irregular shape in fibrils rough surface area. All samples seem to display non-uniform shape.

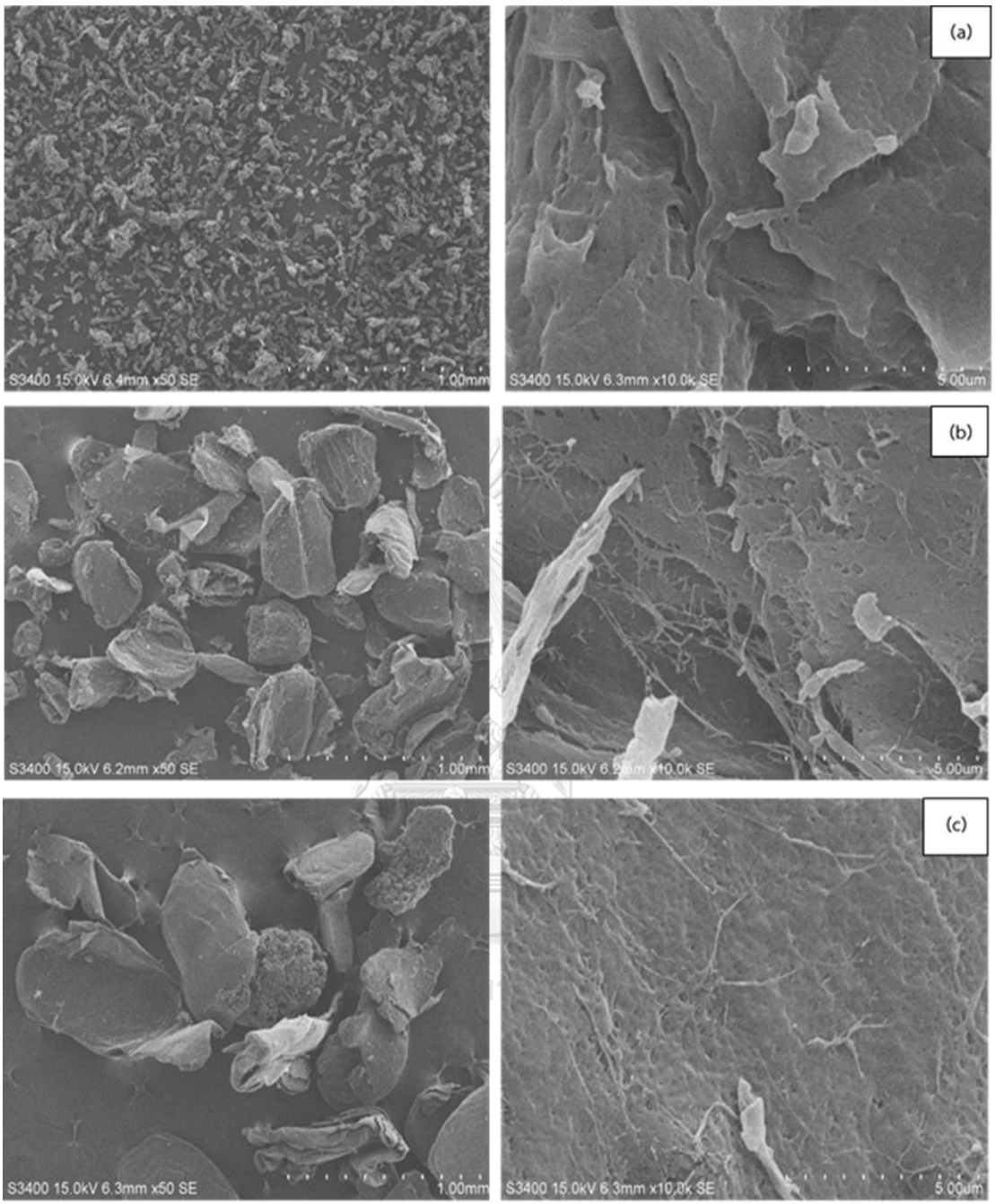

Figure 4.1 SEM micrographs of cellulose material (a) MCC, (b) BAC-P, and (c) BAC-C at 50X and 10.0kX magnification before immobilization

4.1.1.2 Characterization of support with X-ray diffraction (XRD)

The crystalline structure of various cellulose supports before immobilization was investigated by X-ray diffraction (XRD) as shown in (**Figure 4.2**). The XRD patterns of all cellulose supports were likely, presenting the characteristic peaks approximately at 2θ equal to 14.8, 16.2, 22.5, and 34.5, corresponding to planes in the sample with Miller indices (110) (002) (004) [30, 36]. It indicated that cellulose structure of all samples was ordered layer configuration.

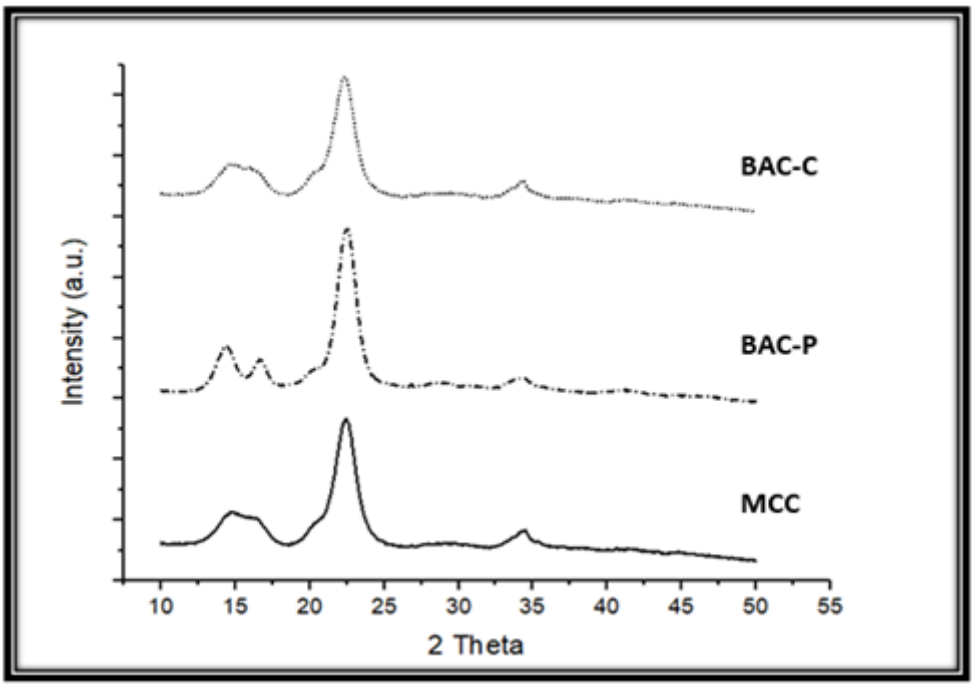

Figure 4.2 XRD patterns of MCC, BAC-P and BAC-C before immobilization

4.1.1.3 Characterization of support with thermal gravimetric analysis (TGA)

The stability of various cellulose supports before immobilization was measured by thermal gravimetric analysis (TGA) as shown in (**Figure 4.3**). The TGA profiles present information on degree of thermal stability in terms of residual weight (%) and temperature (^{o}C). It was observed that the degradation temperature at 5% weight loss of various cellulose supports including MCC, BAC-P, and BAC-C equal 304^{o}C, 284^{o}C and 299^{o}C, respectively. It indicated that MCC had the strongest thermal stability, following by BAC-C and BAC-P. However, the stability of all cellulose supports was not significantly different. Accordingly, the DTA profiles of various cellulose supports before immobilization, which is shown in (**Figure 4.4**), it exhibited percent weight loss of organic volatile components at temperature ranged from 280 to 360 ^{0}C.

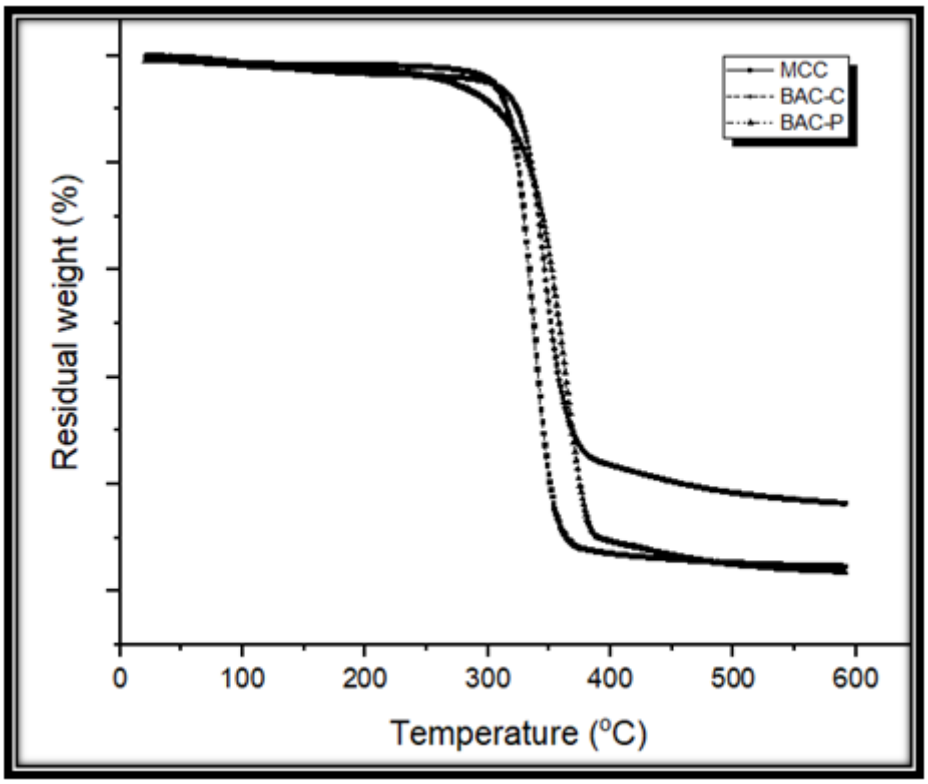

Figure 4.3 TGA profiles of various cellulose supports before immobilization

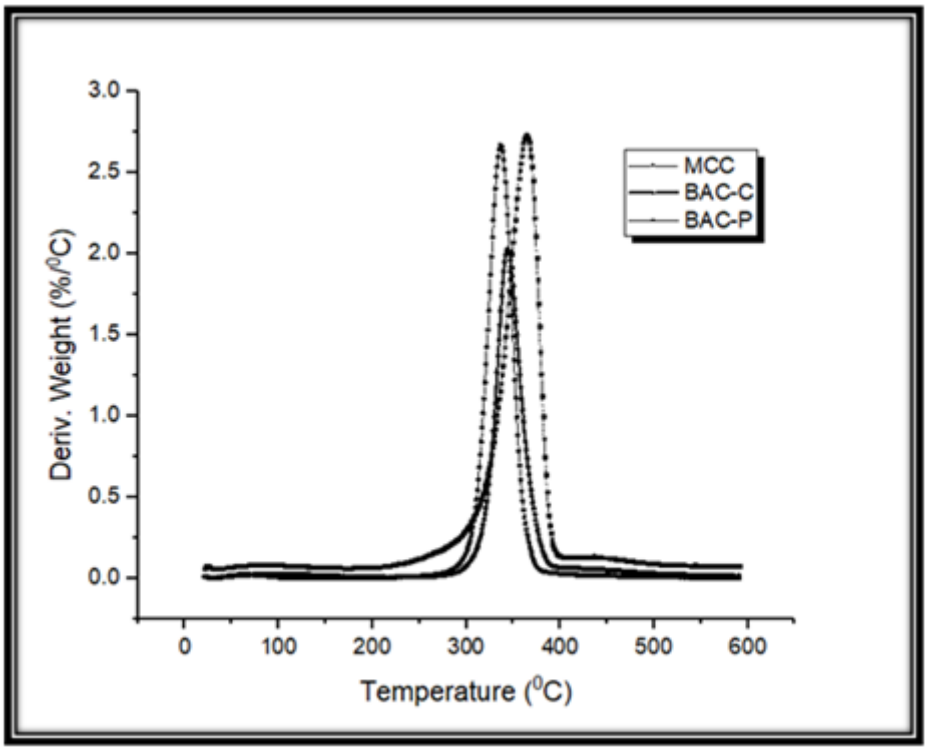

Figure 4.4 DTA profiles of various cellulose supports before immobilization

4.1.1.4 Characterization of support with Fourier transform infrared spectrophotometer (FT-IR)

The functional groups of various cellulose supports were characterized by Fourier transform infrared spectroscopy (FT-IR). The FT-IR spectra of various cellulose supports are shown in (**Figure 4.4**). They displayed the similar wavenumbers of FT-IR peaks. There are broad band at 3331, 3337, 3336 cm^{-1} of MCC, BAC-P, and BAC-C, respectively. Those are shown in (**Figure A.1**, **Figure A.2**, and **Figure A.3**, respectively). It revealed the presence of stretching vibration of the boned hydroxyl group on the various celluloses. The FT-IR peak at 1446 cm^{-1} was assigned to the symmetry of CH_2 bending vibration. The sharp peak of percentage of transmittance at range of 1026-1020 cm^{-1} was corresponded to strong bond of C-C, C-OH, and C-H group vibration [37]. Moreover, it also indicated the FT-IR spectrum of the alcohol functional group corresponding to O-H stretching at 3000-2780 cm^{-1} and C-H stretching at 1500-1300 cm^{-1}, and at 1100 cm^{-1} for C-O stretching [38].

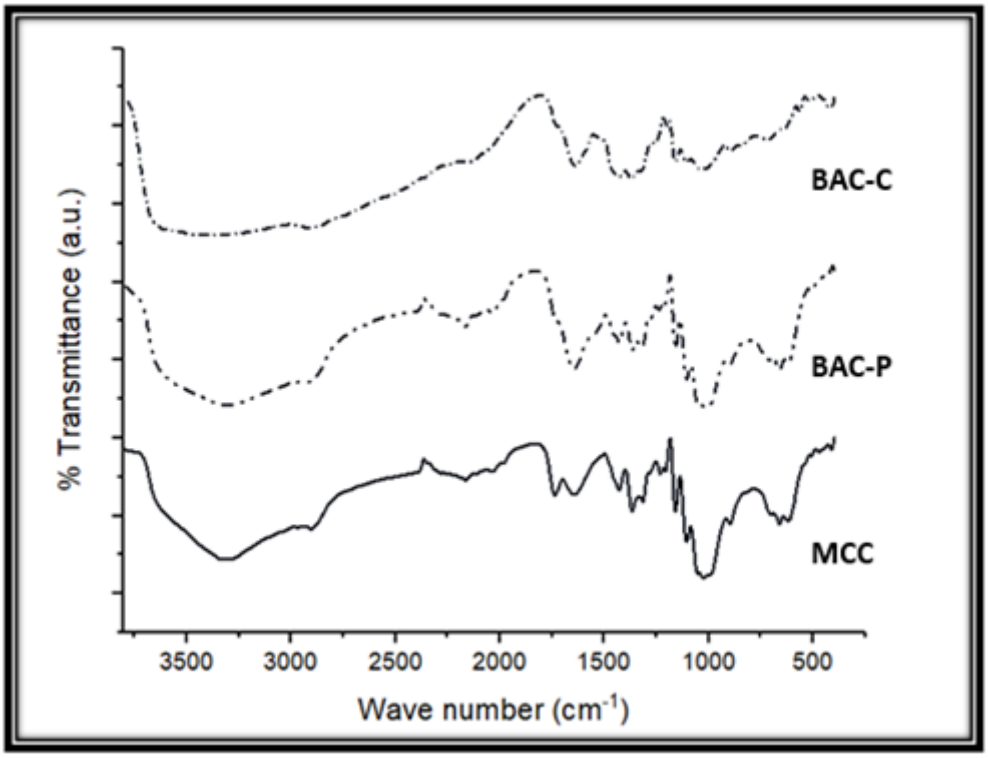

Figure 4.5 FT-IR spectra of MCC, BAC-P, and BAC-C before immobilization

4.1.2 Characterization of cellulose-MMAO support

4.1.2.1 Characterization of cellulose-MMAO support with scanning electron microscopy (SEM) and energy dispersive X-ray spectroscopy (EDX)

After immobilization of MMAO onto cellulose supports, the morphology and elemental dispersion (especially Al from MMAO) of supports were again investigated using SEM-EDX. They are shown in (**Figure 4.6** and **Figure 4.7** of SEM micrograph and dispersion of Al, respectively). It was observed that there are lots of the adhesion of small particle on various support surface indicating the adhesion between cellulose and MMAO. The EDX was also used to determine the distribution of elemental component on cellulose supports showing the good distribution of Al from MMAO on the external support surface.

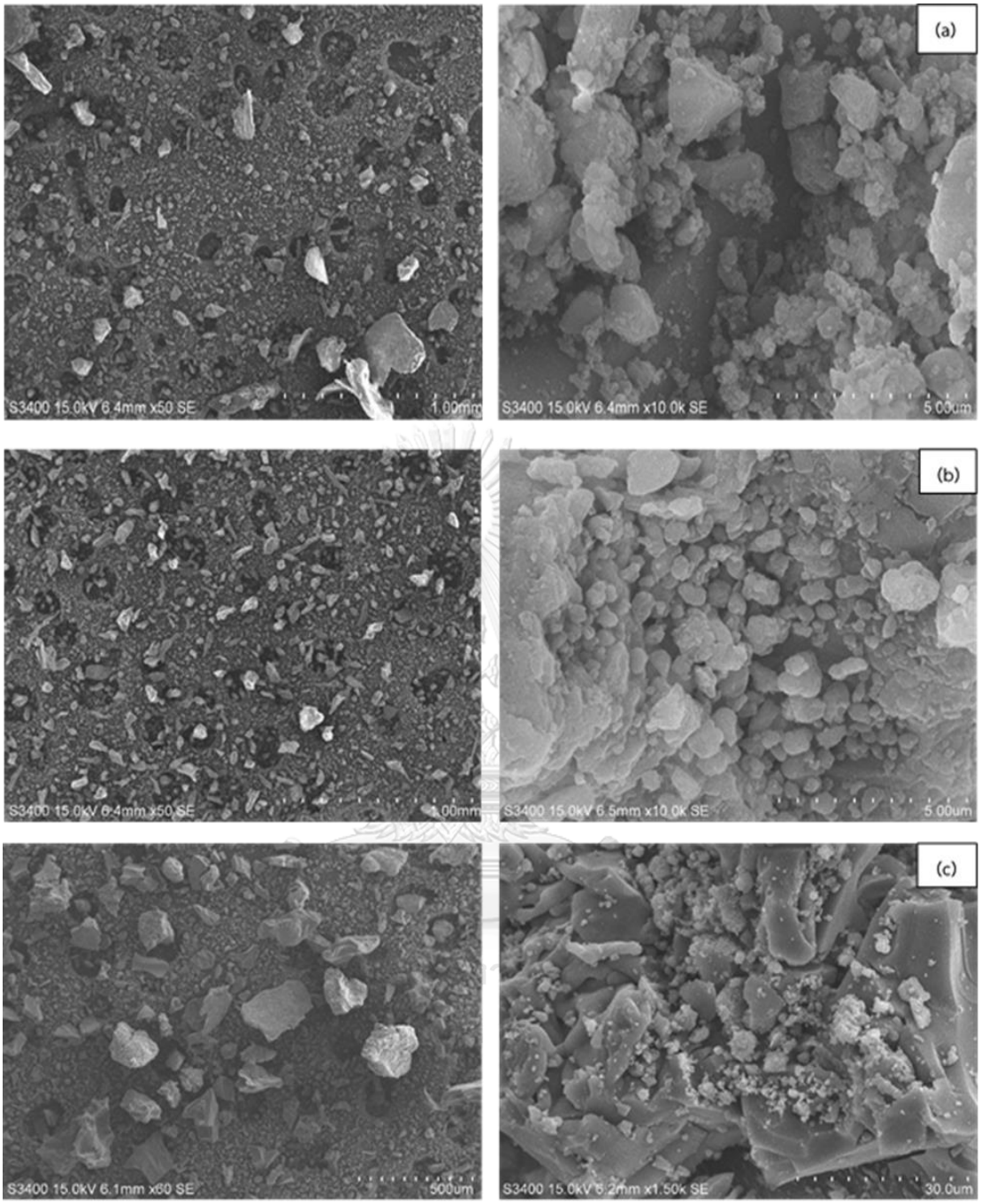

Figure 4.6 SEM micrographs of cellulose materials (a) MCC, (b) BAC-P, and (c) BAC-C at 50X and 10.0kX magnification after immobilization

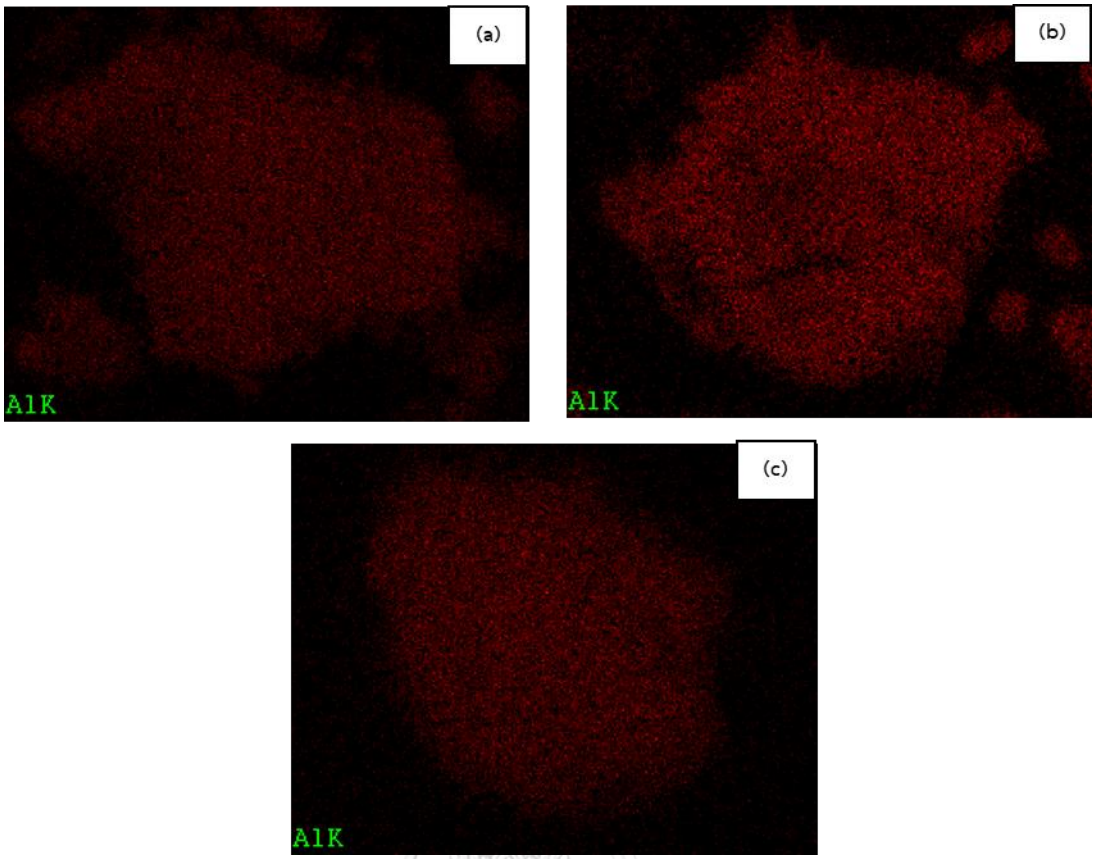

Figure 4.7 Al distribution obtained from EDX of (a) MCC, (b) BAC-P, and (c) BAC-C at 50X and 10.0kX magnification after immobilization

4.1.2.2 Characterization of cellulose-MMAO support with X-ray diffraction (XRD)

After immobilization of MMAO onto the cellulose support, XRD pattern was shown in (**Figure 4.8**). The various supports with immobilized MMAO presented the broad peak of XRD at 2θ equals 22.5, which is similar to the one of characterized XRD peak of cellulose before immobilization. It indicated that Al contents of MMAO were in the highly dispersed form on various cellulose supports.

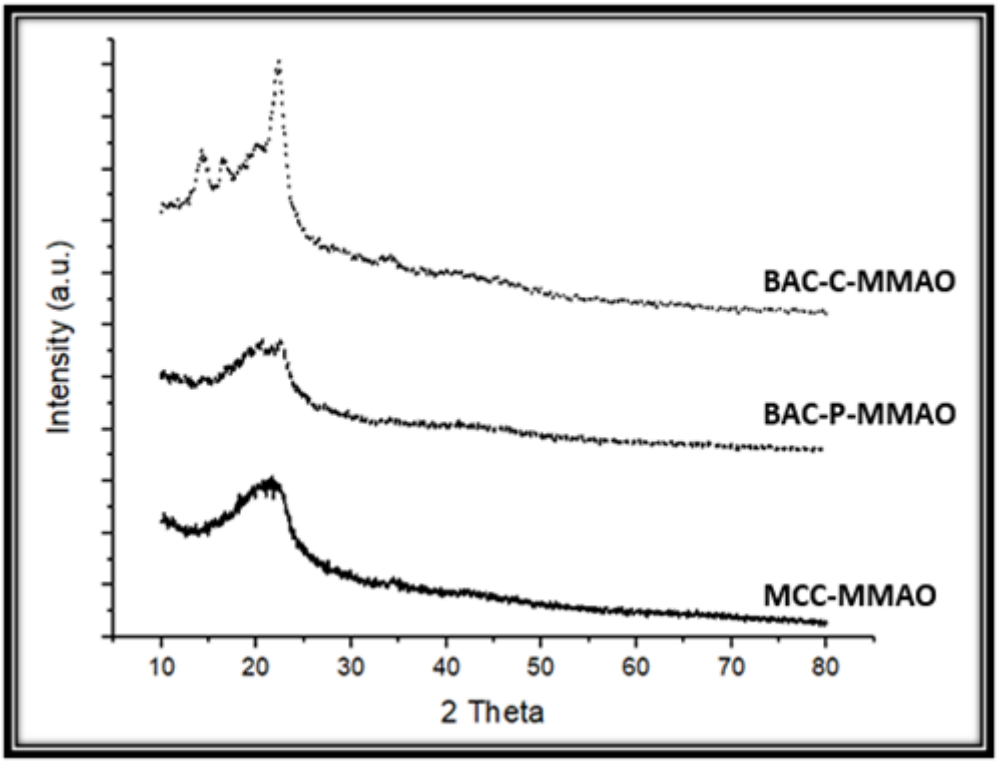

Figure 4.8 XRD patterns of MCC, BAC-P and BAC-C after immobilization

4.1.2.3 Characterization of cellulose-MMAO support with Fourier transform infrared spectrophotometer (FT-IR)

The comparison between various cellulose supports before and after immobilization with MMAO was again investigated using FT-IR to determine the functional group and bonding form. They presented the broad band at the range of wavenumber between 3340-3330 cm^{-1} in MCC and BAC-C after immobilization by MMAO. They still had the hydroxyl group in their structures. For BAC-P after immobilization with MMAO, the FT-IR spectra are shown in (**Figure 4.10**) indicating the broad peak at the wavenumber range of hydroxyl group similarly to those of MCC and BAC-C.

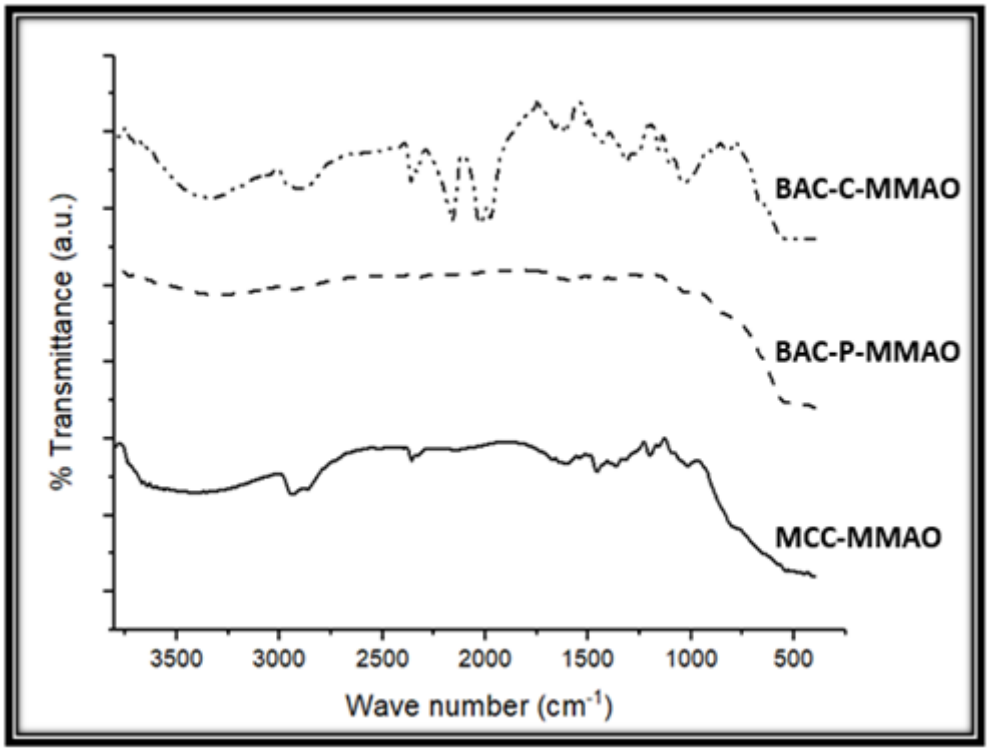

Figure 4.9 FT-IR spectra of MCC, BAC-P, and BAC-C after immobilization

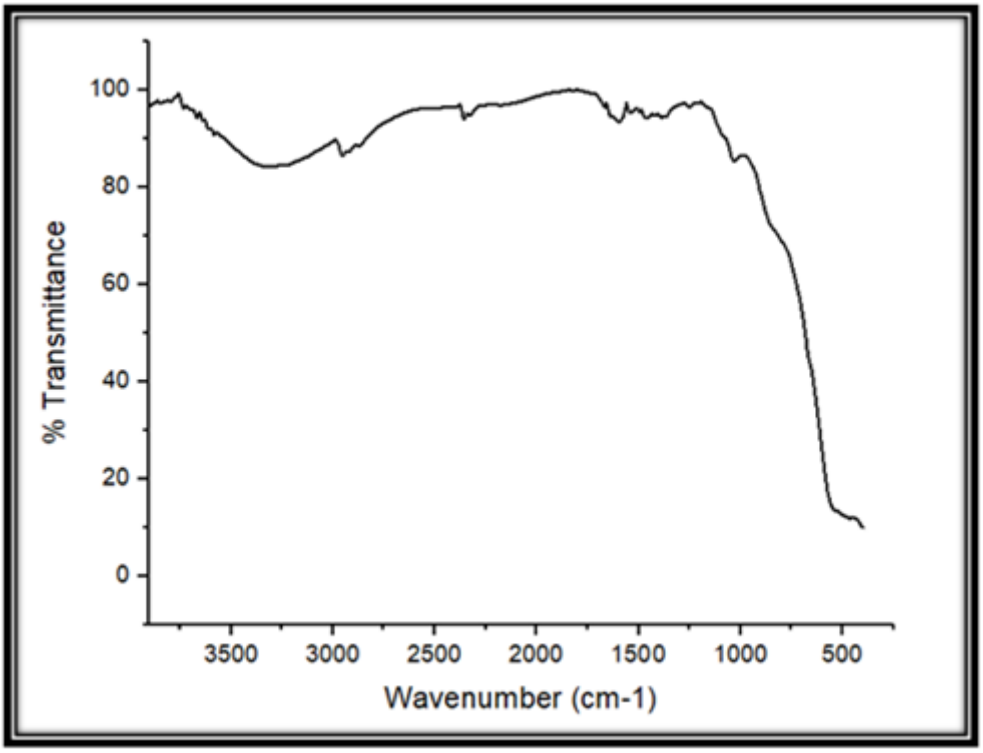

Figure 4.10 FT-IR spectra of BAC-P after immobilization

4.1.2.4 Characterization of cellulose-MMAO support with X-ray photoelectron spectroscopy (XPS)

To determine the binding energy (BE) and the plenty of Al on cellulose supported surfaces, X-ray photoelectron spectroscopy (XPS) was used on this purpose. Actually, the binding energy of Al in orbital 2p core level of $[Al]_{MMAO}$ was determined in various cellulose supported MMAO as shown in (**Figure 4.11** and **Table 4.2**).

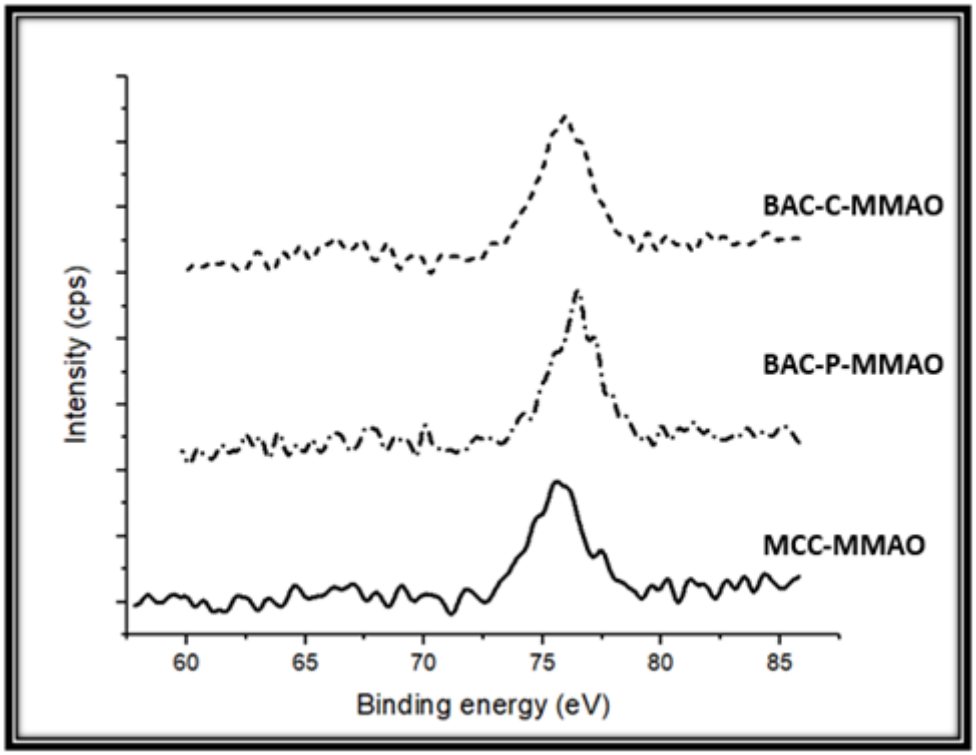

Figure 4.11 XPS spectra of MCC, BAC-P, BAC-C after immobilization

As seen for the binding energy of Al^{3+} in each various cellulose supports compared with Al^{3+} in MMAO, it suggested that, there is no significant change in oxidation state of $[Al]_{MMAO}$ initiated in various cellulose supports, including MCC, BAC-P, and BAC-C. The highest quantity of Al^{3+} at support surface is appeared in BAC-C-MMAO.

Table 4.2 XPS data of Al 2p core level of various cellulose supports

Samples	Binding Energy of Al^{3+} (eV)	Amount of Al^{3+} at surface (%wt.)
MMAO [39]	74.7	28.50
MCC-MMAO	75.6	34.76
BAC-P-MMAO	75.8	23.48
BAC-C-MMAO	74.7	35.38

4.1.2.5 Inductively coupled plasma (ICP)

Inductively coupled plasma (ICP) was used to determine the amount of Al in various cellulose supports in bulk. The ICP result is shown in (**Table 4.3**). It was found that there is the highest quantity of Al in cellulose support in MCC, following by BAC-P and BAC-C, respectively.

Table 4.3 The Al composition of various cellulose supports after immobilization

Sample	Amount of Al in support (%wt.)
MCC-MMAO	19.71
BAP-P-MMAO	22.54
BAC-C-MMAO	23.63

In summary, after characterization of various cellulose support before and after immobilization of MMAO, it was found that in bulk cellulose support contained small quantity of Al as observed by ICP. At cellulose surface, there is Al^{3+} distributed on the support surface without changing the oxidation state of Al from XPS, suggesting that MMAO did not decompose. The determining of crystalline structure before and after immobilization of MMAO in cellulose support using XRD, showed that after immobilization of MMAO on support, it was in the highly dispersed forms, which cannot be detected with XRD (the crystallite size is less than 3 nm) as shown in (**Figure 4.12**).

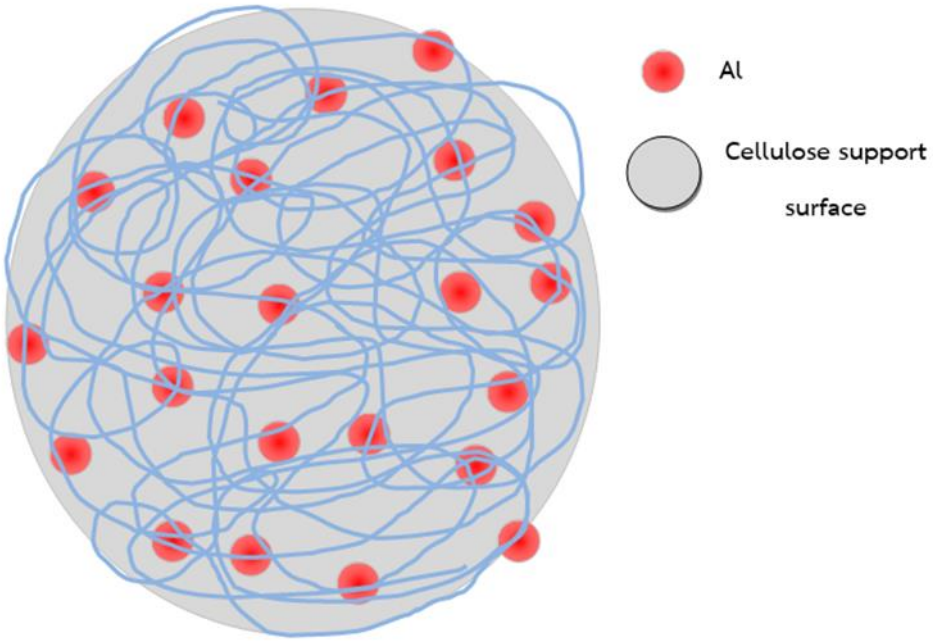

Figure 4.12 Scheme of Al dispersion on cellulose support after immobilization of MMAO

4.1.3 Characterization of polymer

4.1.3.1 Characterization of polymer with scanning electron microscopy (SEM)

The morphology of obtained polyethylene from homogeneous and heterogeneous systems as measured by SEM/EDX are shown in (**Figure 4.13**). Considering the heterogeneous system, it appeared the similar morphologies of polymer obtained from various celluloses, including MCC, BAC-P and BAC-C as supports. However, it was different from homogeneous system. The observed polyethylene from homogeneous system exhibited the larger porosity particles than that from the supported system and polyethylene obtained with the various celluloses display more open structure than the one obtained from homogeneous system. In addition, different celluloses may affect the morphologies in heterogeneous system.

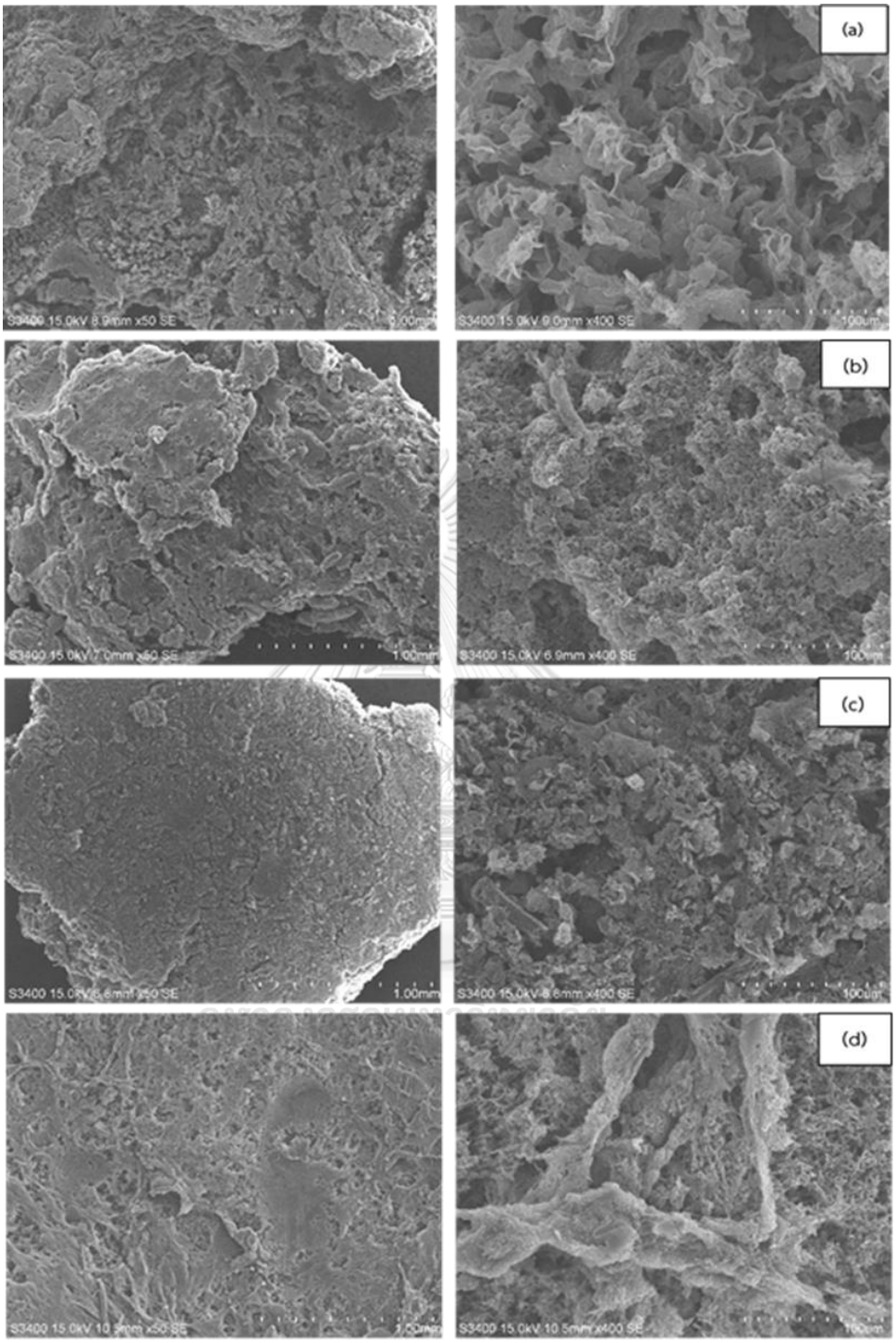

Figure 4.13 SEM micrographs of polyethylene produced via homogeneous system and heterogeneous system (a) PE-HOMO, (b) PE-MCC, (c) PE-BAC-P, and (d) PE-BAC-C at 50X and 400X magnification

4.1.3.2 Characterization of polymer with X-ray diffraction (XRD)

The obtained polyethylenes were characterized using XRD technique. **Figure 4.14** shows the XRD patterns of polyethylenes synthesized with different cellulose supports compared to polyethylene from homogeneous system. It indicates that, the XRD patterns for all produced polyethylene were similar. All samples exhibited two peaks at 2θ of the orthorhombic crystalline form in polyethylene at 21.4° and 24.1° [40].

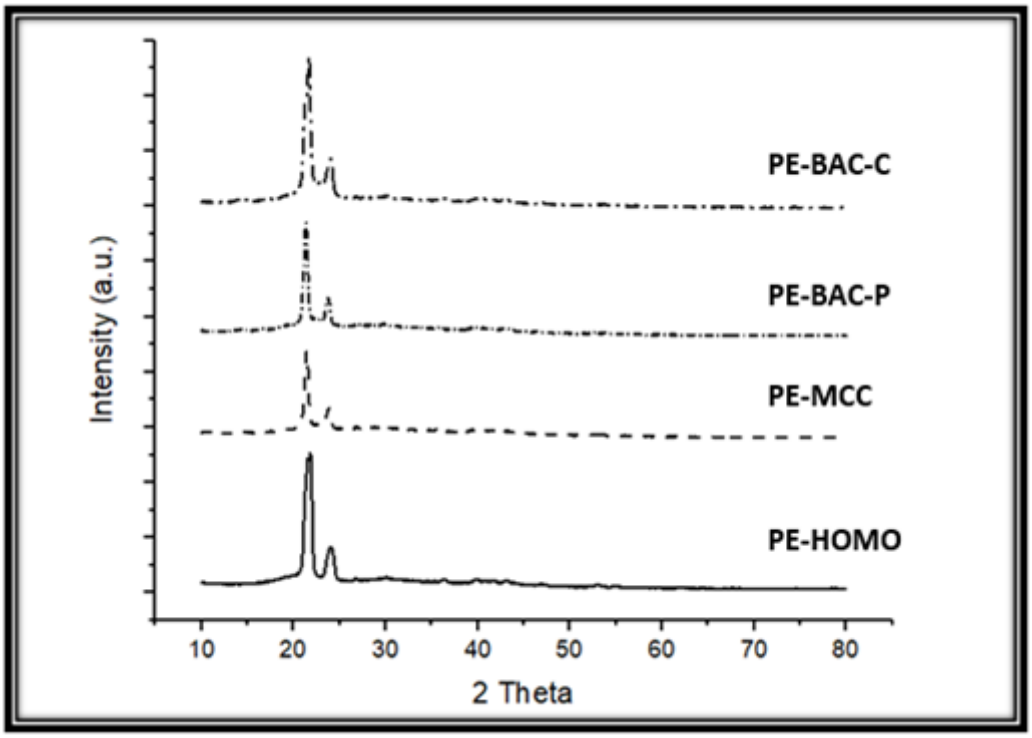

Figure 4.14 XRD patterns of polyethylene produced via homogeneous system and heterogeneous system

4.1.1.3 Characterization of polymer with thermal gravimetric analysis-differential scanning calorimetry (TGA-DSC)

To investigate the stability of produced polyethylene from homogeneous and heterogeneous system, TGA technique was performed as shown in **Figure 4.15**. The TGA profile displays degree of thermal stability in terms of residual weight (%) and temperature (°C). It was found that the degradation temperature at 5% weight loss of polyethylene from homogeneous system (PE-HOMO) and polyethylene from heterogeneous system, including PE-MCC, PE-BAC-P, and BAC-C equal to 144°C, 118°C, 307°C, and 300°C, respectively. PE-BAC-P exhibited the strongest thermal stability, following by PE-BAC-C, PE-HOMO, and PE-MCC. In addition, the DTA profile was also performed as shown in **Figure 4.16**, it appeared percent weight loss of organic volatile components at temperature range between 260 and 350 ^{0}C, 410 and 500 ^{0}C, and percent weight loss of moisture at 100 ^{0}C.

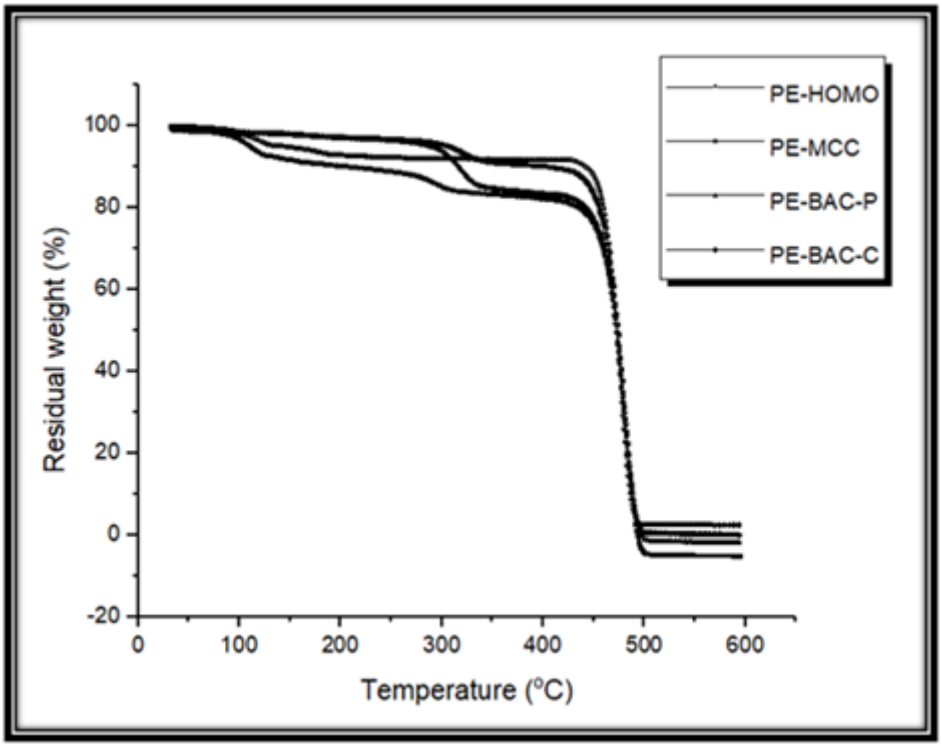

Figure 4.15 TGA profiles of polyethylenes produced via homogeneous system and heterogeneous system

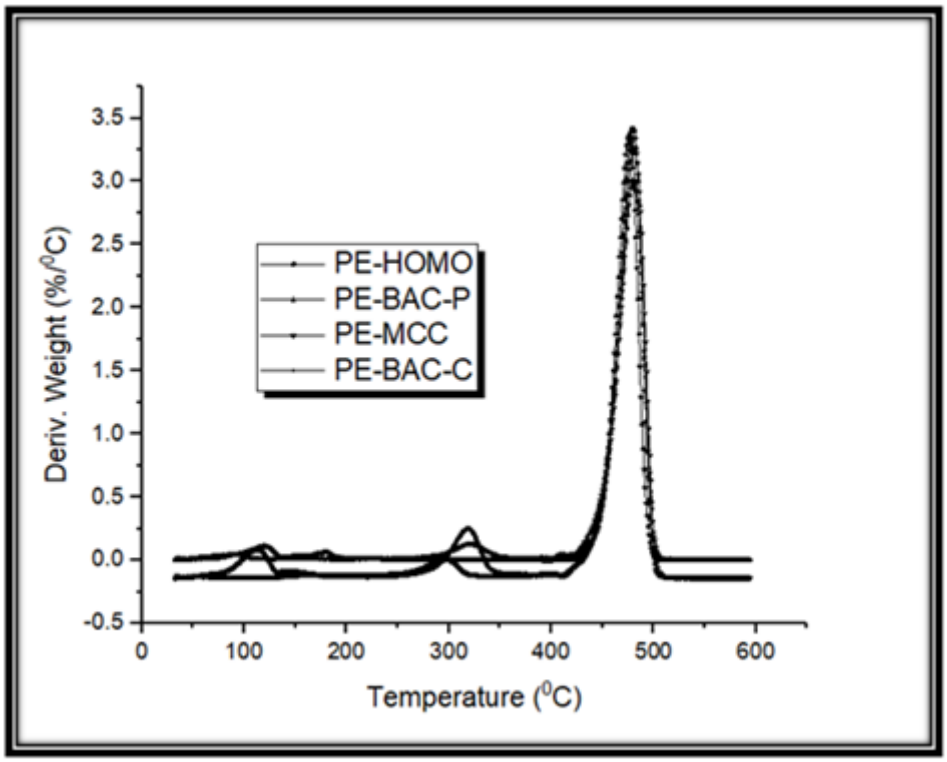

Figure 4.16 DTA profiles of polyethylenes produced via homogeneous system and heterogeneous system

The obtained polyethylenes were determined by differential scanning calorimeter (DSC). The melting enthalpy and melting temperature of the polymer are listed in (**Table 4.4**) and the DSC curve are shown in (**Figure C-1**), (**Figure C-2**), (**Figure C-3**) and (**Figure C-4**), respectively as referred to **Appendix C**. For heterogeneous system, it was found that there was no significant change in the melting temperature for all produced polyethylenes. The melting temperature of produced polyethylenes was in the range between (122 and 125 °C). In contrast, it was observed that produced polyethylenes with addition of cellulose exhibited different crystallinity. The highest crystallinity was obtained in PE-BAC-P, following by PE-MCC, PE-HOMO and PE-BAC-C, respectively.

Table 4.4 Melting and crystallization behaviors of polyethylenes produced via homogeneous system and heterogeneous system

Samples	Melting Temperature, T_m[a] (°c)	ΔH_{exp}[b] (J/g)	X_c[c] (%)
PE-HOMO	124	164.4	57.5
PE-MCC	122	167.2	58.5
PE-BAC-P	123	215.9	75.5
PE-BAC-C	125	167.4	58.5

[a] Melting temperature (T_m) was obtained from DSC measurement.

[b] Heat of fusion (ΔH_{exp}) was obtained from DSC measurement.

[c]Crystallinity (X_c) was calculated from this equation; %crystallinity = ($\Delta H_{sample}/\Delta H_{100\%}$crystallinity)x100, the $\Delta H_{100\%}$ crystallinity of polyethylene is 286 J/g.

4.1.4 Ethylene consumption

The ethylene consumption rate (ml/min) was recorded as shown in **Figure 4.17**. It indicated that produced polyethylene in homogeneous system exhibited the steady rate since the first minute to the last minute in overall time of 15 minutes. For produced polyethylene in heterogeneous system, they showed the irregular rate since the first minute. Therefore, no deactivation of catalysts was observed in all runs.

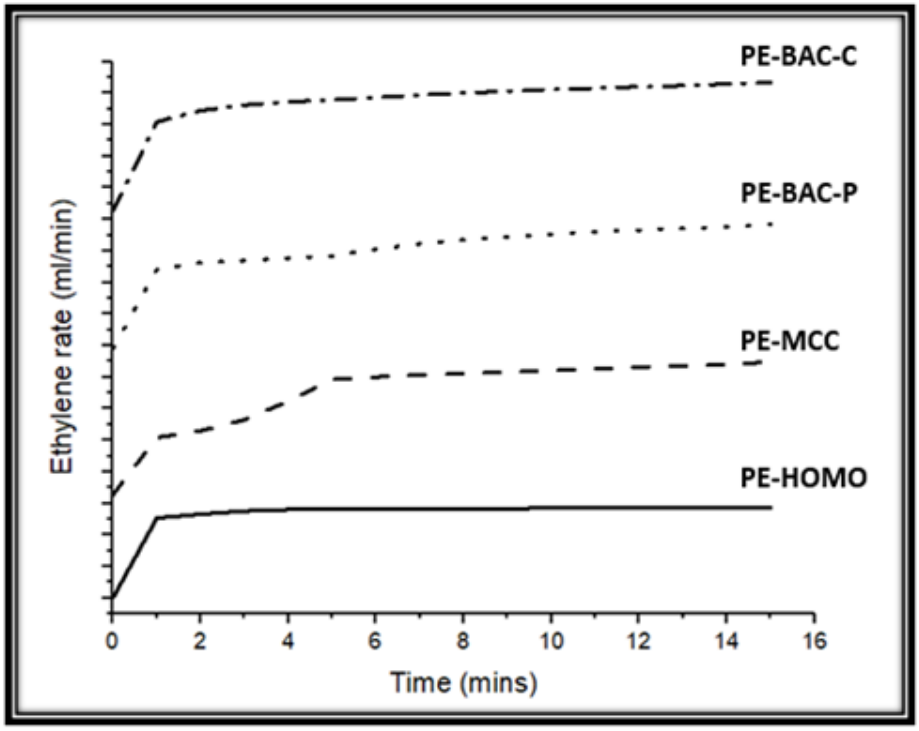

Figure 4.17 The ethylene consumption of polyethylene produced via homogeneous system and heterogeneous system

4.1.5 Catalytic activity

The reported catalytic activity of catalysts in ethylene polymerization following homogeneous and heterogeneous system is shown in **Table 4.5**. In fact, it is assigned to the *in situ* polymerization of ethylene using catalyst precursors prepared by *ex situ* immobilization method. For this immobilization system the various cellulose supports were reacted with the desired amount of cocatalyst, namely MMAO at room temperature for 30 minutes, which were allowed the preparation of supports in form of suspensions. Afterwards, the *in situ* polymerization was finished, the yield and ethylene consumption rate were collected. In addition to **Table 4.5**, the produced polyethylene from homogeneous system displayed the highest catalytic activity and polymer yield. On the contrary, the produced polyethylene from heterogeneous system exhibited lower catalytic activity and polymer yield compared to the homogeneous system. It is well known that the supported system results in decreased catalytic activity for heterogeneous catalysts. This is mostly due to the presence of support interaction resulting in lower active sites for the polymerization process. Another reason maybe caused by steric hindrance of the support surface that acts as the roles of ligand [41, 42].

Table 4.5 The catalytic activity of catalysts via homogeneous system and heterogeneous system

Samples	Polymer yield[a] (g)	Catalytic activity[b] (kg of pol/molZr h)
PE-HOMO	0.7894	380
PE-MCC	0.4943	238
PE-BAC-P	0.4291	207
PE-BAC-C	0.4196	202

[a] The polymerization time was 15 min.

[b]Activities were measured at polymerization temperature of 70 °C, [ethylene] = 0.018 mole, $[Al]_{MMAO}/[Zr]_{Cat}$ = 1135, in toluene with total volume = 30 mL, and $[Zr]_{Cat}$ =5 x 10^{-5} M.

4.2 Effect of cellulose from different biomass on heterogeneous system compared with commercial cellulose (part 2)

In part 2, the study of characteristics and activity of polyethylene using biomass celluloses as supports compared to commercial cellulose was investigated. This part consists of 3 portions. First, biomass celluloses are characterized to identify physicochemical properties. Next, effect of MMAO immobilization on biomass cellulose supports is presented in the second segment. Finally, produced polyethylene was also characterized in terms of morphology, crystallization and thermal behaviors.

4.2.1 Characterization of support

4.2.1.1 Characterization of support with scanning electron microscopy (SEM)

The morphology of several cellulose supports derived from biomass were also examined using scanning electron microscopy (SEM) as shown in (**Figure 4.18** and **Figure 4.19**). The raw material of cellulose was prepared by drying all materials by exposing to sunlight. Then, dried materials were blended using moulinex machine. The selected sizes 40-60 μm of cellulose powder was collected. From SEM micrographs, it was observed that the biomass celluloses presented slightly irregular shape in unfebrile rough and it could not identify the average size of them.

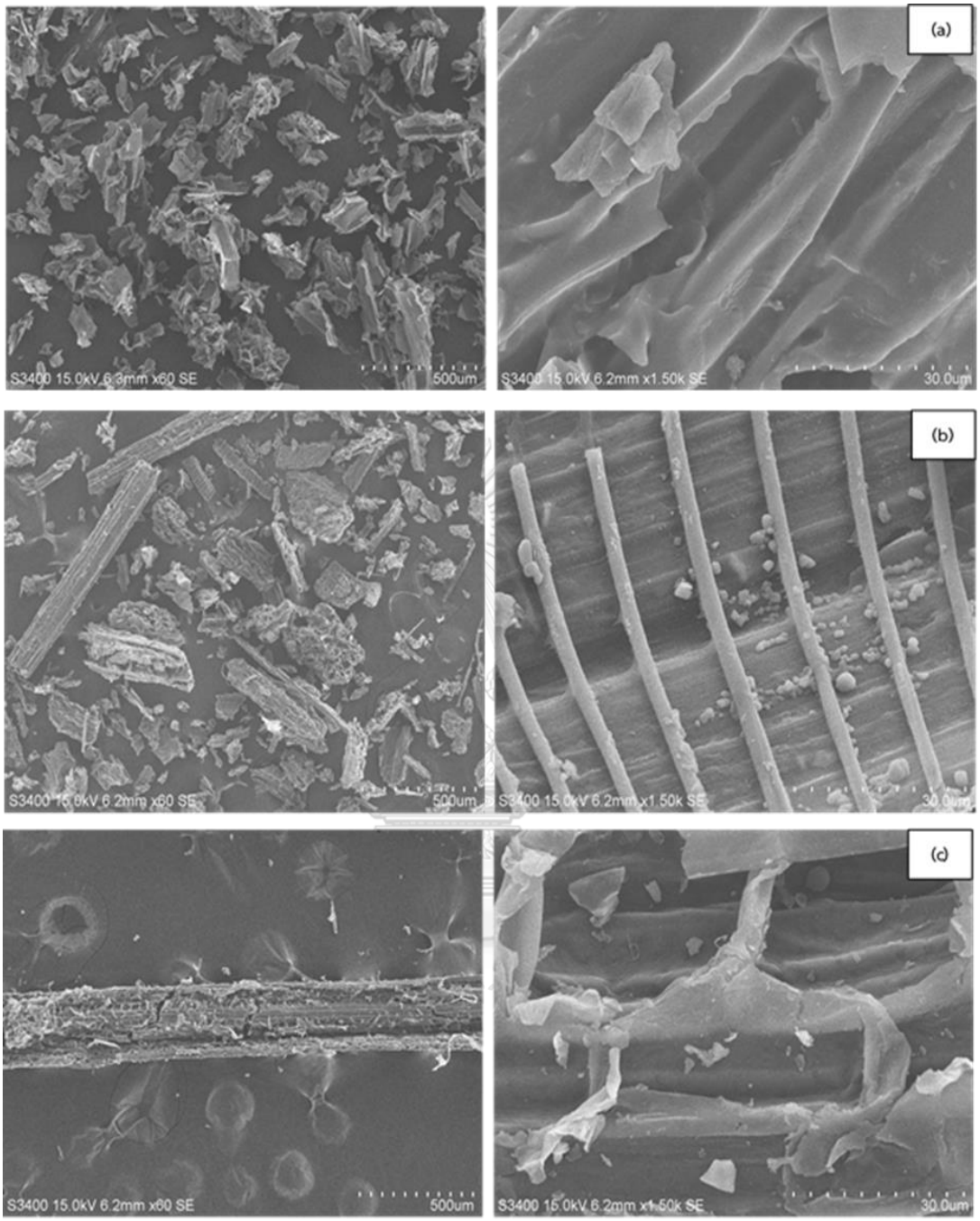

Figure 4.18 SEM micrographs of biomass cellulose material (a) SC, (b) BS, and (c) RS at 60X and 1.50kX magnification before immobilization

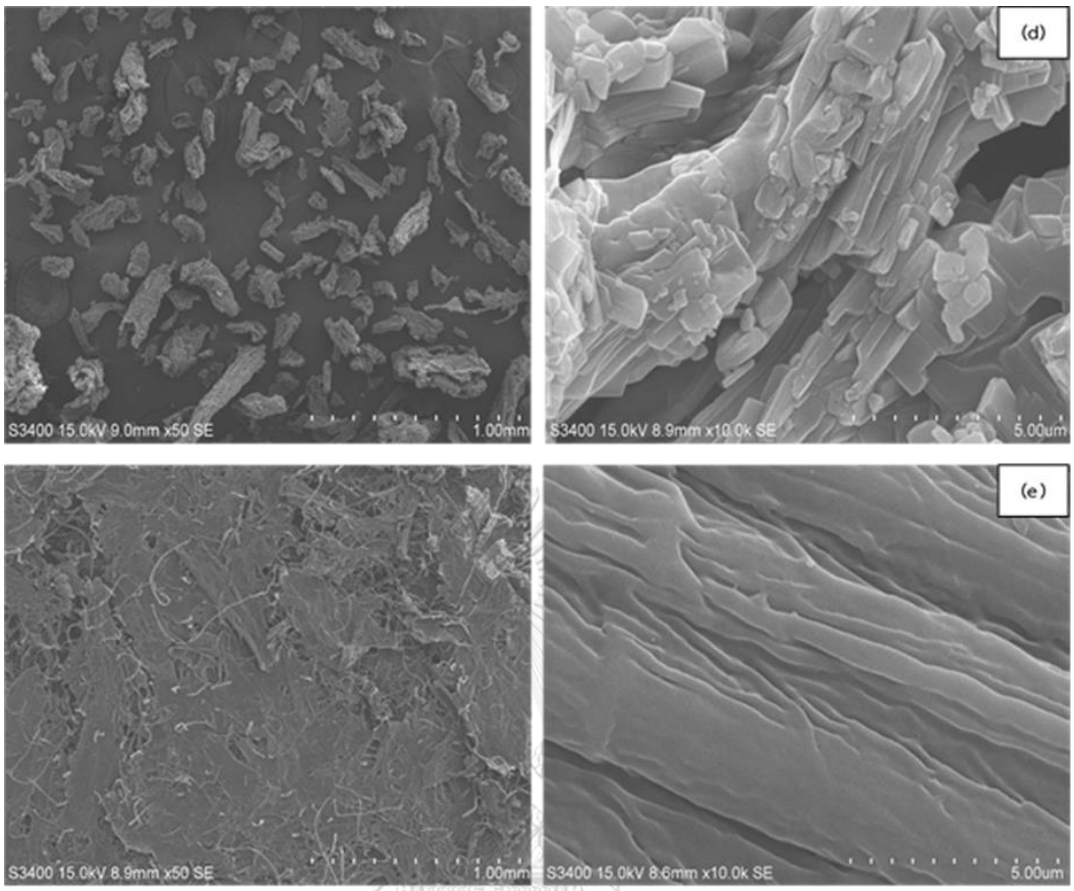

Figure 4.19 SEM micrographs of biomass cellulose material (d) WH, and (e) PA at 50X and 10.0kX magnification before immobilization

4.2.1.2 Characterization of support with X-ray diffraction (XRD)

The crystalline structure of various biomass cellulose supports before immobilization was also analyzed by X-ray diffraction (XRD) as shown in (**Figure 4.21** and **Figure 4.22**). When compared to commercial cellulose, namely MCC, the XRD patterns of it, presents the characteristic peaks approximately at 2θ equal to 14.8, 16.2, 22.5, and 34.5° as shown in (**Figure 4.20**). In addition, the various biomass cellulose supports demonstrate only one characteristic XRD peak of cellulose at 2θ equals to 22.5°. It can be observed another peak in WH, corresponding to another organic composition. However, PA mostly exhibits the similar peak as MCC.

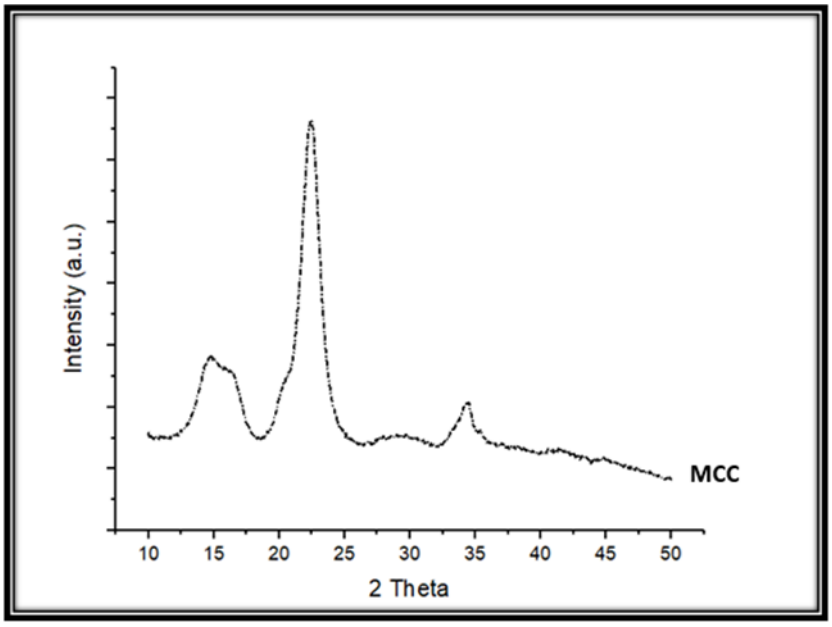

Figure 4.20 XRD pattern of MCC before immobilization

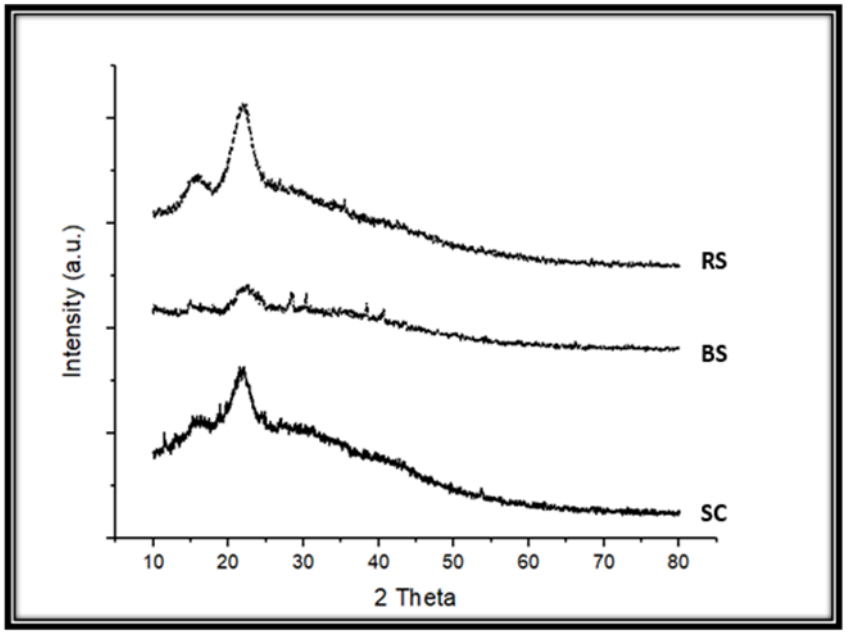

Figure 4.21 XRD patterns of biomass cellulose before immobilization (1; SC, BS, and RS)

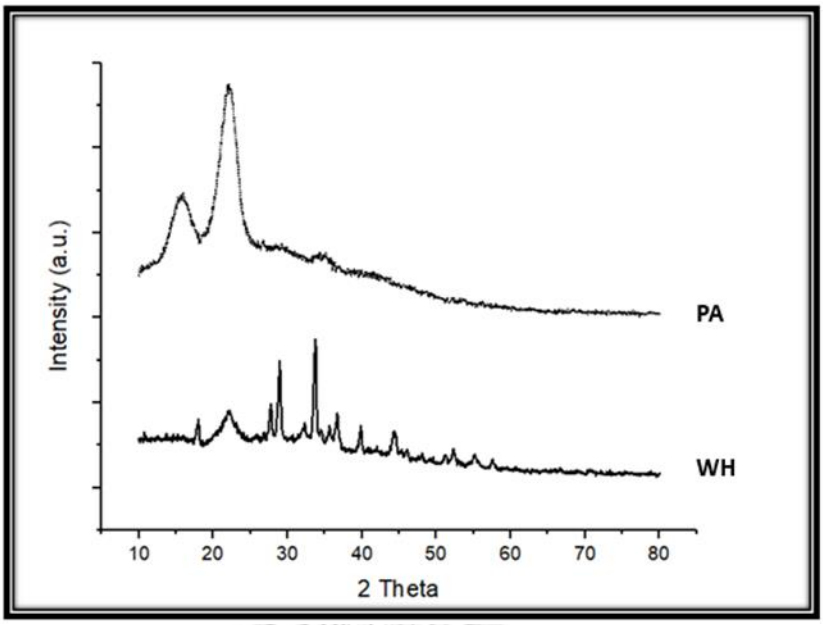

Figure 4.22 XRD patterns of biomass cellulose before immobilization (2; WH and PA)

4.2.1.3 Characterization of support with thermal gravimetric analysis (TGA)

The stability of different biomass cellulose supports before immobilization was also measured by thermal gravimetric analysis (TGA) as shown in (**Figure 4.23**). The TGA profiles present information on degree of thermal stability in terms of residual weight (%) and temperature (^{o}C). It demonstrated that the degradation temperature at 5% weight loss of different biomass cellulose supports including SC, BS, RS, WH, and PA equal 181^{o}C, 174^{o}C, 262 ^{o}C, 259 ^{o}C, and 266^{o}C, respectively. It was found that PA has the strongest thermal stability, following by RS, WH, SC and BS. It is worth noting that the stability of all biomass cellulose supports was slightly different. Moreover, the DTA profiles of various biomass cellulose supports before immobilization as shown in (**Figure 4.24**), display percent weight loss of organic volatile components at temperature ranging from 150 to 380 ^{0}C.

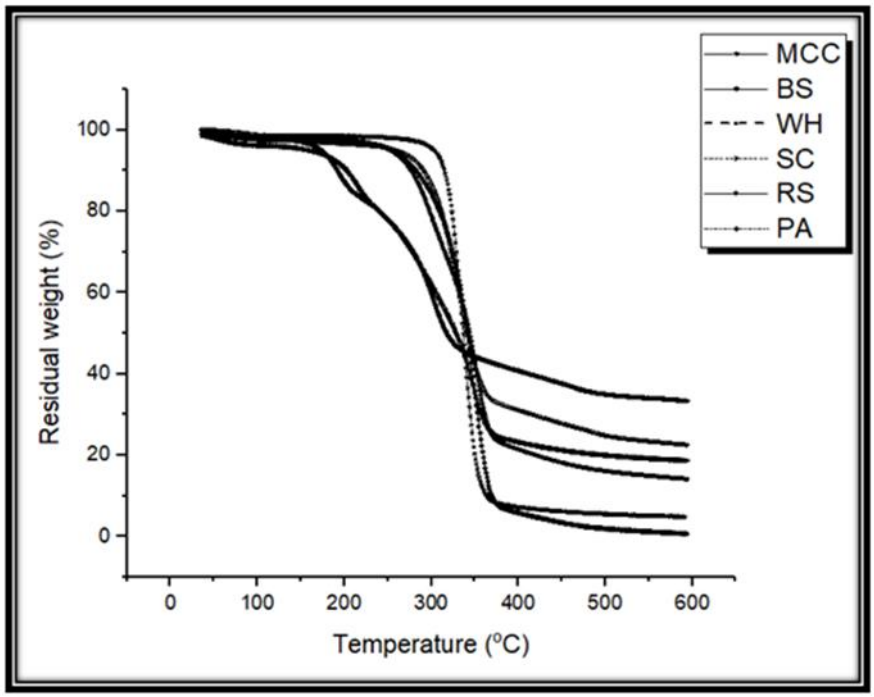

Figure 4.23 TGA profiles of biomass cellulose supports before immobilization

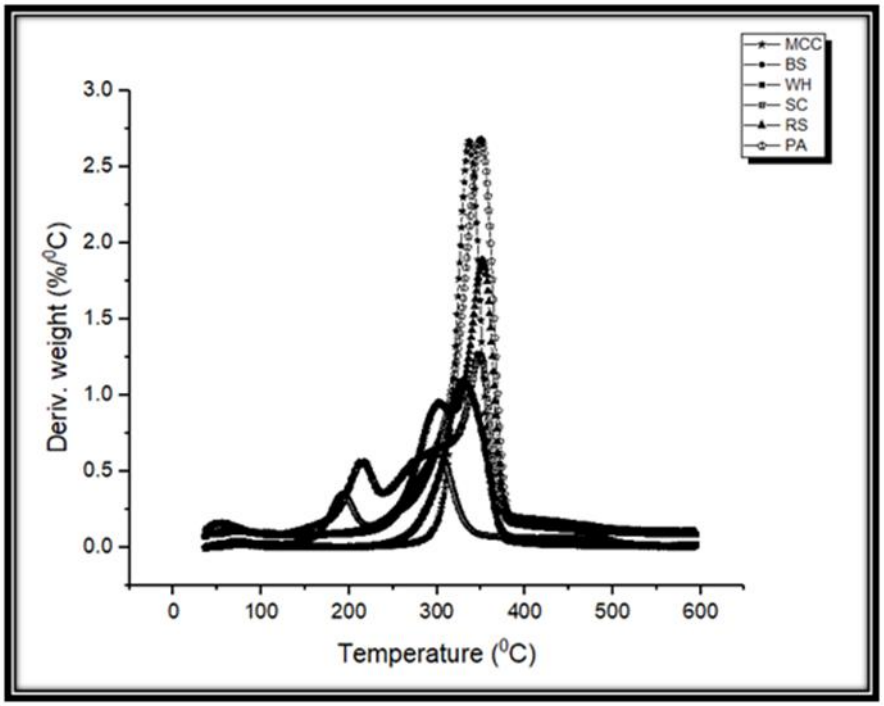

Figure 4.24 DTA profiles of biomass cellulose supports before immobilization

4.2.1.4 Characterization of support with Fourier transform infrared spectrophotometer (FT-IR)

The functional groups of different biomass cellulose supports were investigated by Fourier transform infrared spectroscopy (FT-IR). The FT-IR spectra of various biomass cellulose supports are shown in (**Figure 4.25**). They displayed the similar FT-IR peaks when compared to MCC. There are broad bands at 3342, 3278, 3342, 3334, and 3338 cm^{-1} of SC, BS, RS, WH, and PA, respectively. Those are shown in (**Figure A.4**, **Figure A.5**, **Figure A.6**, **Figure A.7** and **Figure A.8**, respectively). It revealed the presence of stretching vibration of the boned hydroxyl group on the various celluloses. The FT-IR peak at 1446 cm^{-1} was corresponding to the symmetry of CH_2 bending vibration. The sharp peak of percentage of transmittance at range of 1026-1020 cm^{1} was corresponded to strong bond of C-C, C-OH, and C-H group vibration [37], Accordingly, it also indicated the FT-IR spectrum of the alcohol functional group assigned to O-H stretching at 3000-2780 cm^{-1} and C-H stretching at 1500-1300 cm^{-1}, and at 1100 cm^{-1} for C-O stretching [38]. All FT-IR spectra of different biomass cellulose were also similar to various celluloses in part 1.

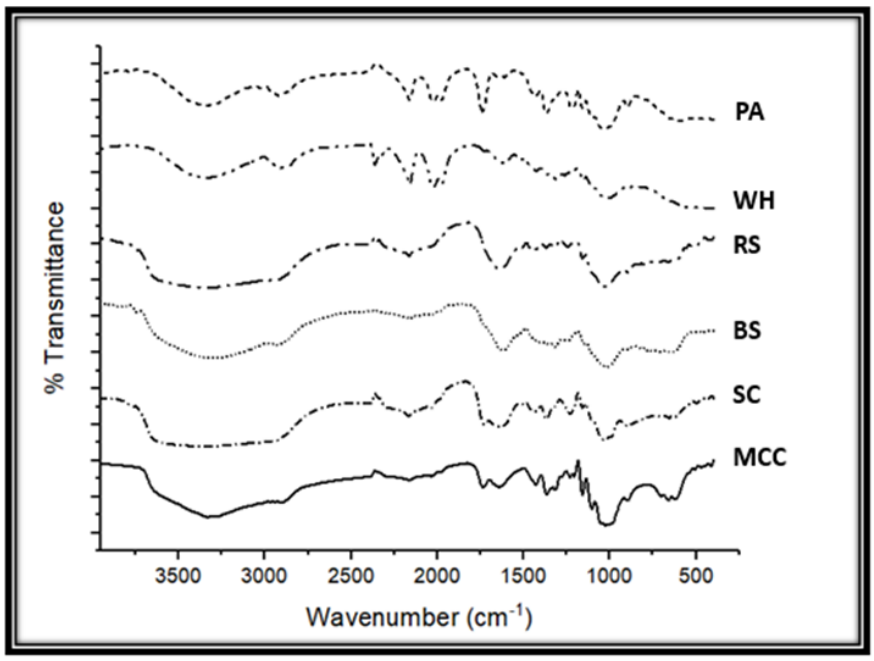

Figure 4.25 FT-IR spectra of biomass cellulose supports before immobilization

4.2.2 Characterization of cellulose-MMAO support

4.2.2.1 Characterization of cellulose-MMAO support with scanning electron microscopy (SEM) and energy dispersive X-ray spectroscopy (EDX)

After immobilization of MMAO onto different biomass cellulose supports, the morphology and elemental distribution (especially, for Al from MMAO) of supports were again investigated using SEM-EDX. They are shown in (**Figure 4.26, Figure 4.27** and **Figure 4.28** of SEM micrograph and dispersion of Al, respectively). It suggested that there are lots of the adhesion of small particle on different biomass cellulose support surface indicating the adhesion between cellulose and MMAO. However, in biomass cellulose, namely RS presented slightly small particle on surface when compared to other biomass cellulose including SC, BS, WH and PA. The EDX was also used to determine the distribution of elemental component on different biomass cellulose supports showing the good distribution of Al from MMAO on the external support surface in all biomass celluloses after immobilization of MMAO.

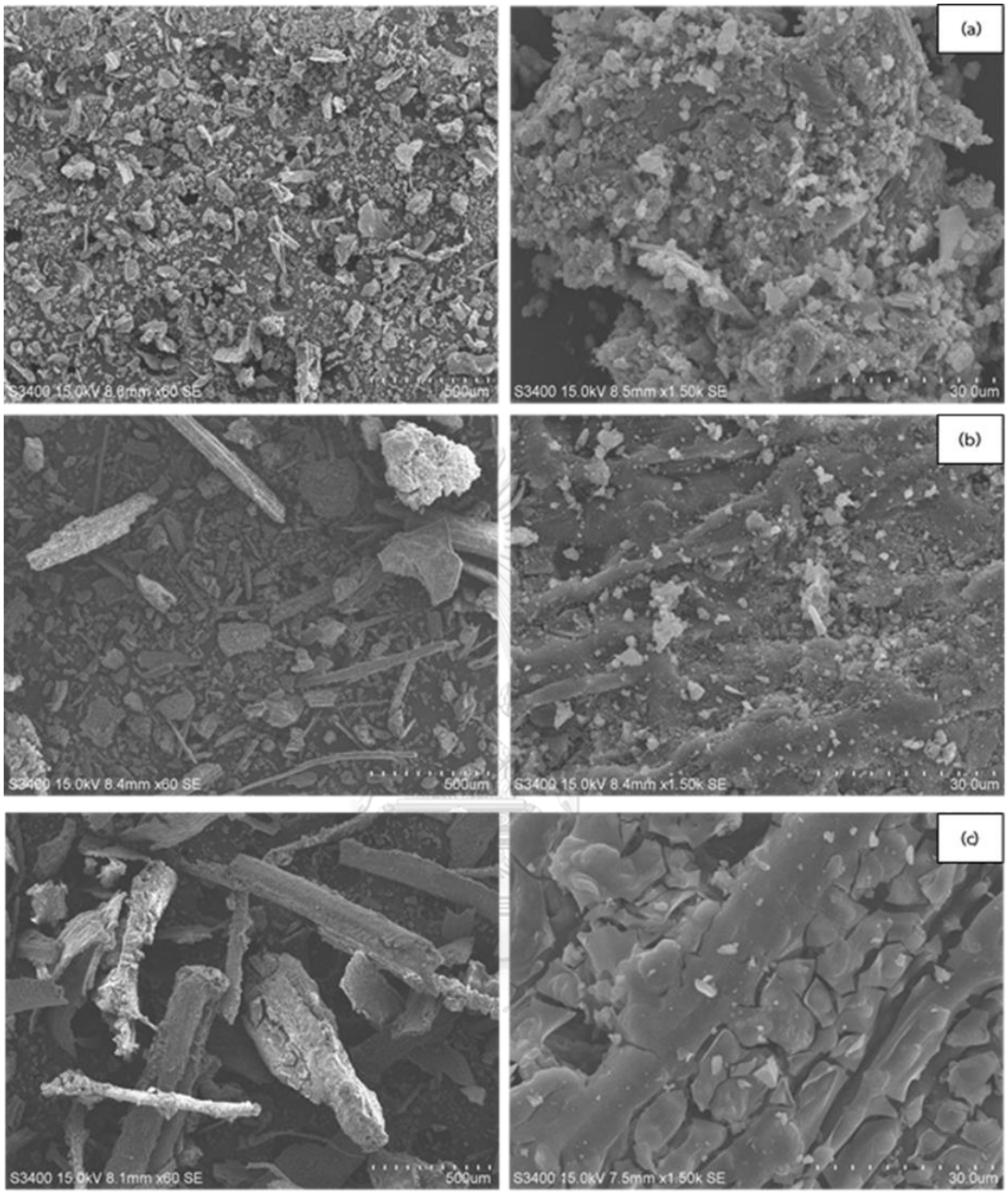

Figure 4.26 SEM micrographs of biomass cellulose material (a) SC, (b) BS, and (c) RS at 60X and 1.50kX magnification after immobilization

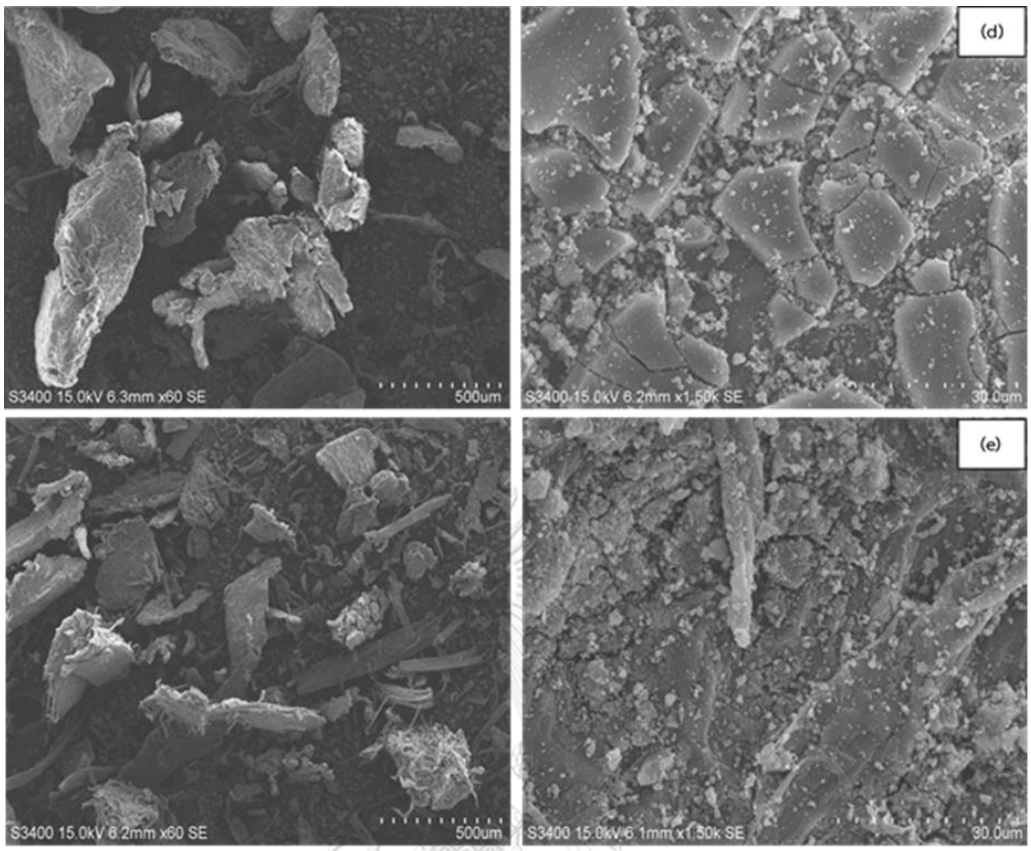

Figure 4.27 SEM micrographs of biomass cellulose materials (d) WH and (e) PA at 60X and 1.50kX magnification after immobilization

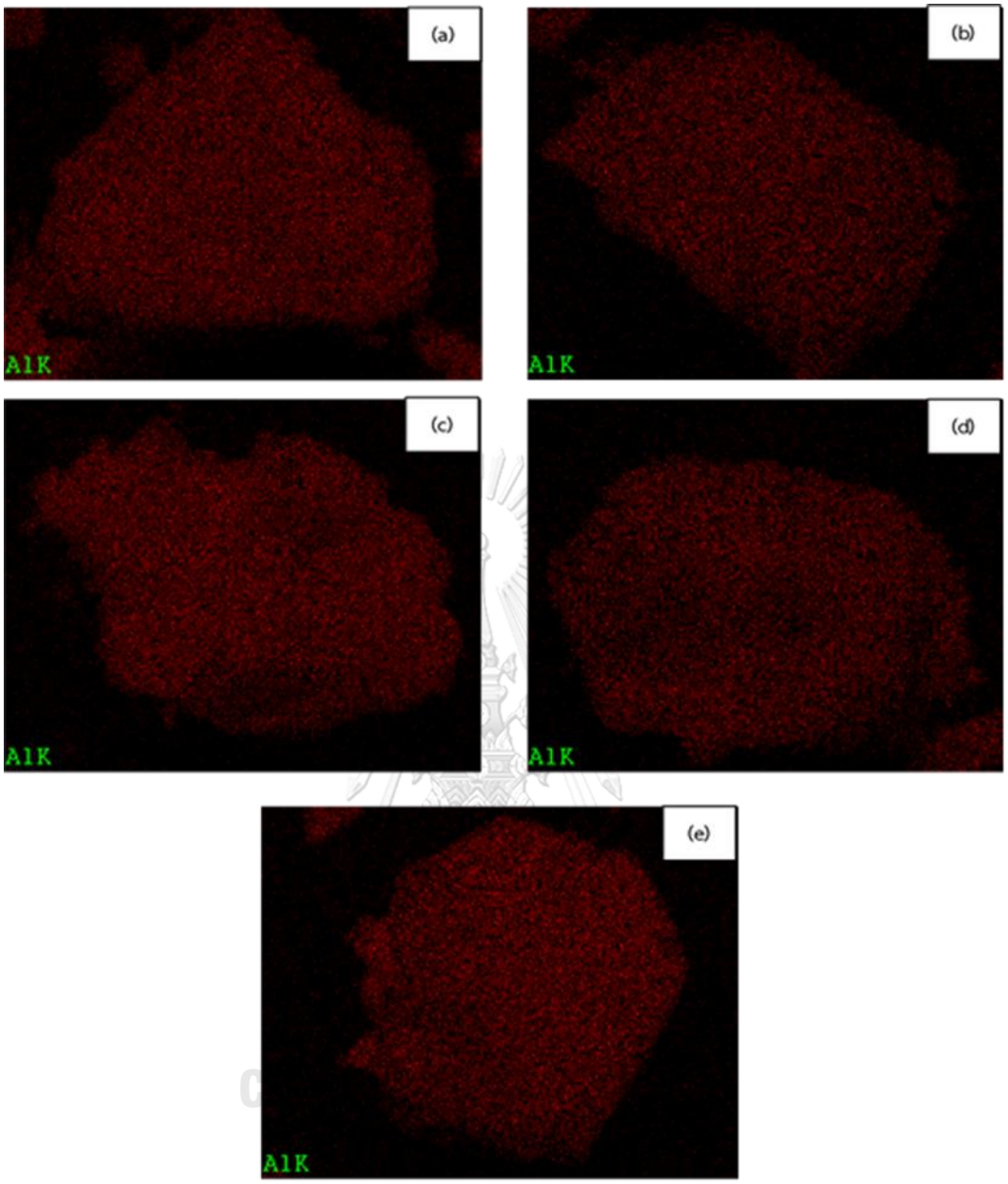

Figure 4.28 Al distribution obtained from EDX of (a) SC, (b) BS, (c) RS, (d) WH and (e) PA at 60X and 1.50kX magnification after immobilization

4.2.2.2 Characterization of cellulose-MMAO support with X-ray diffraction (XRD)

After immobilization of MMAO onto the cellulose support, XRD pattern was detected and shown in (**Figure 4.29, Figure 4.30** and **Figure 4.31**). The different biomass cellulose supports with immobilized MMAO presented the broad peak of XRD at 2θ equals 22.5°, which is similar to the characteristic XRD peak of cellulose before immobilization. It was similar to XRD pattern of MCC after immobilization with MMAO, which was shown in (**Figure 4.29**). It indicated that Al contents of MMAO were in the highly dispersed form on various cellulose supports.

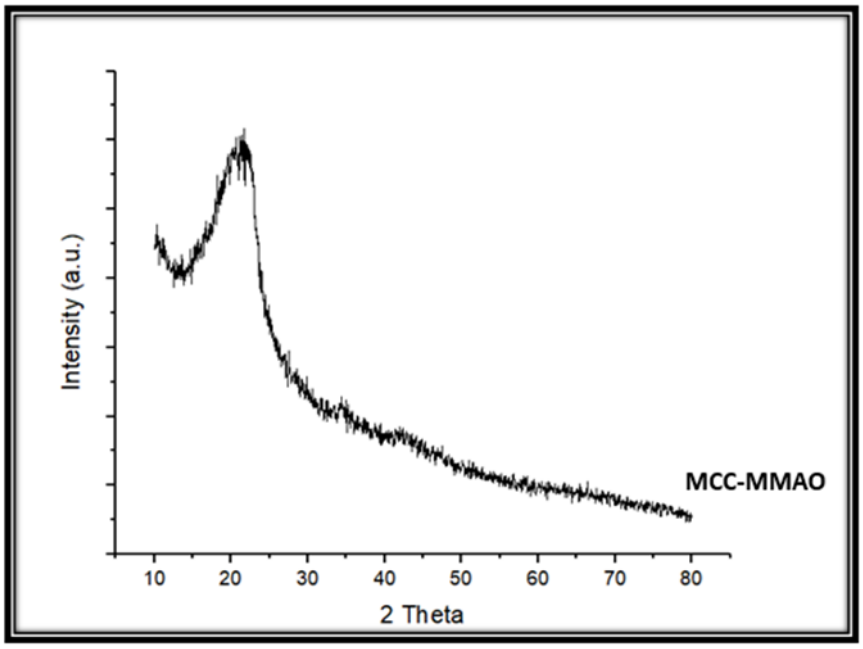

Figure 4.29 XRD pattern of MCC after immobilization

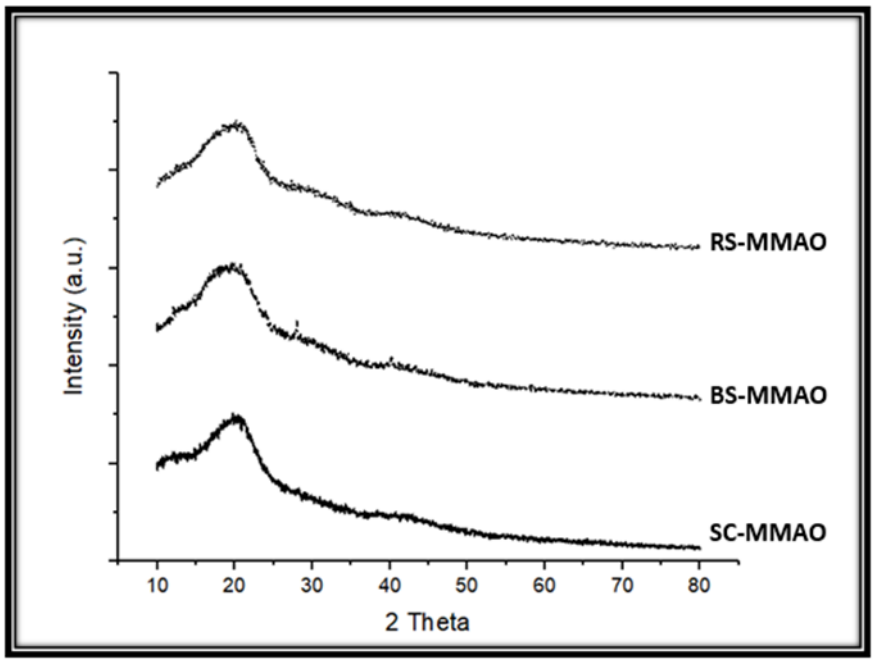

Figure 4.30 XRD patterns of biomass cellulose after immobilization (1; SC, BS, and RS)

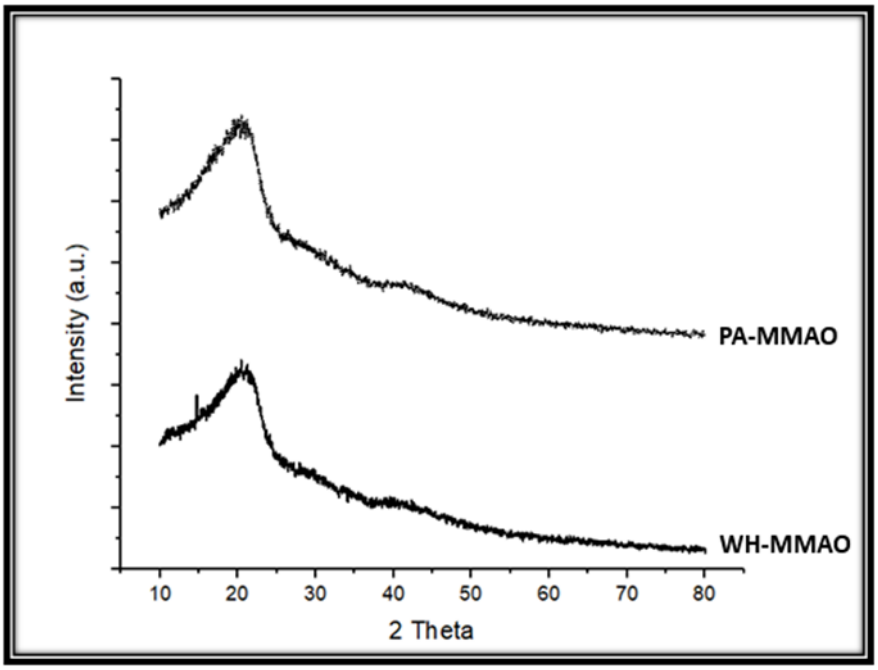

Figure 4.31 XRD patterns of biomass cellulose after immobilization (2; WH, and PA)

4.2.2.3 Characterization of cellulose-MMAO support with Fourier transform infrared spectrophotometer (FT-IR)

The comparison between different biomass cellulose supports before and after immobilization with MMAO was again investigated using FT-IR to analyze the functional group and bonding form. They presented the changing of broad band at the range of wavenumber between 3340-3330 cm^{-1} in all biomass supports after immobilization by MMAO. They still had only slight the hydroxyl groups in their structures when compared to MCC. The FT-IR spectra after immobilization with MMAO are shown in (**Figure 4.32** and **Figure 4.33**).

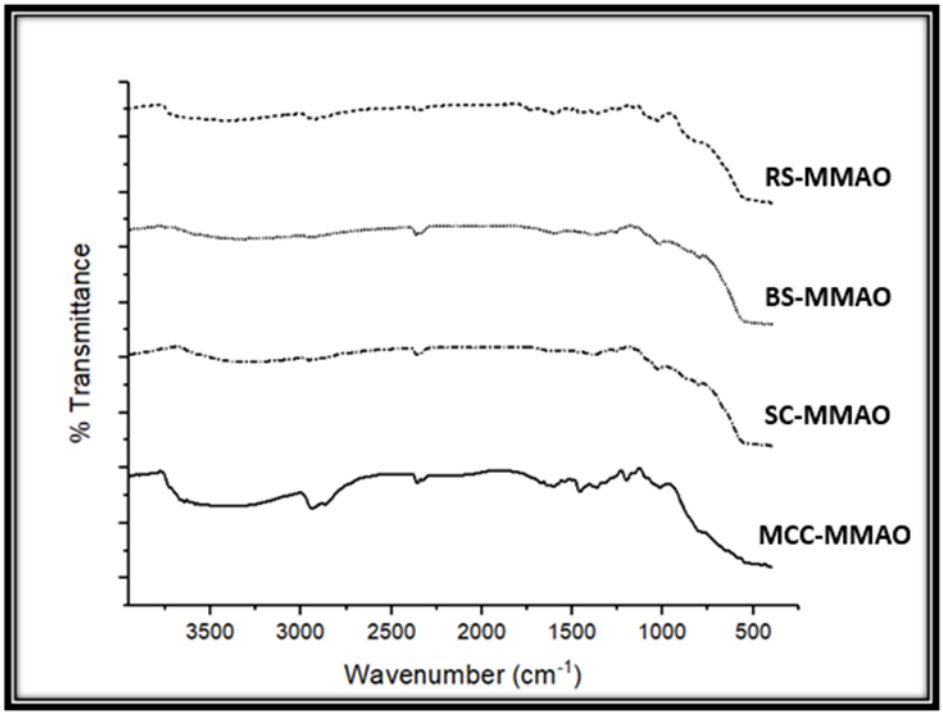

Figure 4.32 FT-IR spectra of SC, BS, and RS compared to MCC after immobilization

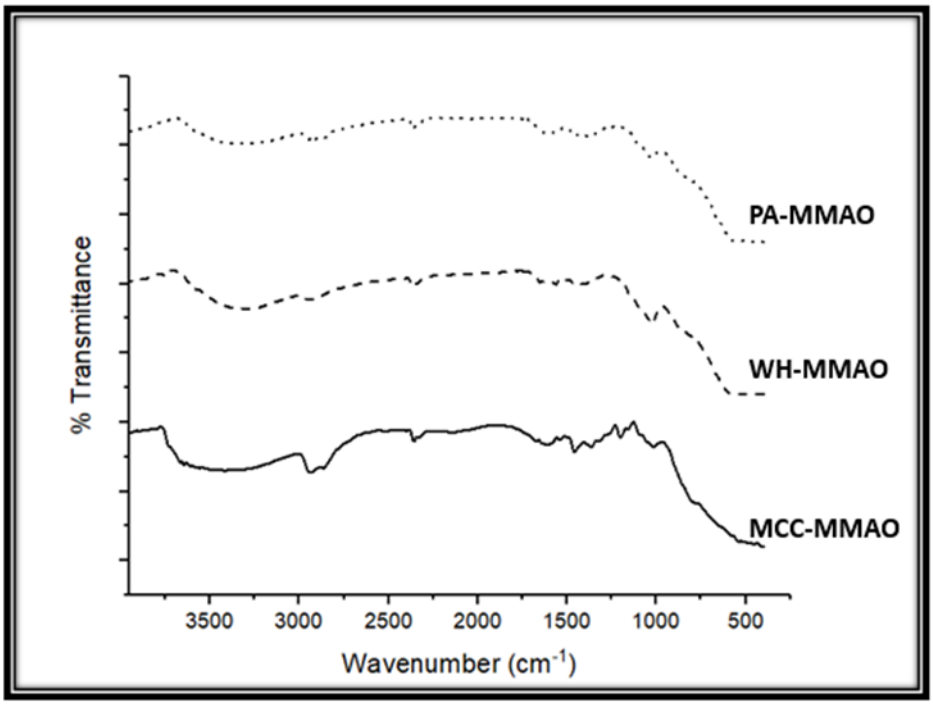

Figure 4.33 FT-IR spectra of WH and PA compared to MCC after immobilization

4.2.2.4 Characterization of cellulose-MMAO support with X-ray photoelectron spectroscopy (XPS)

To consider the binding energy (BE) and a large number of Al on cellulose support surfaces, X-ray photoelectron spectroscopy (XPS) was also used on this purpose in part 2. Actually, the binding energy of Al in orbital 2p core level of $[Al]_{MMAO}$ was determined in different biomass cellulose-supported MMAO as shown in (**Figure 4.34** and **Table 4.6**).

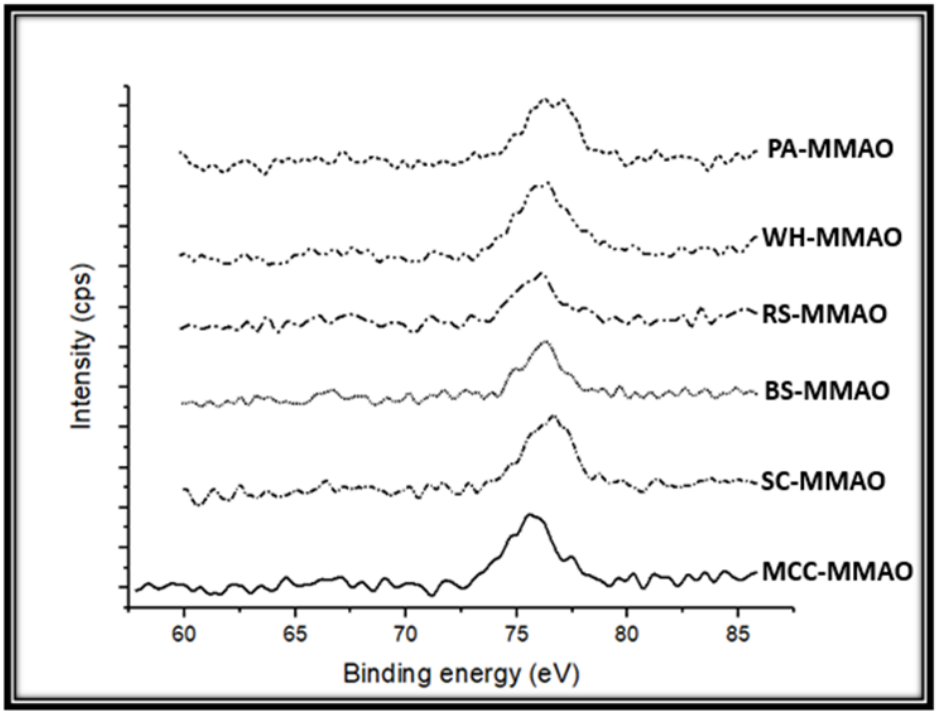

Figure 4.34 XPS spectra of biomass cellulose supports after immobilization

As seen for the binding energy of Al^{3+} in each different biomass cellulose supports compared with Al^{3+} in MMAO, it indicated that, there is no significant change in oxidation state of $[Al]_{MMAO}$ initiated in different biomass cellulose supports, including SC, BS, RS, WH and PA. The highest quantity of Al^{3+} at support surface is appeared in PA followed by SC, WH, MCC, RS and BS, respectively.

Table 4.6 XPS data of Al 2p core level of biomass cellulose supports

Samples	Binding Energy of Al^{3+} (eV)	Amount of Al^{3+} at surface (%wt.)
MMAO [39]	74.7	28.50
MCC-MMAO	75.6	34.76
SC-MMAO	74.4	44.97
BS-MMAO	75.9	23.50
RS-MMAO	76.0	26.42
WH-MMAO	80.0	36.10
PA-MMAO	75.3	54.66

4.2.2.5 Inductively coupled plasma (ICP)

Inductively coupled plasma (ICP) was also used to conclude the amount of Al in different biomass cellulose supports in bulk. The ICP result is shown in (**Table 4.7**). It was found that there is the highest quantity of Al in cellulose support in WH, following by PA, BS, SC, MCC, and RS, respectively.

Table 4.7 The Al composition of biomass cellulose supports after immobilization

Sample	Amount of Al on support (%wt.)
MCC-MMAO	19.71
SC-MMAO	19.76
BS-MMAO	24.05
RS-MMAO	14.56
WH-MMAO	34.10
PA-MMAO	25.74

As referred to part 1, in summary, after characterization of different biomass cellulose support before and after immobilization of MMAO, it was found that in bulk cellulose support contained small quantity of Al as observed by ICP. At cellulose surface, there is Al^{3+} distributed on the support surface without changing the oxidation state of Al from XPS, suggesting that MMAO did not decompose. The determining of crystalline structure before and after immobilization of MMAO in cellulose support using XRD, showed that after immobilization of MMAO on support, it was in the highly dispersed forms, which cannot be detected with XRD (the crystallite size is less than 3 nm) as shown in (**Figure 4.35**).

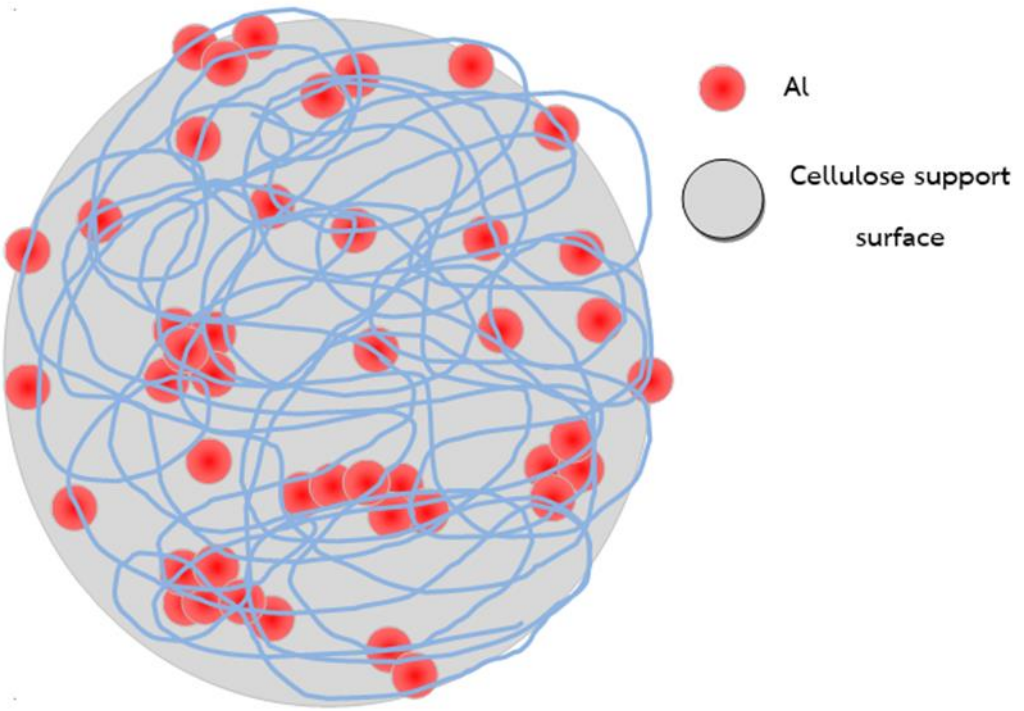

Figure 4.35 Scheme of Al dispersion on external surface of biomass cellulose support after immobilization of MMAO

4.2.3 Characterization of polymer

4.2.3.1 Characterization of polymer with scanning electron microscopy (SEM)

The morphology of obtained polyethylene from heterogeneous systems as measured by SEM is shown in (**Figure 4.36** and **Figure 4.37**). Determining the heterogeneous system, it appeared the slightly similar morphologies of polymer obtained from different biomass celluloses, including SC, BS, RS, WH and PA as supports. However, they were also different. The observed polyethylene from SC, RS, WH, and PA exhibited the larger porosity particles than that from BS and polyethylenes obtained with the different biomass celluloses display more open structure.

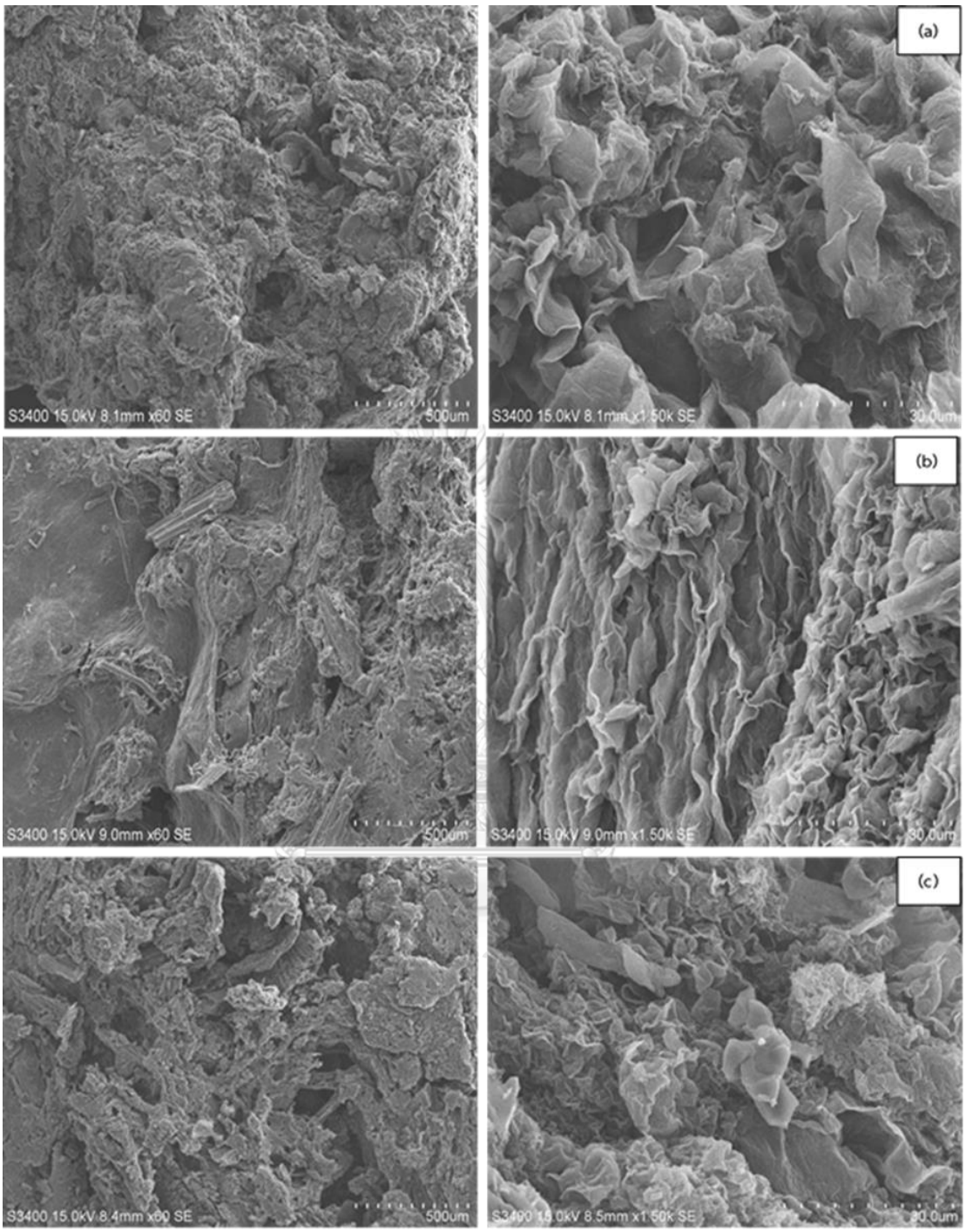

Figure 4.36 SEM micrographs of polyethylene produced via heterogeneous system (a) PE-SC, (b) PE-BS, (c) PE-RS, (d) PE-WH and (e) PE-PA at 60X and 1.50kX magnification

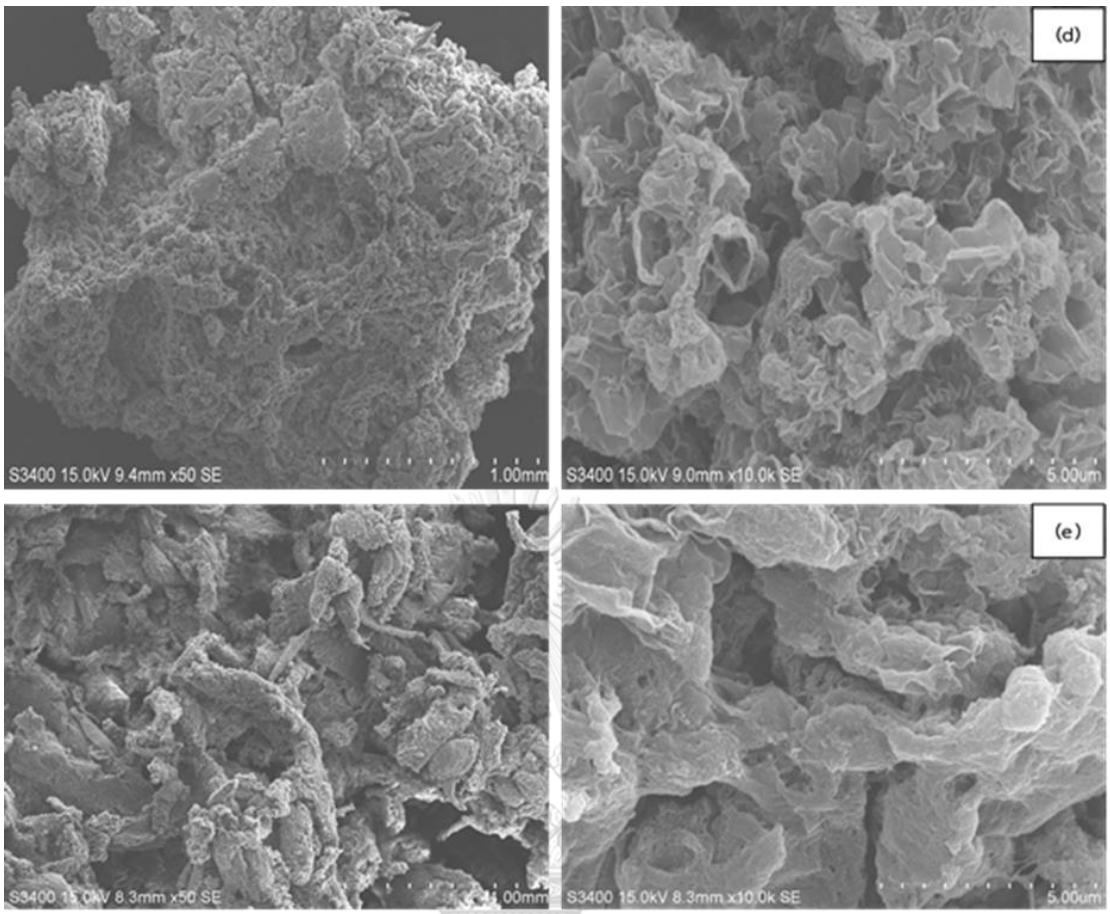

Figure 4.37 SEM micrographs of polyethylene produced via heterogeneous system (d) PE-WH and (e) PE-PA at 60X and 10.0kX magnification

4.2.3.2 Characterization of polymer with X-ray diffraction (XRD)

As referred to part 1, the obtained polyethylenes were characterized using XRD technique. **Figure 4.38** shows the XRD patterns of polyethylenes synthesized with different cellulose supports compared to polyethylene from commercial cellulose. It indicates that, the XRD patterns for all produced polyethylene were similar. All samples exhibited two peaks at 2θ of the orthorhombic crystalline form in polyethylene at 21.4° and 24.1° [40].

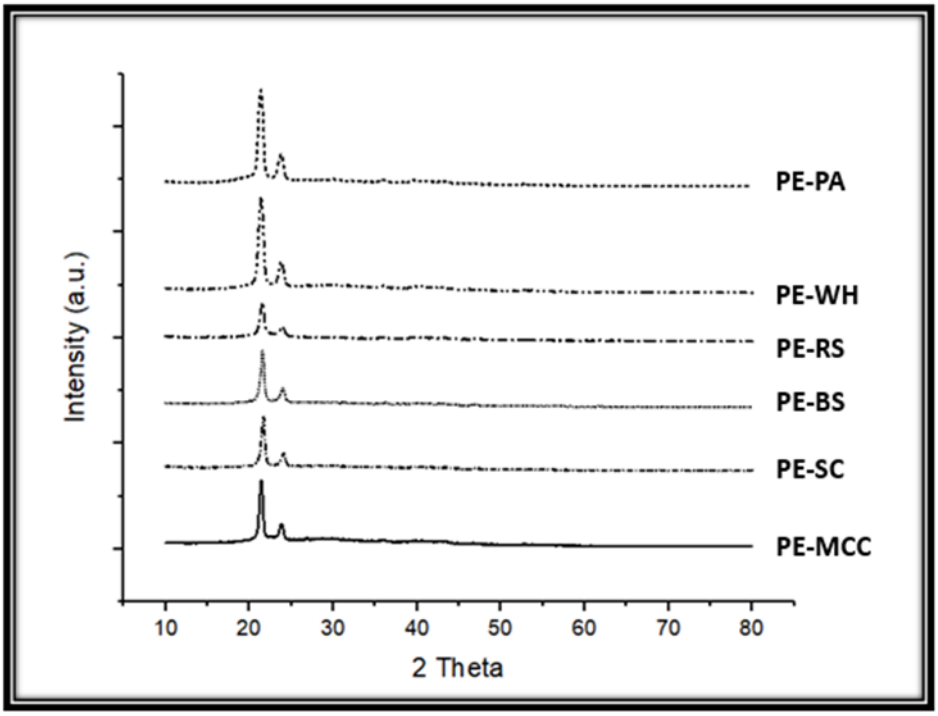

Figure 4.38 XRD patterns of polyethylene produced via heterogeneous system using biomass cellulose as support compared to commercial cellulose

4.2.3.3 Characterization of polymer with thermal gravimetric analysis-differential scanning calorimetry (TGA-DSC)

To determine the stability of produced polyethylene from heterogeneous system using different biomass cellulose as support for metallocene catalyst, TGA technique was carried out as shown in **Figure 4.39**. The TGA profile exhibits degree of thermal stability in terms of residual weight (%) and temperature (^{o}C). It was found that the degradation temperature at 5% weight loss of polyethylene from heterogeneous system, including PE-MCC PE-SC, PE-BS, PE-RS, PE-WH and PE-PA equal to 118^{o}C, 334^{o}C, 276^{o}C, 234^{o}C, 435^{o}C, and 304^{o}C, respectively. PE-WH exhibited the strongest thermal stability, following by PE-SC, PE-PA, PE-BS, PE-RS and PE-MCC. In addition, the DTA profile was also implemented as shown in **Figure 4.40**, it appeared percent weight loss of organic volatile components at temperature range between 210 and 500 ^{0}C and percent weight loss of moisture at 100 ^{0}C.

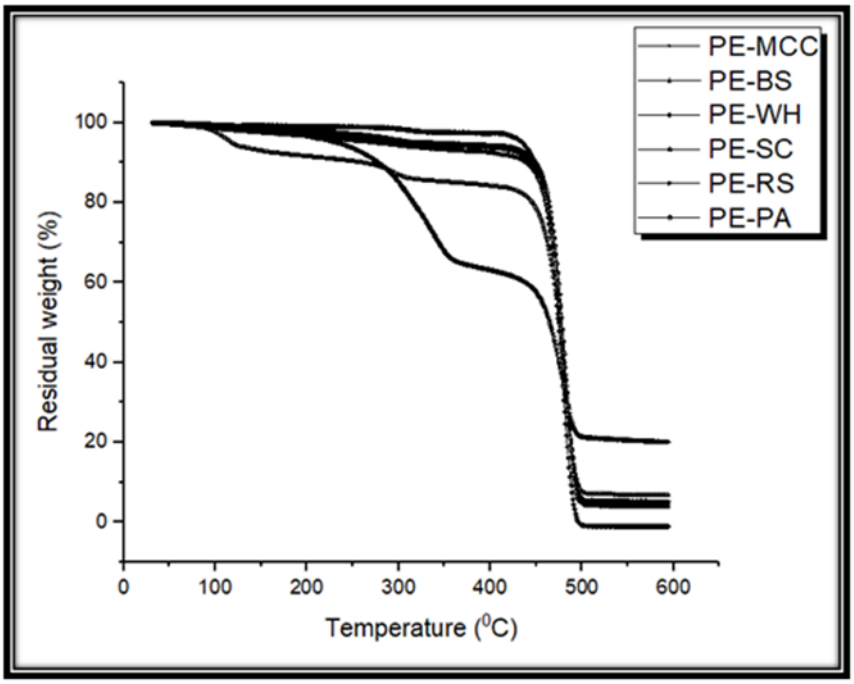

Figure 4.39 TGA profiles of polyethylenes produced via heterogeneous system using biomass cellulose as support compared to commercial cellulose

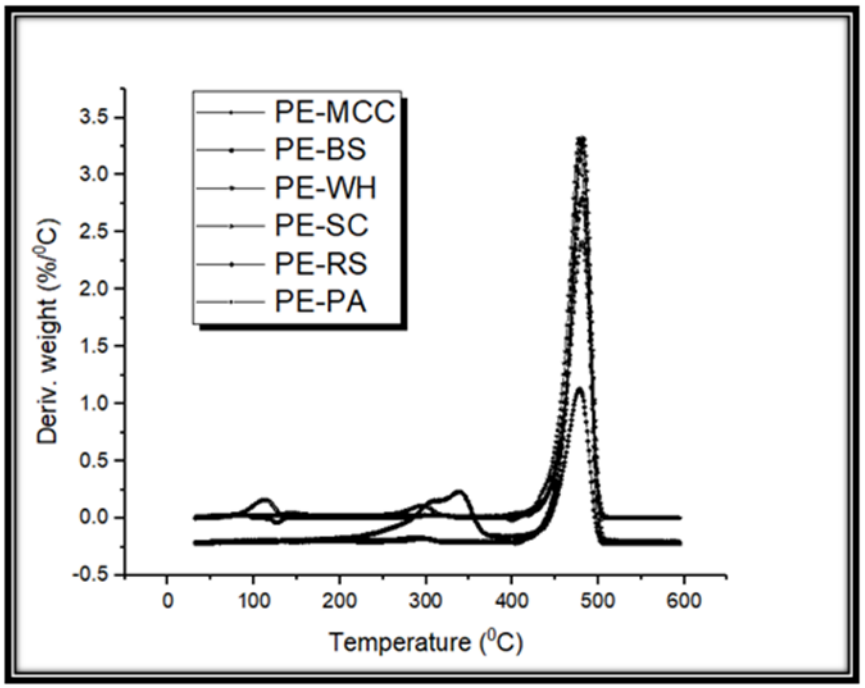

Figure 4.40 DTA profiles of polyethylenes produced via heterogeneous system using biomass cellulose as support compared to commercial cellulose

The obtained polyethylenes from heterogeneous system were determined by differential scanning calorimeter (DSC). The melting enthalpy and melting temperature of the polymer are listed in (**Table 4.8**) and the DSC curves are shown in (**Figure C-1**), (**Figure C-5**), (**Figure C-6**), (**Figure C-7**) (**Figure C-8**) and (**Figure C-9**), for MCC, SC, BS, RS, WH, and PA, respectively as referred to **Appendix C**. For this heterogeneous system, it was seen that there was no significant change in the melting temperature for all produced polyethylenes. The melting temperature of produced polyethylenes was in the range between (121 and 128°C). On the contrary, it was observed that produced polyethylenes with addition of cellulose exhibited different crystallinity. The highest crystallinity was obtained in PE-SC, following by PE-BS, PE-WH, PE-PA, PE-MCC, and PE-RS, respectively.

Table 4.8 Melting and crystallization behaviors

Samples	Melting Temperature, T_m [a] (°c)	ΔH_{exp} [b] (J/g)	X_c [c] (%)
PE-MCC	124	164.4	57.5
PE-SC	128	196.2	68.6
PE-BS	128	180.0	62.9
PE-RS	127	85.5	29.9
PE-WH	123	178.0	62.24
PE-PA	121	169.9	59.41

[a] Melting temperature (T_m) was obtained from DSC measurement.

[b] Heat of fusion (ΔH_{exp}) was obtained from DSC measurement.

[c] Crystallinity (X_c) was calculated from this equation; %crystallinity = ($\Delta H_{sample}/\Delta H_{100\%}$ crystallinity)x100, the $\Delta H_{100\%}$ crystallinity of polyethylene is 286 J/g.

4.2.4 Ethylene consumption

As referred to part 1, the ethylene consumption rate (ml/min) in part 2 was also recorded as shown in **Figure 4.41**. It indicated that produced polyethylene in homogeneous system exhibited the steady rate since the first minute to the last minute in overall time of 15 minutes. For produced polyethylene in heterogeneous system, they showed the irregular rate since the first minute. Therefore, no deactivation of catalysts was observed in all runs.

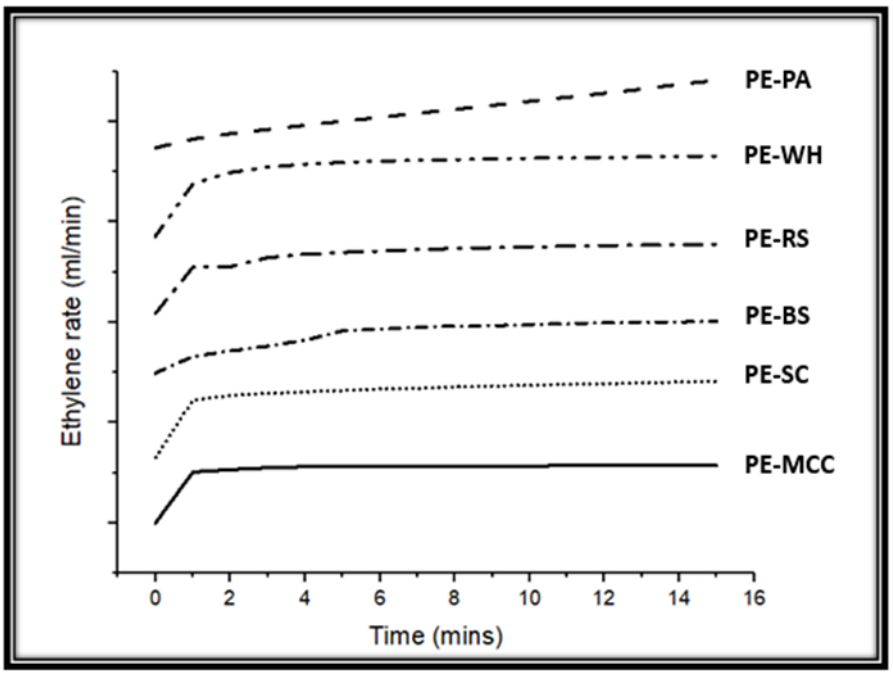

Figure 4.41 The ethylene consumption of polyethylene produced via heterogeneous system using biomass cellulose compared to commercial cellulose

4.2.5 Catalytic activity

The reported catalytic activity of catalysts in ethylene polymerization following heterogeneous system using different biomass cellulose as support for metallocene catalyst, is shown in **Table 4.9**. In addition to **Table 4.9**, the produced polyethylene from pineapple leaf (PA) displayed the highest catalytic activity and polymer yield following by PE-WH, PE-RS, PE-SC, PE-BS, and PE-MCC respectively.

Table 4.9 The catalytic activity of catalysts via heterogeneous system using biomass cellulose as support compared to commercial cellulose

Samples	Polymer yield[a] (g)	Catalytic activity[b] (kg of pol/mol Zr h)
PE-MCC	0.4943	238
PE-SC	0.5980	288
PE-BS	0.5487	263
PE-RS	0.7290	351
PE-WH	0.9054	436
PE-PA	1.0406	502

[a] The polymerization time was 15 min.

[b] Activities were measured at polymerization temperature of 70 ^{o}C, [ethylene] = 0.018 mole, $[Al]_{MMAO}/[Zr]_{Cat}$ = 1135, in toluene with total volume = 30 mL, and $[Zr]_{Cat}$ =5 x 10^{-5} M.

CHAPTER 5
CONCLUSION AND RECOMMENDATIONS

5.1 CONCLUSION

In the first part, the various celluloses, including microcrystalline cellulose (MCC, commercial cellulose), and two types of bacteria cellulose from different natural biomass were used as support for metallocene catalyst in *in situ* polymerization reaction compared to polyethylene obtained from the homogeneous system. It was found that polyethylene produced from homogeneous system displayed the highest activity due to the larger particle size of cellulose, it may slightly interact with MMAO resulting in reduced catalytic activity. In contrast, using two kinds of bacteria cellulose tended to increase crystallinity because bacteria celluloses have similar crystalline structure like microcrystalline cellulose, which may increase the order of polyethylene structure, whereas the melting temperature of all polyethylene was in range between (122-125 ^{o}C) indicating no significant change.

In the second part, the different types of biomass celluloses, including biomass cellulose from sugarcane, leaf sheath of banana tree, rice straw, water hyacinth and pineapple leaf were also used as support for metallocene catalyst in *in situ* polymerization reaction compared to commercial cellulose, namely microcrystalline cellulose (MCC) from the first part. It indicated the produced polyethylene using pineapple leaf as support exhibited the highest activity, and produced polyethylene from different biomass cellulose presented the higher activity than commercial cellulose. On the contrary, it was displayed that produced polyethylenes with addition of cellulose presented different crystallinity due to the irregular shape in each different biomass celluloses compared to cellulose commercial, different biomass celluloses, excepting for the obtained polyethylene using rice straw as support, were in the same range of crystallinity presenting the semi-crystalline form.

5.2 RECOMMENDATION

- Investigating of the other type of organic support, such as starch should be applied.
- Effect of calcination temperature should be investigated.
- Effect of another cocatalyst should be studied.

REFERENCES

1. Mitani, M., et al., *FI Catalysts: new olefin polymerization catalysts for the creation of value-added polymers.* The Chemical Record, 2004. 4(3): p. 137-158.
2. Tritto, I., et al., *Dimethylzirconocene– Methylaluminoxane Catalyst for Olefin Polymerization: NMR Study of Reaction Equilibria.* Macromolecules, 1997. 30(5): p. 1247-1252.
3. Cho, H.S., J.S. Chung, and W.Y. Lee, *Control of molecular weight distribution for polyethylene catalyzed over Ziegler–Natta/Metallocene hybrid and mixed catalysts.* Journal of Molecular Catalysis A: Chemical, 2000. 159(2): p. 203-213.
4. Baran, N.Y., T. Baran, and A. Menteş, *Fabrication and application of cellulose Schiff base supported Pd (II) catalyst for fast and simple synthesis of biaryls via Suzuki coupling reaction.* Applied Catalysis A: General, 2017. 531: p. 36-44.
5. Reddy, K.R., et al., *Cellulose supported palladium (0) catalyst for Heck and Sonogashira coupling reactions.* Journal of Molecular Catalysis A: Chemical, 2006. 252(1): p. 12-16.
6. Hamielec, A.E. and J.B. Soares, *Polymerization reaction engineering—metallocene catalysts.* Progress in polymer science, 1996. 21(4): p. 651-706.
7. Wannaborwon, M., *COPOLYMERIZATION OF ETHYLENE/1-OLEFIN WITH TITANOCENE AND ZIRCONOCENE CATALYSTS IN HOMOGENEOUS SYSTEM*, in *Chemical Engineering*. 2013, Chulalongkorn University: Chulalongkorn University.
8. Wilkinson, G., and Birmingham, I.M., Journal of the American Chemical Society 76, 1954: p. 4281.
9. Fisher, E.O., Journal of AngewandteChemie 22, 1962: p. 620.
10. Kaminsky, W. and F. Renner, *High melting polypropenes by silica-supported zirconocene catalysts.* Macromolecular Rapid Communications, 1993. 14(4): p. 239-243.

11. Desharun, C., B. Jongsomjit, and P. Praserthdam, *Study of LLDPE/alumina nanocomposites synthesized by insitu polymerization with zirconocene/d-MMAO catalyst.* Catalysis Communications, 2008. 9(4): p. 522-528.
12. Wannaborworn, M., P. Praserthdam, and B. Jongsomjit, *LLDPE synthesis via SiO 2–Ga-supported zirconocene/MMAO catalyst.* Journal of Industrial and Engineering Chemistry, 2012. 18(1): p. 373-377.
13. Shlieout, G., K. Arnold, and G. Müller, *Powder and mechanical properties of microcrystalline cellulose with different degrees of polymerization.* AAPS PharmSciTech, 2002. 3(2): p. 45-54.
14. Thomas, C. and Y. Pourcelot, *Preformulation of five commercial celluloses in drug development: rheological and mechanical behaviour.* Drug development and industrial pharmacy, 1993. 19(15): p. 1947-1964.
15. Carlin, B.A., *Direct compression and the role of filler-binders.* Pharmaceutical dosage forms: tablets, 2008. 2: p. 173-216.
16. Trache, D., et al., *Microcrystalline cellulose: Isolation, characterization and bio-composites application—A review.* International journal of biological macromolecules, 2016. 93: p. 789-804.
17. Albers, J., K. Knop, and P. Kleinebudde, *Brand-to-brand and batch-to-batch uniformity of microcrystalline cellulose in direct tableting with a pneumohydraulic tablet press.* Pharmazeutische Industrie, 2006. 68(12): p. 1420-1428.
18. Suzuki, T. and H. Nakagami, *Effect of crystallinity of microcrystalline cellulose on the compactability and dissolution of tablets.* European journal of pharmaceutics and biopharmaceutics, 1999. 47(3): p. 225-230.
19. Wannaborworn, M., P. Praserthdam, and B. Jongsomjit, *Observation of different catalytic activity of various* 1*-olefins during ethylene/*1*-olefin copolymerization with homogeneous metallocene catalysts.* Molecules, 2011. 16(1): p. 373-383.
20. Zhang, F., et al., *Mechanochemical preparation and properties of a cellulose–polyethylene composite.* Journal of Materials Chemistry, 2002. 12(1): p. 24-26.

21. Jonas, R. and L.F. Farah, *Production and application of microbial cellulose.* Polymer Degradation and Stability, 1998. 59(1-3): p. 101-106.
22. Kirdponpattara, S., *PROPERTIES AND APPLICATIONS OF BACTERIAL CELLULOSE-ALGINATE COMPOSITE SPONGES*, in 2012. 2012, Chulalongkorn University: Chulalongkorn University.
23. Krajewska, B., *Application of chitin-and chitosan-based materials for enzyme immobilizations: a review.* Enzyme and microbial technology, 2004. 35(2): p. 126-139.
24. Kingkaew, J., et al., *Effect of molecular weight of chitosan on antimicrobial properties and tissue compatibility of chitosan-impregnated bacterial cellulose films.* Biotechnology and bioprocess engineering, 2014. 19(3): p. 534-544.
25. Shah, J. and R.M. Brown, *Towards electronic paper displays made from microbial cellulose.* Applied microbiology and biotechnology, 2005. 66(4): p. 352-355.
26. PEACOCK, A.J., *HANDBOOK OF POLYETHYLENE*. Stuctures, Properties, and Application. 2000, Baytown, Texas: Exxon Chemical Company.
27. Rodphon, P., *CHARACTERISTICS AND CATALYTIC PROPERTIES OF SILICA-SUPPORTED ZIRCONOCENE/MAO CATALYSTS FOR ETHYLENE POLYMERIZATION*, in *Chemical Engineering*. 2011, Chulalongkorn University: Chulalongkorn University.
28. Brent, S.A., *Plastics materials and processing.* Prentice Hall, 2000.
29. Bergstra, M.F., *Catalytic ethylene polymerization*. 2004: University of Twente.
30. Suttivutnarubet, C., *MODIFICATION OF CELLULOSE SUPPORTED ZIRCONOCENE CATALYST WITH BORON AND GALLIUM FOR ETHYLENE COPOLYMERIZATION*, in *Chemical Engineering*. 2012, Chulalongkorn University: Chulalongkorn University.
31. Jamnongphol, S., *PREPARATION OF SILICA COATED WITH POLYETHYLENE BY IN SITU POLYMERIZATION WITH METALLOCENE CATALYST*, in 2016. 2016, Chulalongkorn University: Chulalongkorn University.

32. Chu, K.J., J.B. Soares, and A. Penlidis, *Polymerization mechanism for in situ supported metallocene catalysts.* Journal of Polymer Science Part A: Polymer Chemistry, 2000. 38(3): p. 462-468.

33. Li, W., et al., *Disentangled UHMWPE/POSS nanocomposites prepared by ethylene in situ polymerization.* Polymer, 2014. 55(7): p. 1792-1798.

34. Malpass, D.B., *Introduction to industrial polyethylene: properties, catalysts, and processes*. Vol. 45. 2010: John Wiley & Sons.

35. Piel, C., *Polymerization of ethylene and ethylene-co-α-olefin; Investigations on short- and long-chain branching and structure-property relationships*, in *Department of Chemistry*. 2005, University of Hamburg: University of Hamburg.

36. Park, S., et al., *Cellulose crystallinity index: measurement techniques and their impact on interpreting cellulase performance.* Biotechnology for biofuels, 2010. 3(1): p. 10.

37. Fan, M., D. Dai, and B. Huang, *Fourier transform infrared spectroscopy for natural fibres*, in *Fourier Transform-Materials Analysis*. 2012, InTech.

38. Magalhaes, D.T., O. Do Coutto Filho, and F. Coutinho, *Ziegler-natta catalyst for ethylene and propylene polymerization supported on adducts of magnesium chloride with methyl and ethyl alcohols.* European Polymer Journal, 1991. 27(8): p. 827-830.

39. Ketloy, C., B. Jongsomjit, and P. Praserthdam, *Characteristics and catalytic properties of [t-BuNSiMe 2 Flu] TiMe 2/dMMAO catalyst dispersed on various supports towards ethylene/1-octene copolymerization.* Applied Catalysis A: General, 2007. 327(2): p. 270-277.

40. Kuo, S.-W., et al., *Syntheses and characterizations of in situ blended metallocence polyethylene/clay nanocomposites.* Polymer, 2003. 44(25): p. 7709-7719.

41. Chien, J.C. and T. Nozaki, *Ethylene–hexene copolymerization by heterogeneous and homogeneous Ziegler–Natta catalysts and the "comonomer" effect.* Journal of Polymer Science Part A: Polymer Chemistry, 1993. 31(1): p. 227-237.

42. Jongsomjit, B., S. Ngamposri, and P. Praserthdam, *Catalytic activity during copolymerization of ethylene and* 1*-hexene via mixed TiO2/SiO2-supported MAO with rac-Et [Ind]* 2*ZrCl*2 *metallocene catalyst.* Molecules, 2005. 10(6): p. 672-678.

APPENDIX

APPENDIX A: FOURIER TRANSFORM INFRARED SPECTROSCOPY

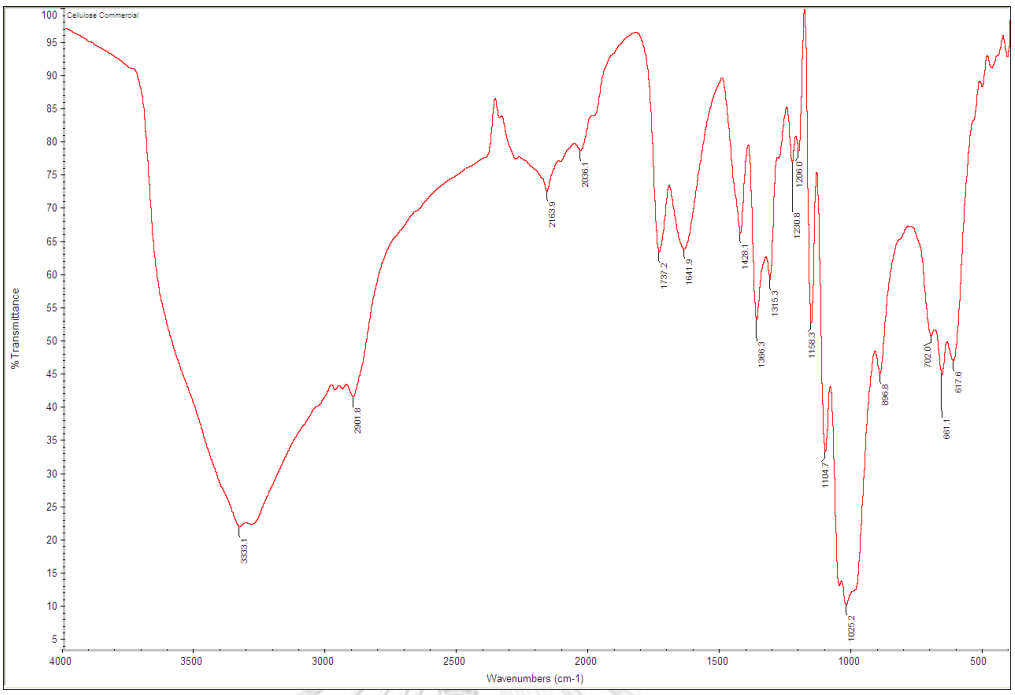

Figure A-1 FT-IR of MCC before immobilization with MMAO

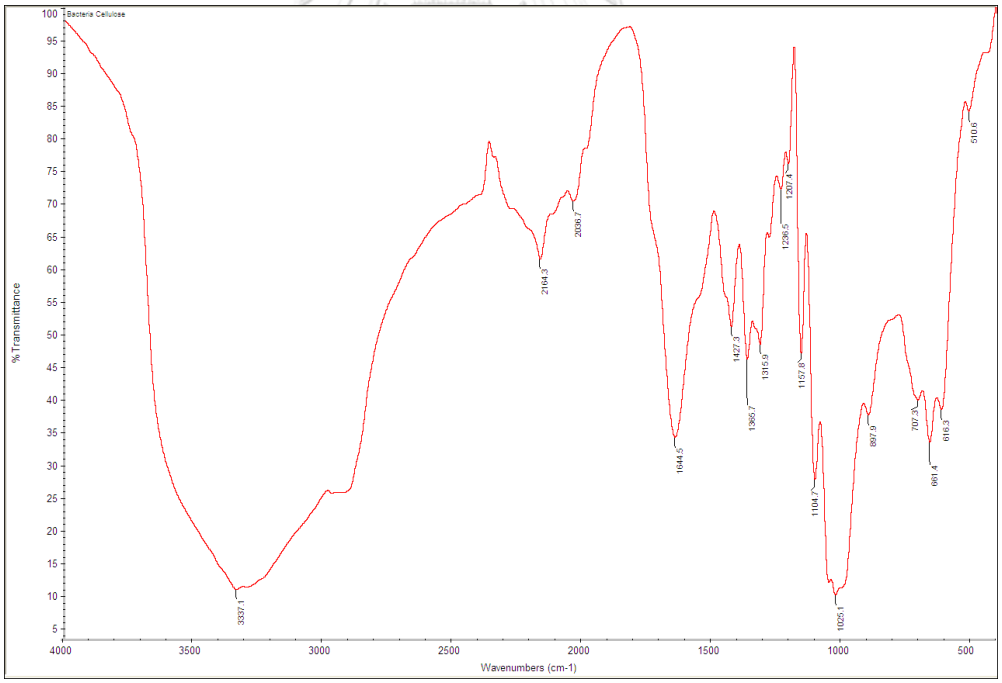

Figure A-2 FT-IR of BAC-P before immobilization with MMAO

Figure A-3 FT-IR of BAC-C before immobilization with MMAO

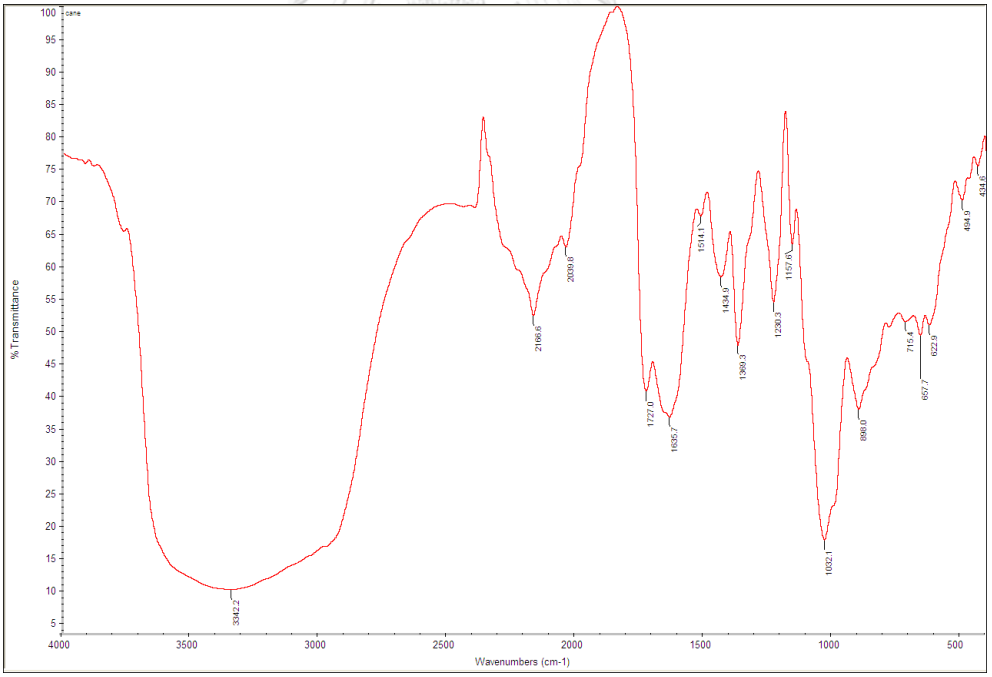

Figure A-4 FT-IR of SC before immobilization with MMAO

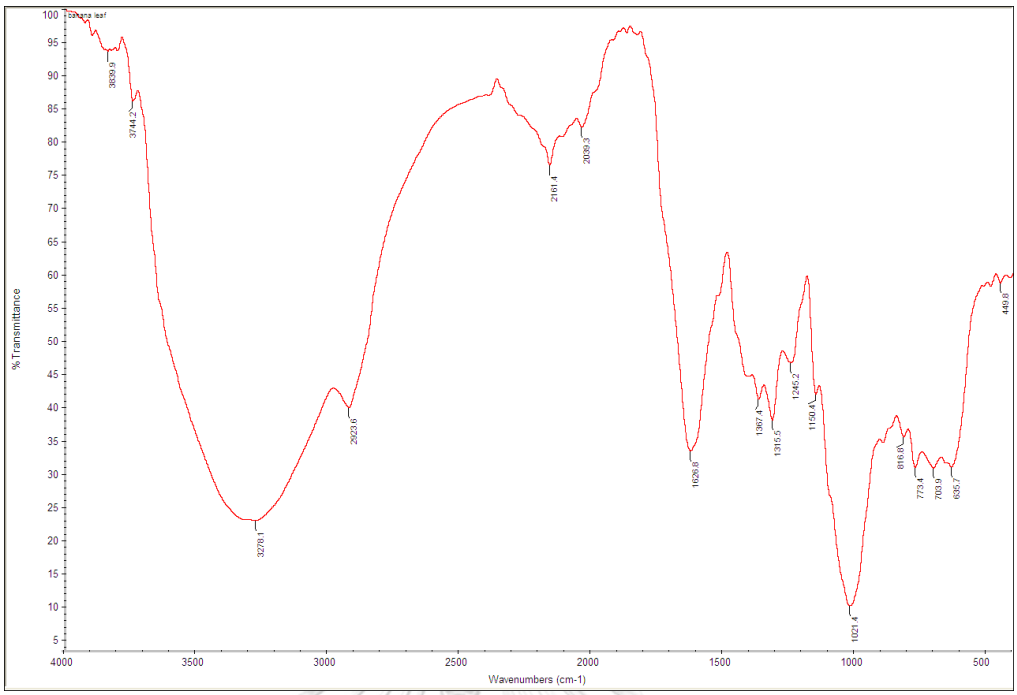

Figure A-5 FT-IR of BS before immobilization with MMAO

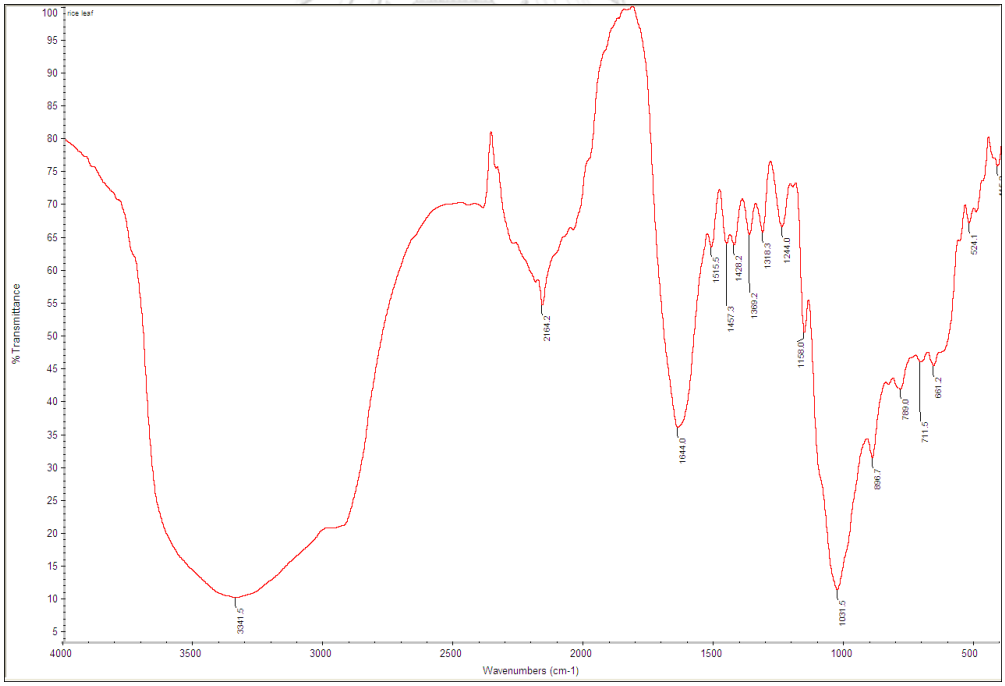

Figure A-6 FT-IR of RS before immobilization with MMAO

Figure A.-7 FT-IR of WH before immobilization with MMAO

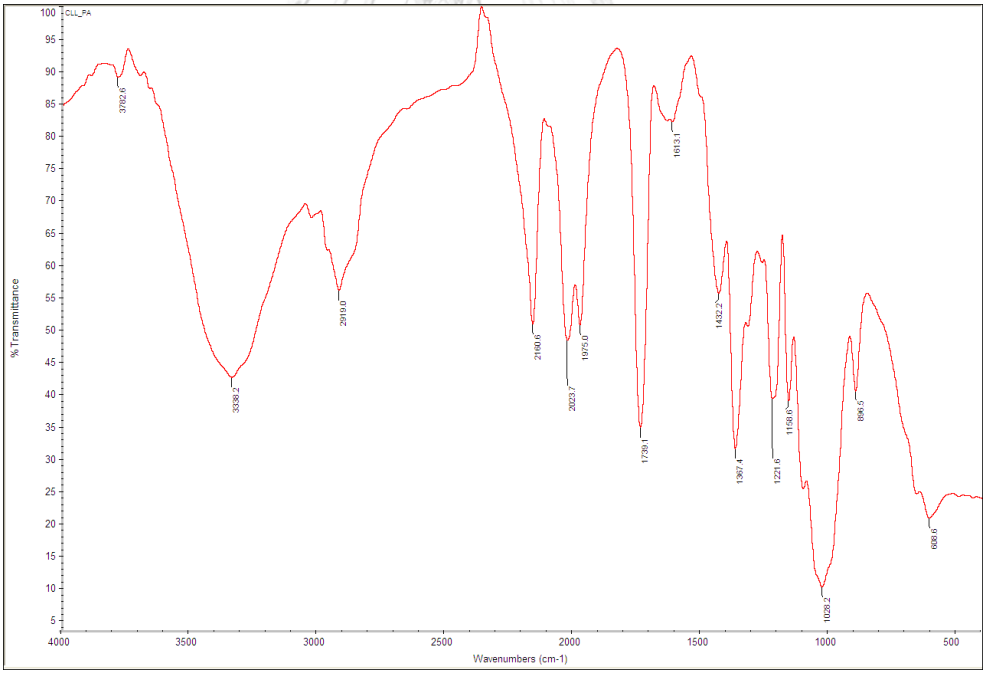

Figure A-8 FT-IR of PA before immobilization with MMAO

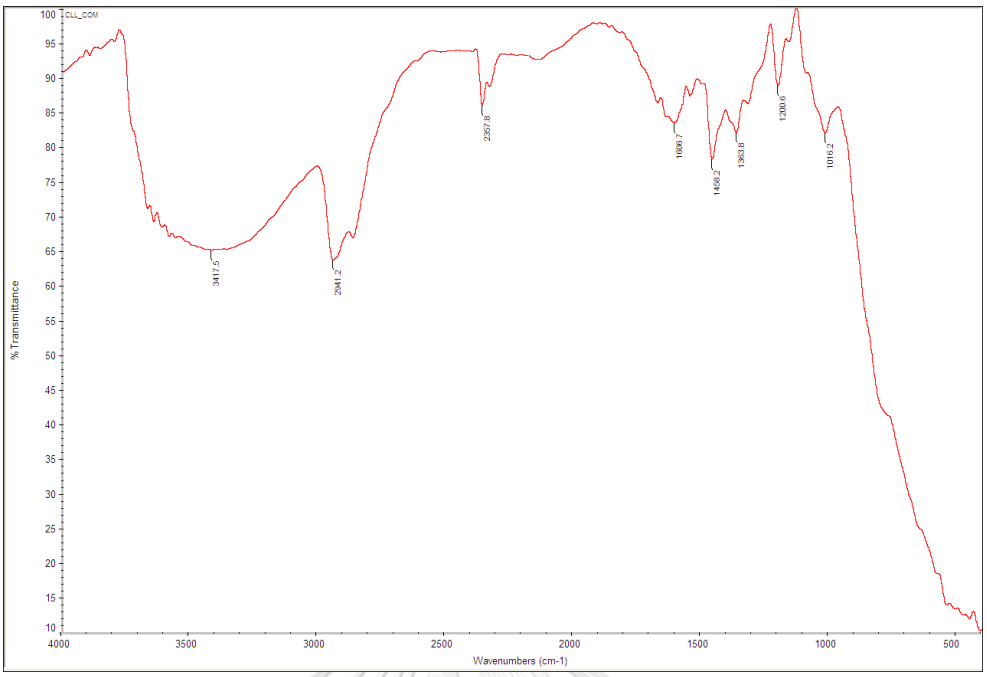

Figure A-9 FT-IR of MCC after immobilization with MMAO

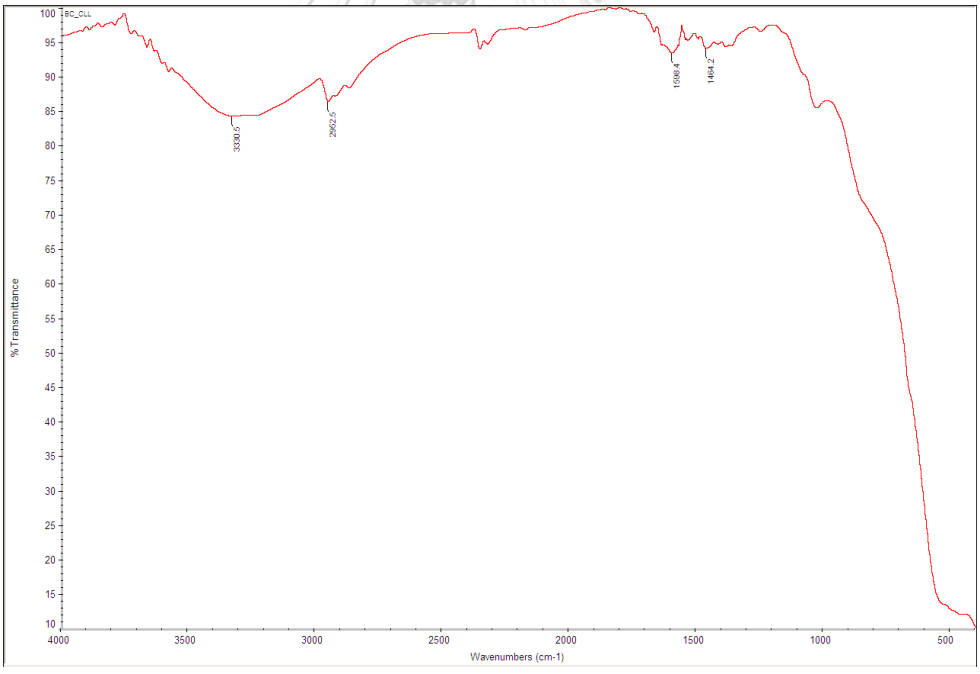

Figure A-10 FT-IR of BAC-P after immobilization with MMAO

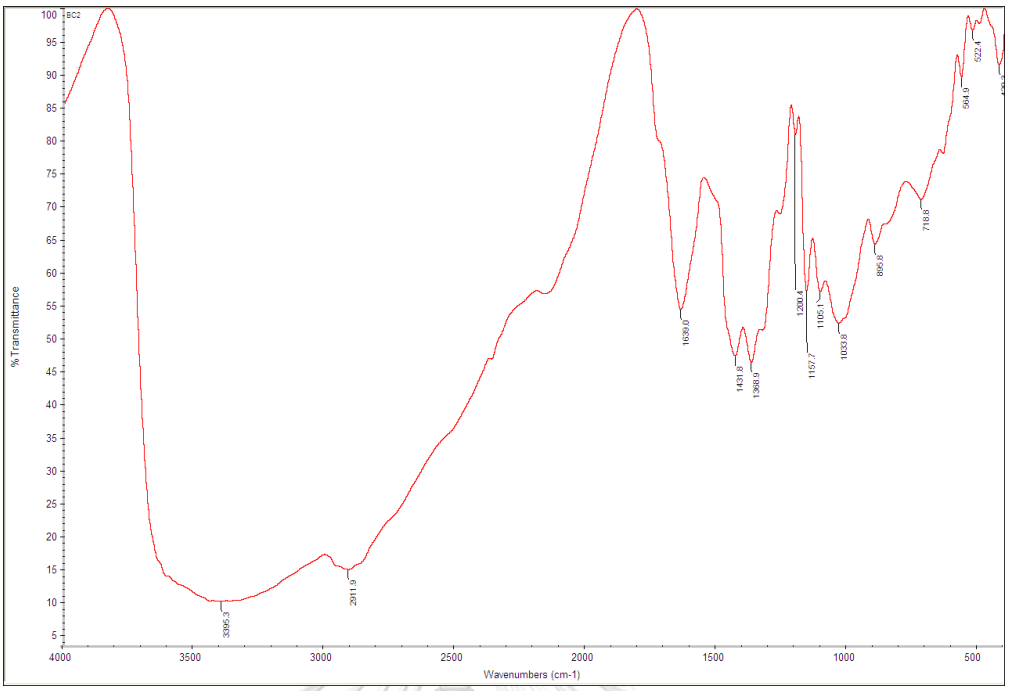

Figure A-11 FT-IR of BAC-C after immobilization with MMAO

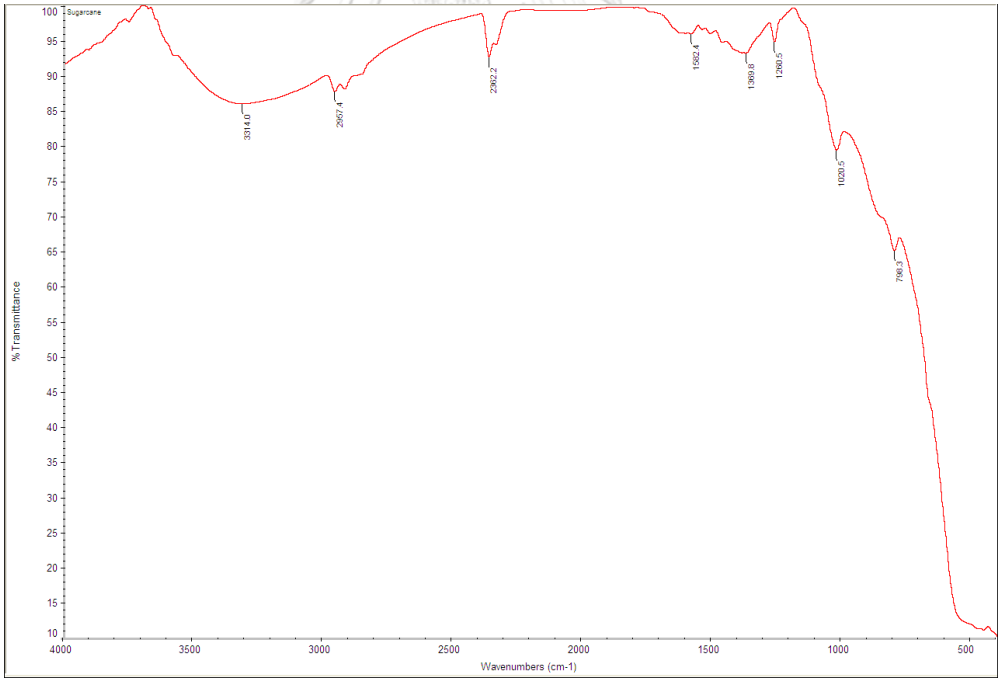

Figure A-12 FT-IR of SC after immobilization with MMAO

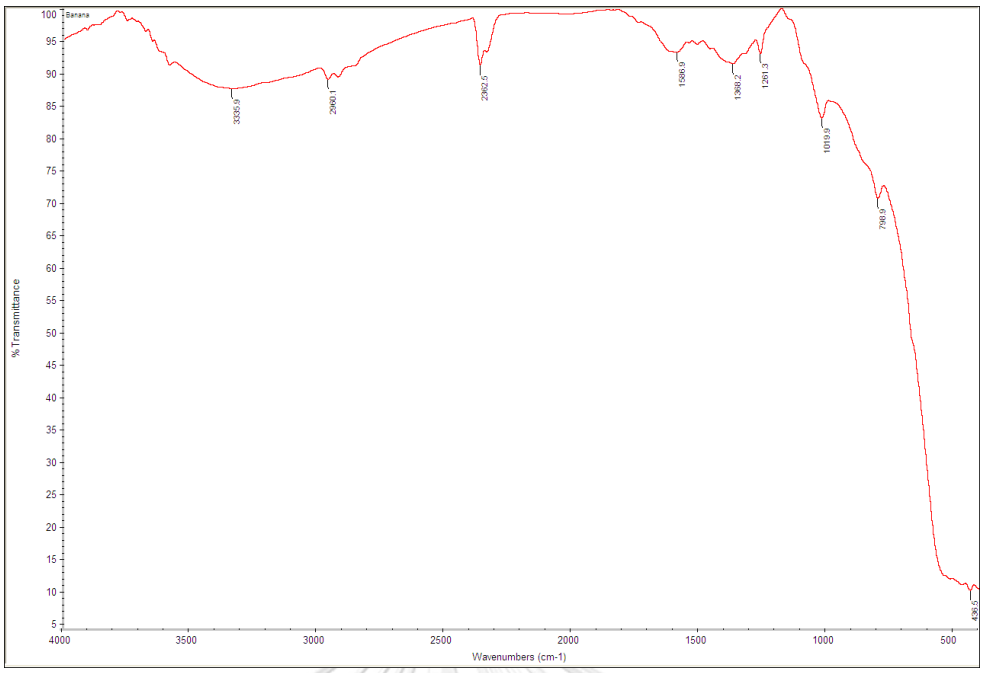

Figure A-13 FT-IR of BS after immobilization with MMAO

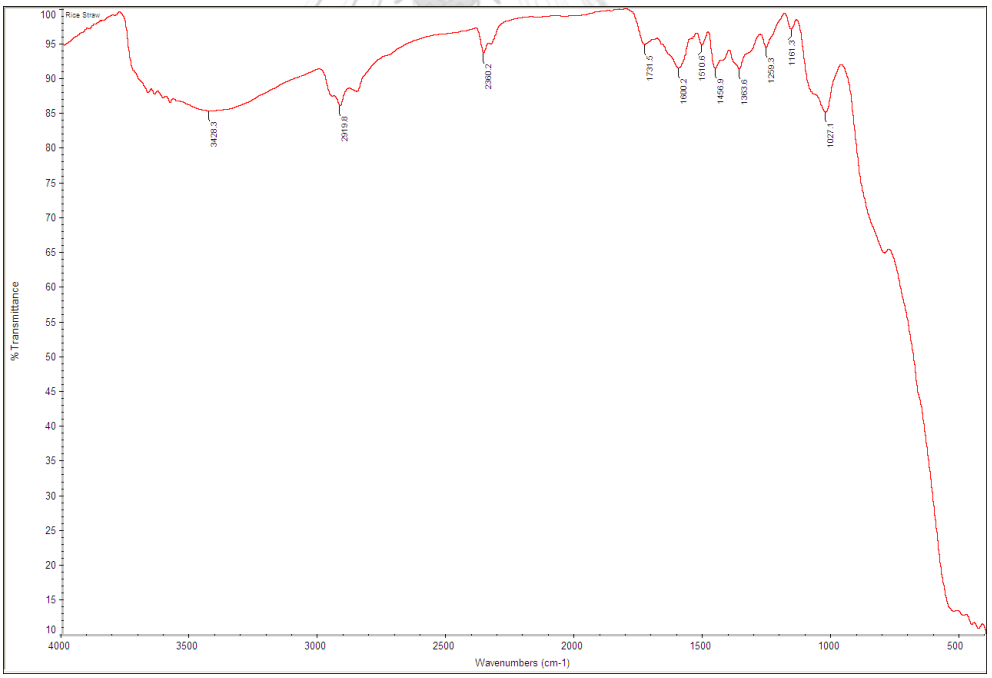

Figure A-14 FT-IR of RS after immobilization with MMAO

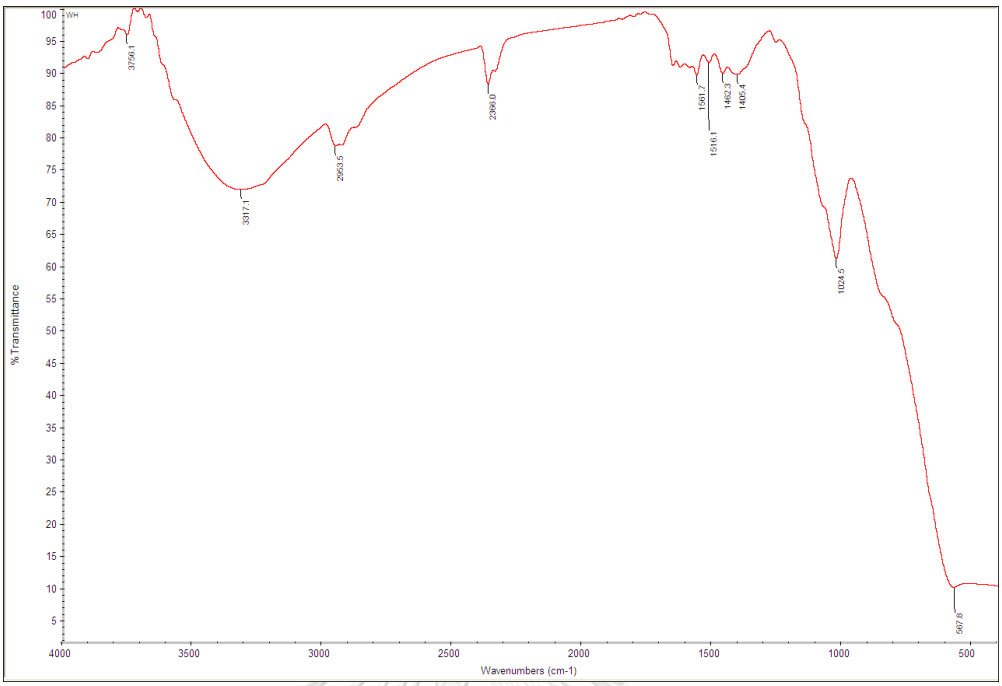

Figure A-15 FT-IR of WH after immobilization with MMAO

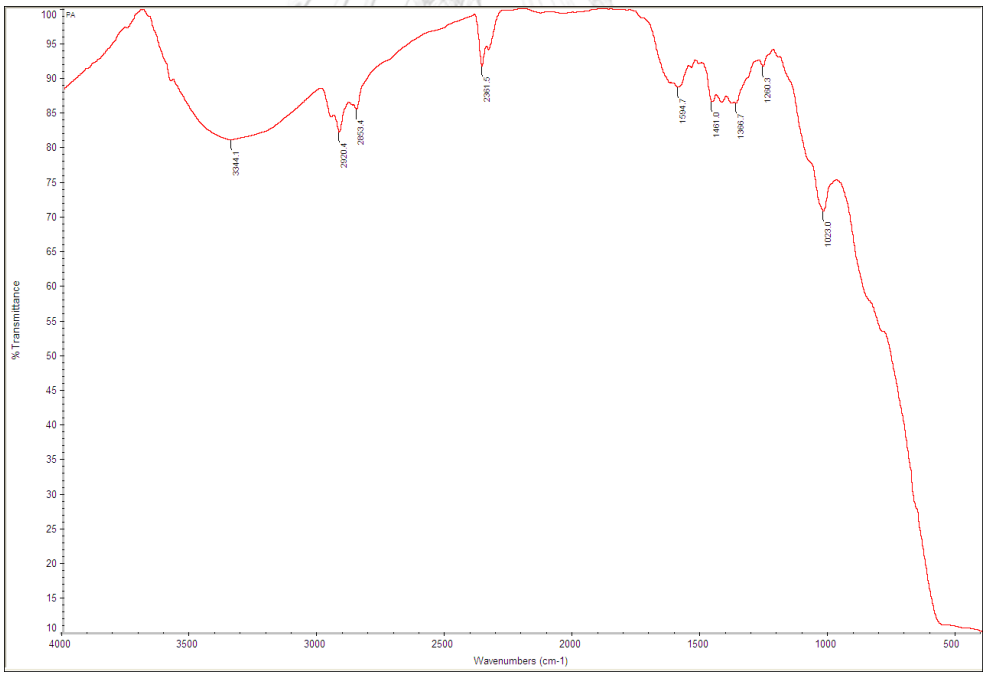

Figure A-16 FT-IR of PA after immobilization with MMAO

APPENDIX B : THERMAL GRAVIMETRIC ANALYSIS

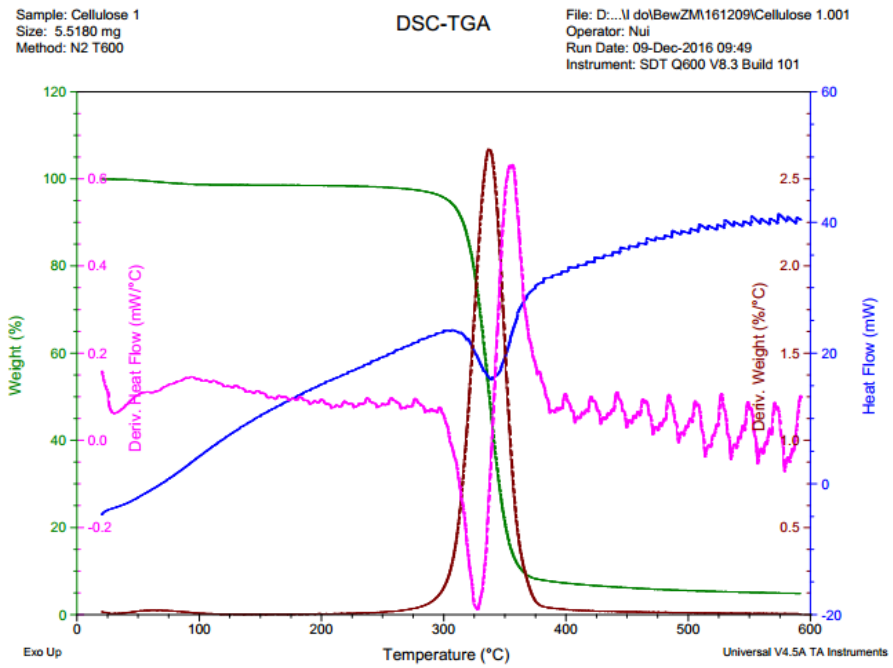

Figure B-1 TGA of MCC before immobilization with MMAO

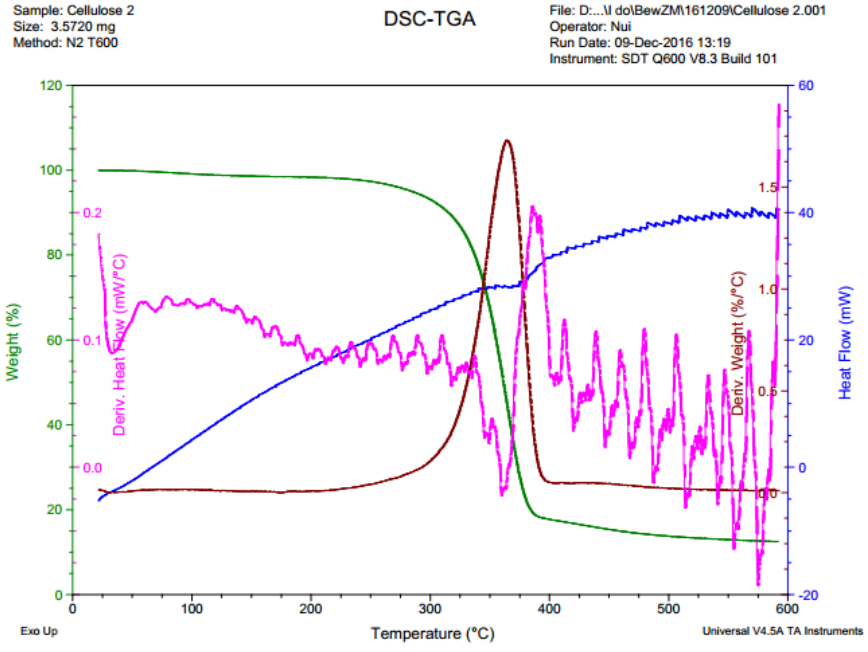

Figure B-2 TGA of BAC-P before immobilization with MMAO

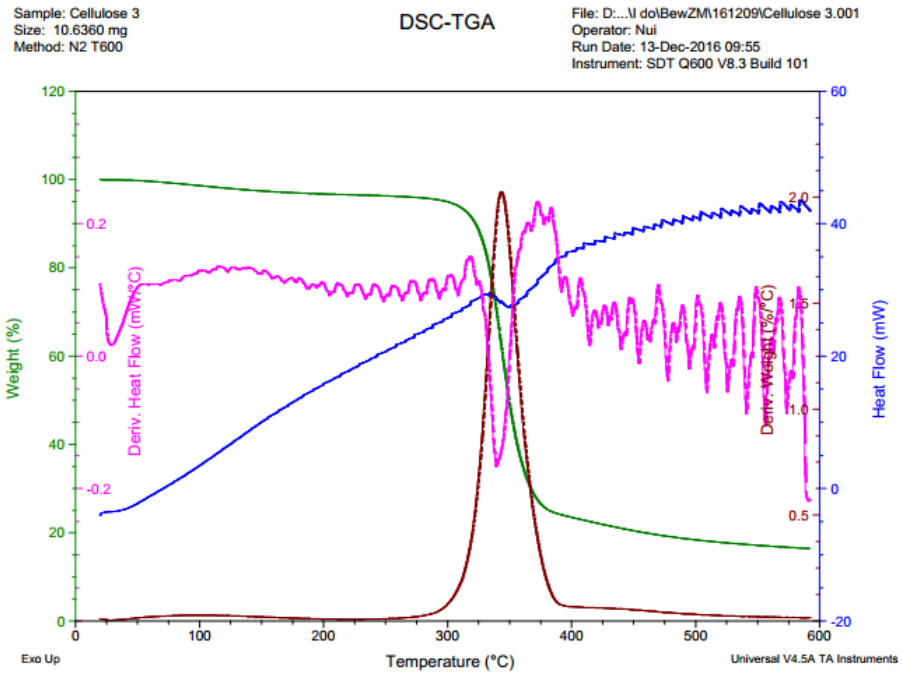

Figure B-3 TGA of BAC-C before immobilization with MMAO

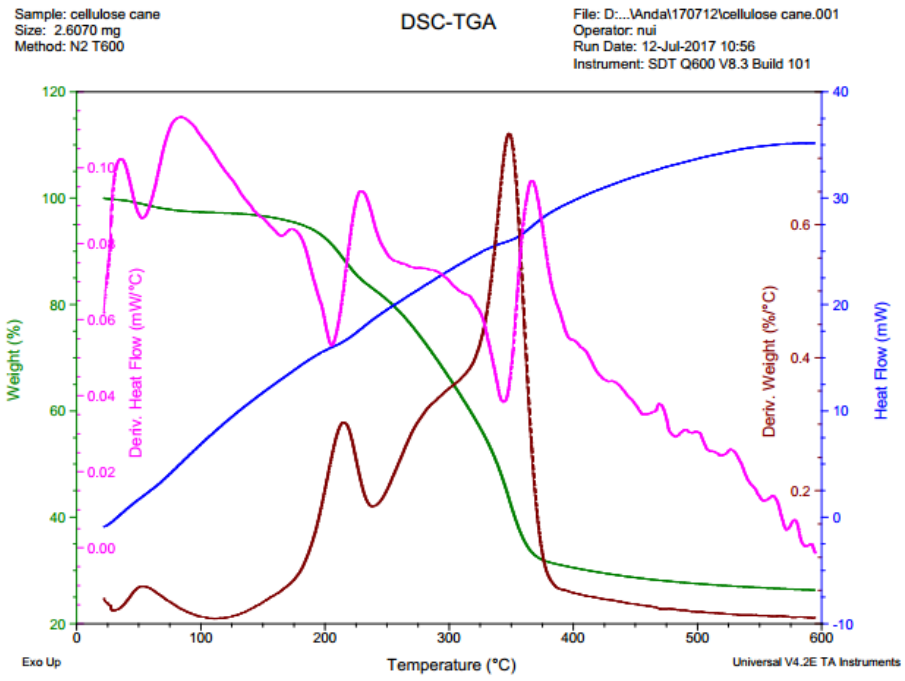

Figure B-4 TGA of SC before immobilization with MMAO

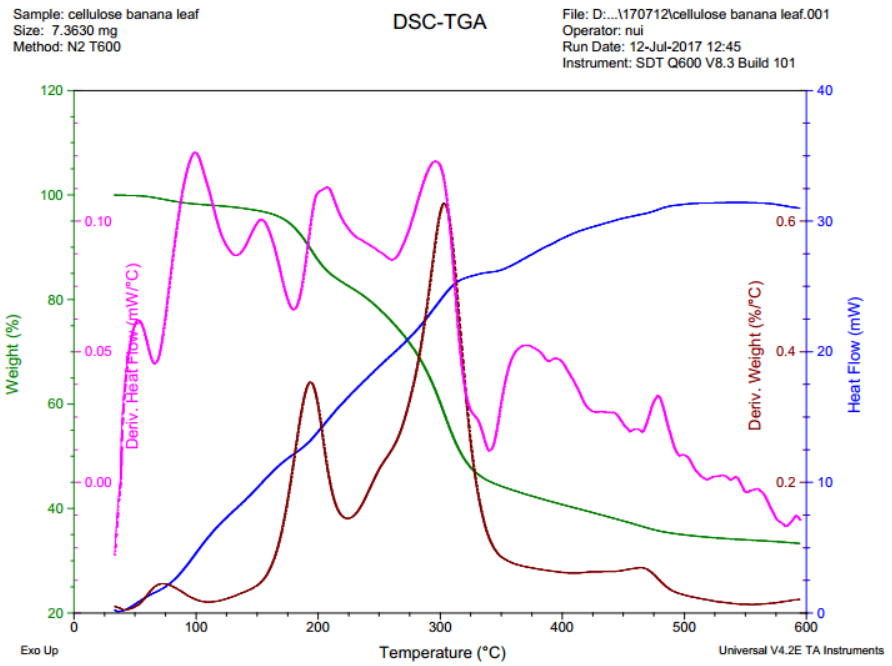

Figure B-5 TGA of BS before immobilization with MMAO

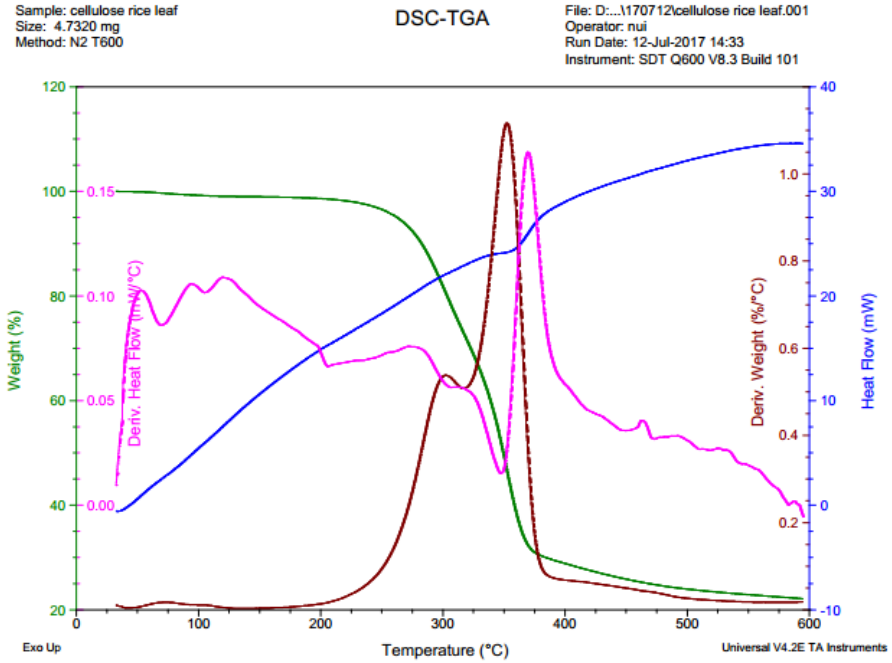

Figure B-6 TGA of RS before immobilization with MMAO

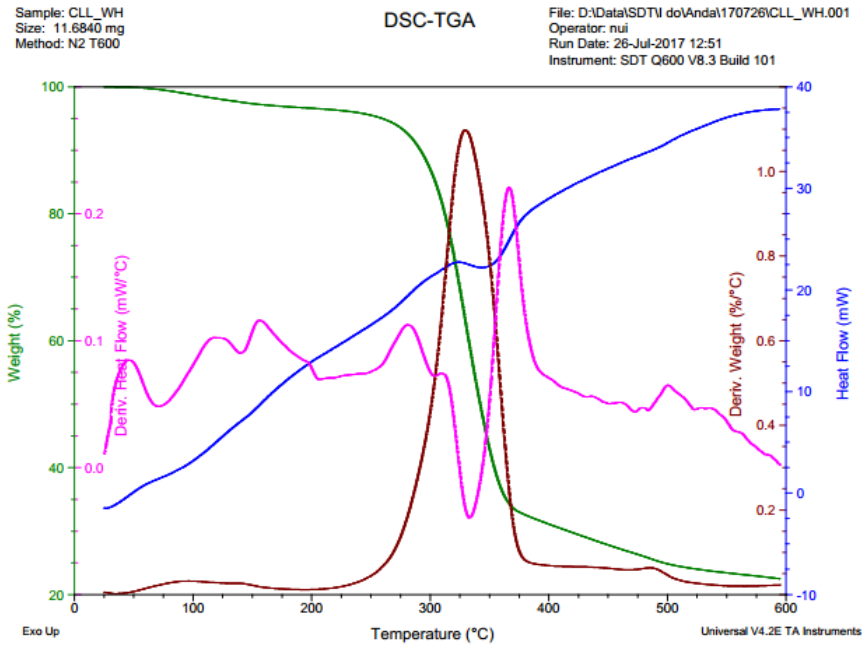

Figure B-7 TGA of WH before immobilization with MMAO

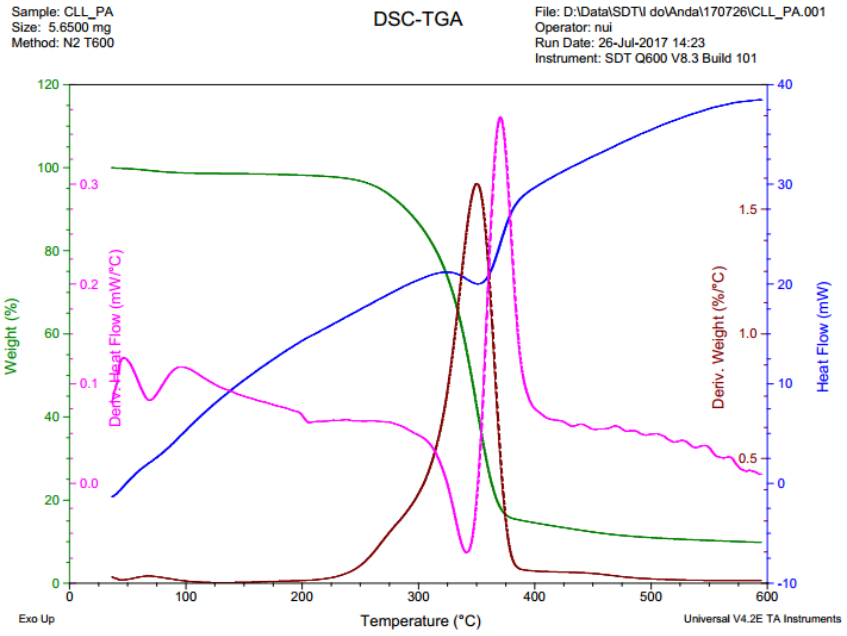

Figure B-8 TGA of PA before immobilization with MMAO

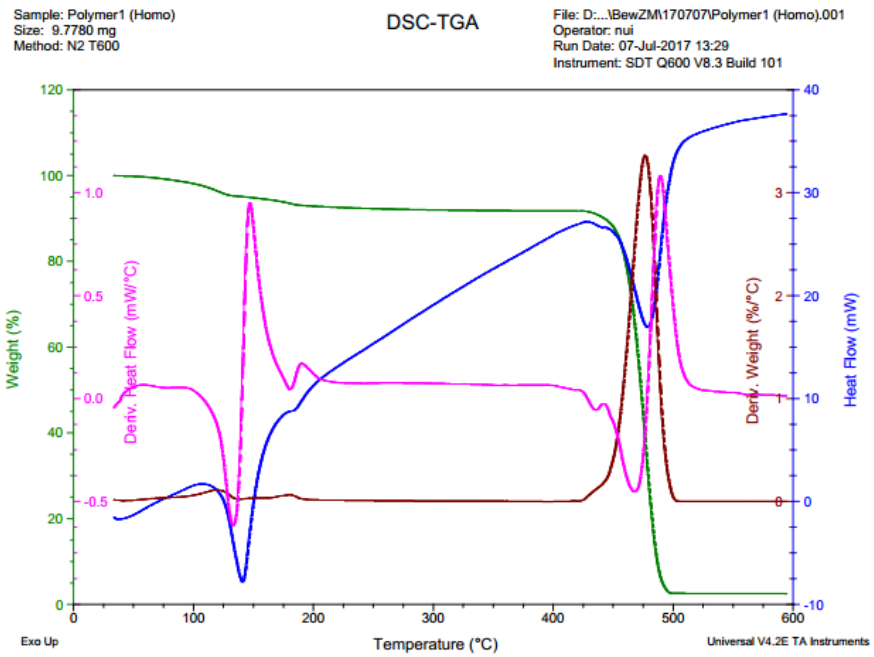

Figure B-9 TGA of Polyethylene by homogeneous system

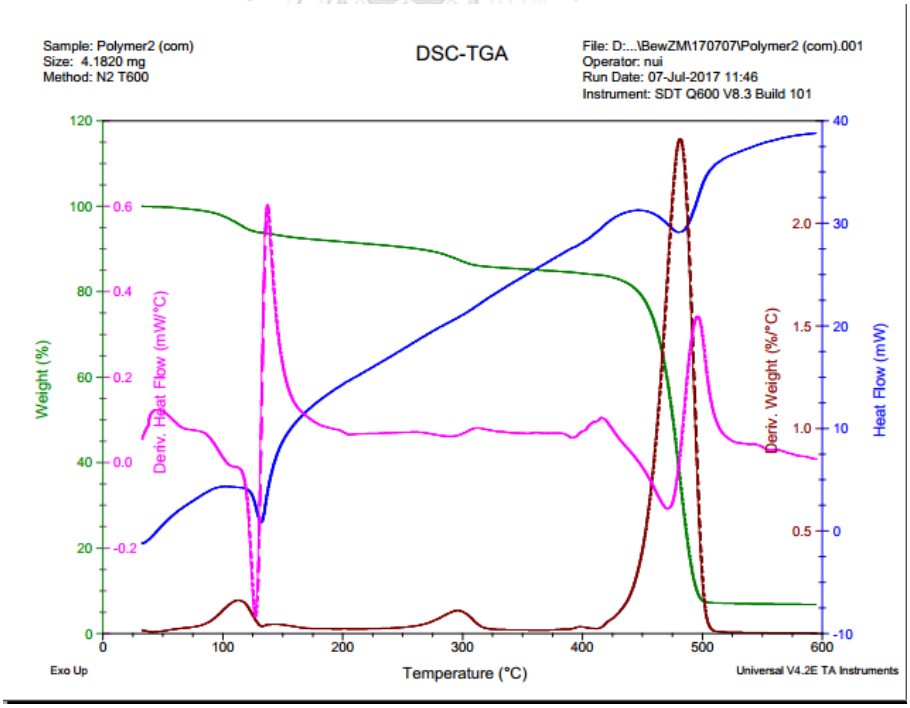

Figure B-10 TGA of Polyethylene using MCC as support

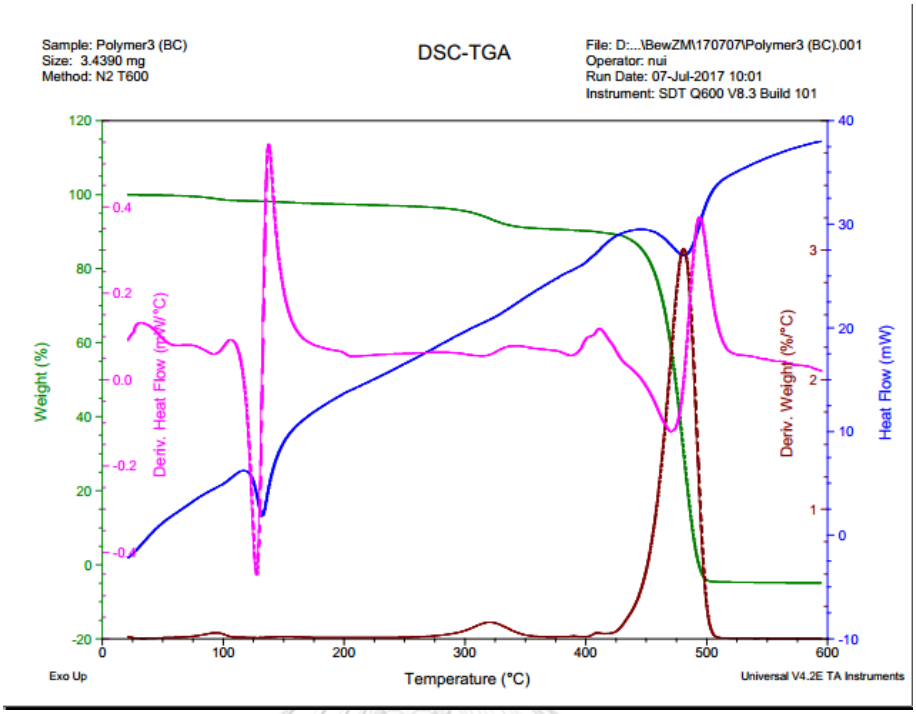

Figure B-11 TGA of Polyethylene using BAC-P as support

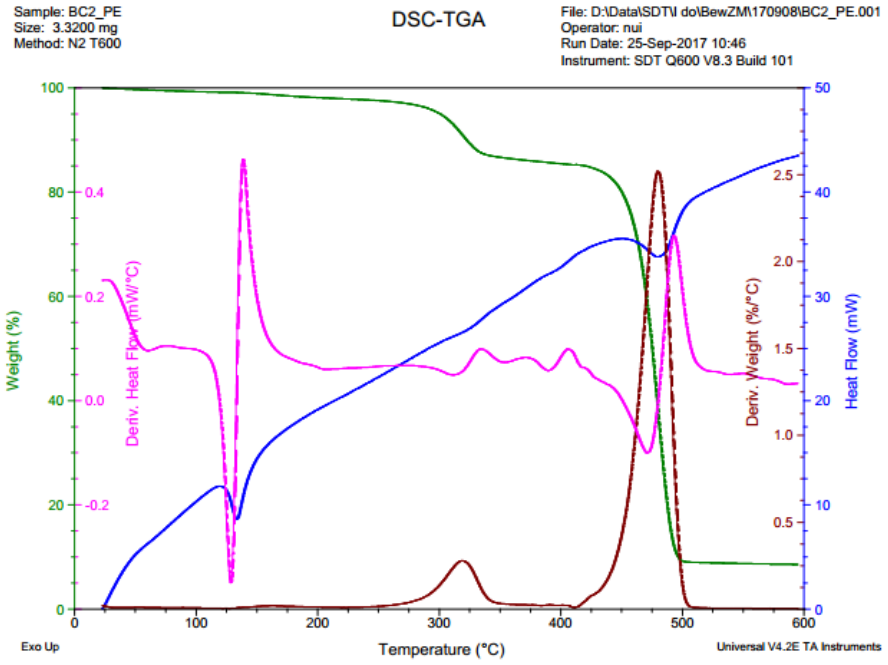

Figure B-12 TGA of Polyethylene using BAC-C as support

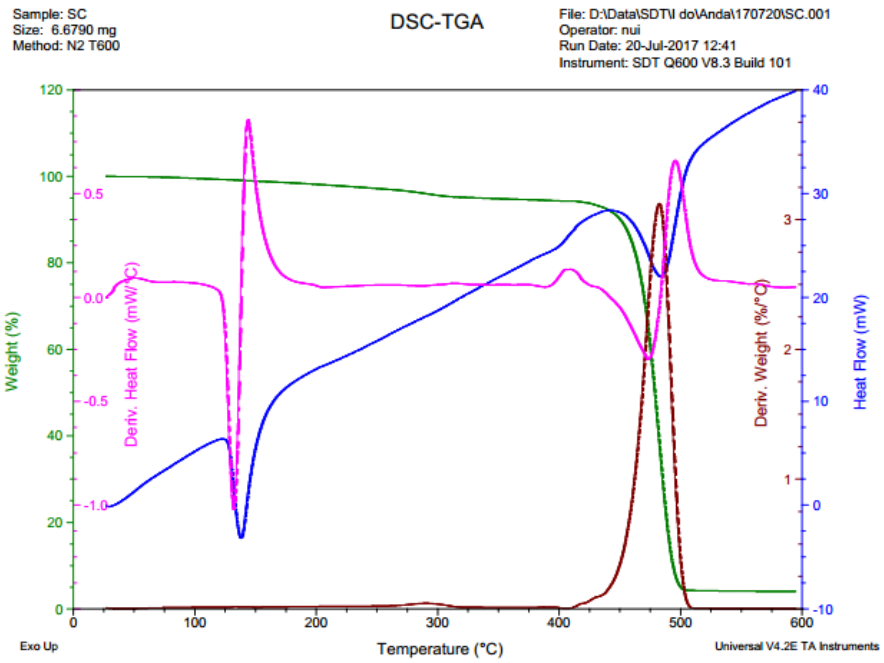

Figure B-13 TGA of Polyethylene using SC as support

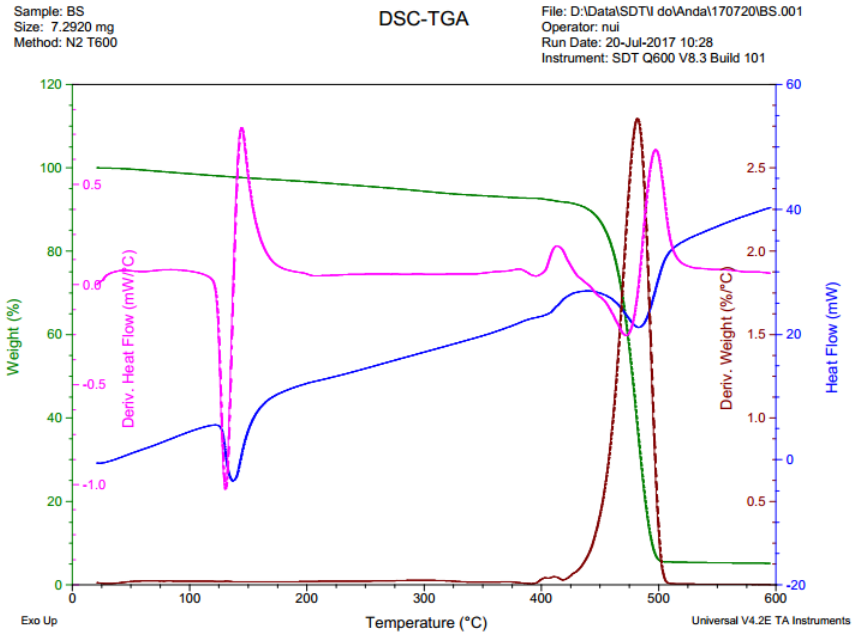

Figure B-14 TGA of Polyethylene using BS as support

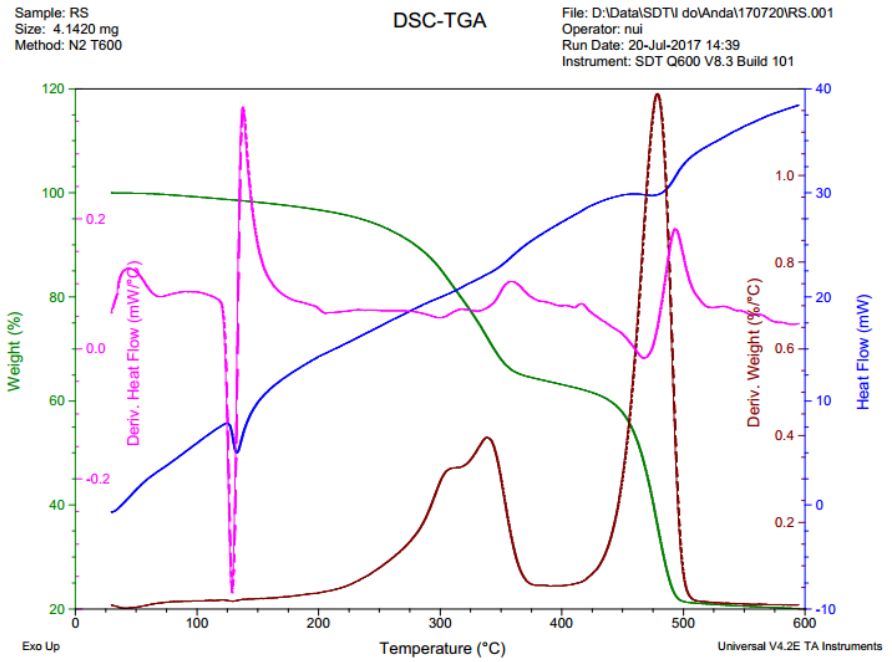

Figure B-15 TGA of Polyethylene using RS as support

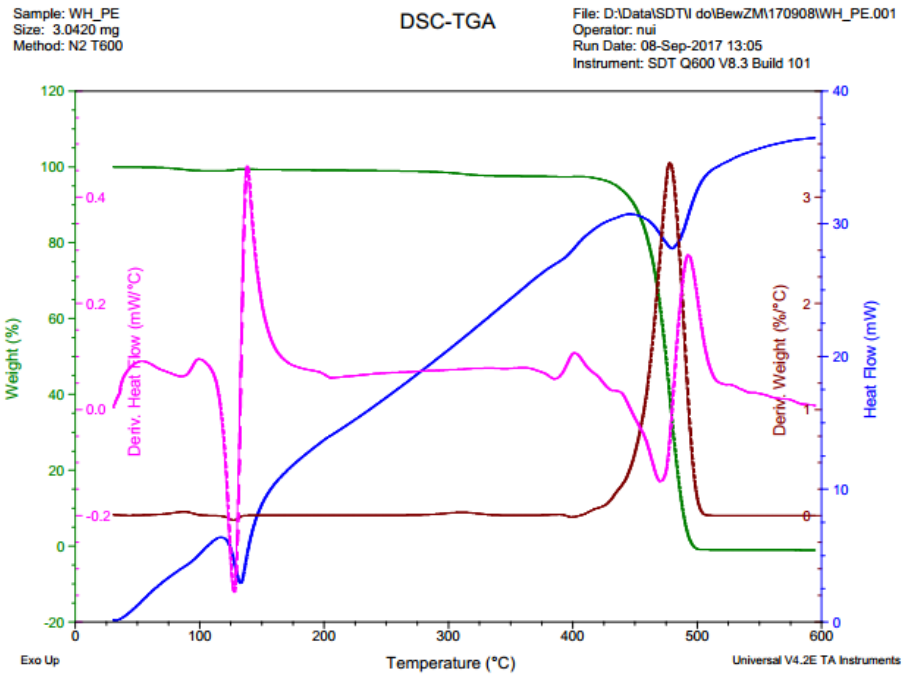

Figure B-16 TGA of Polyethylene using WH as support

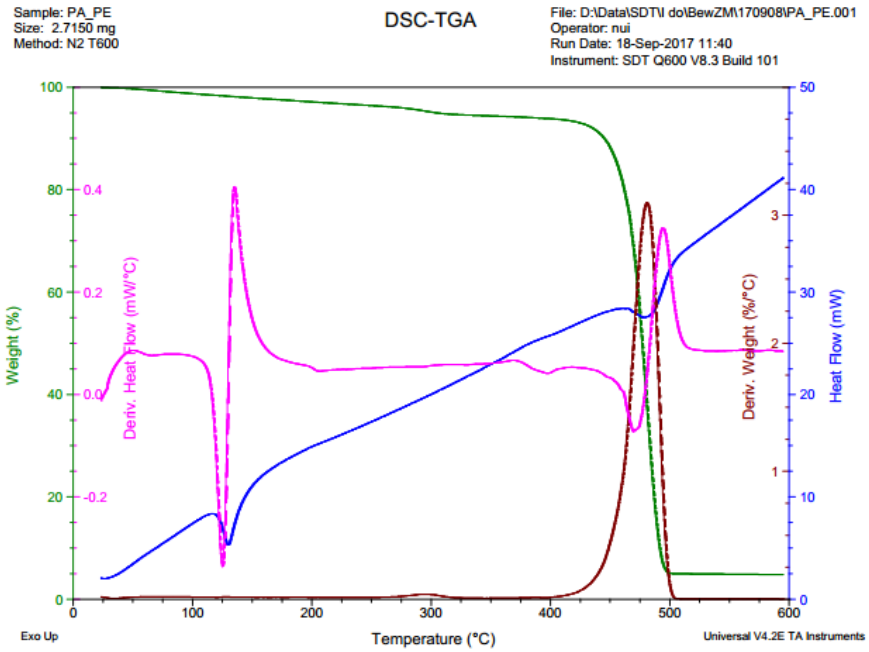

Figure B-17 TGA of Polyethylene using PA as support

APPENDIX C : DIFFERENTIAL SCANNING CAROLIMETRY

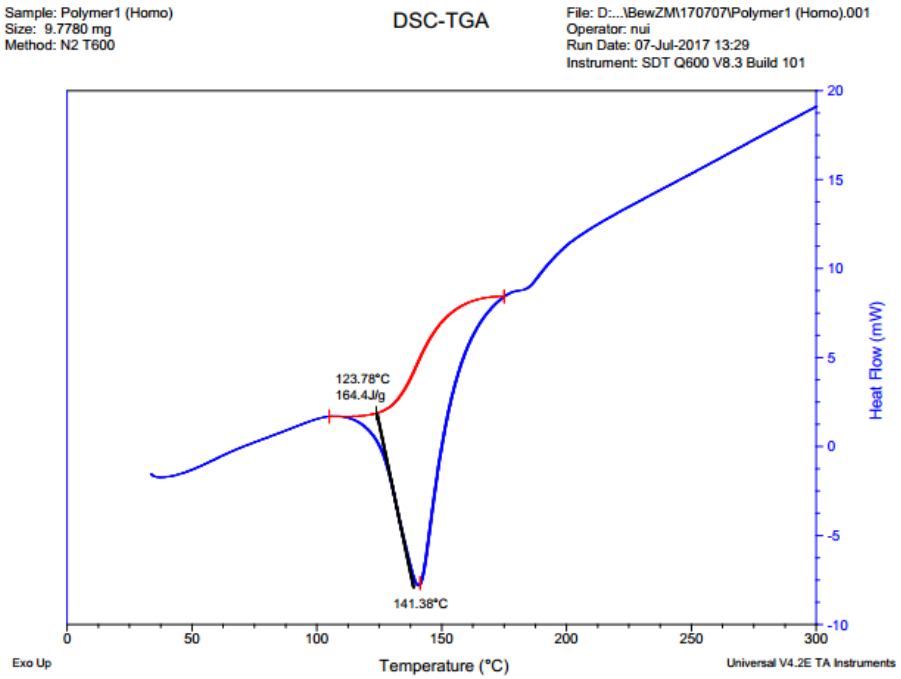

Figure C-1 DSC of Polyethylene by homogeneous system

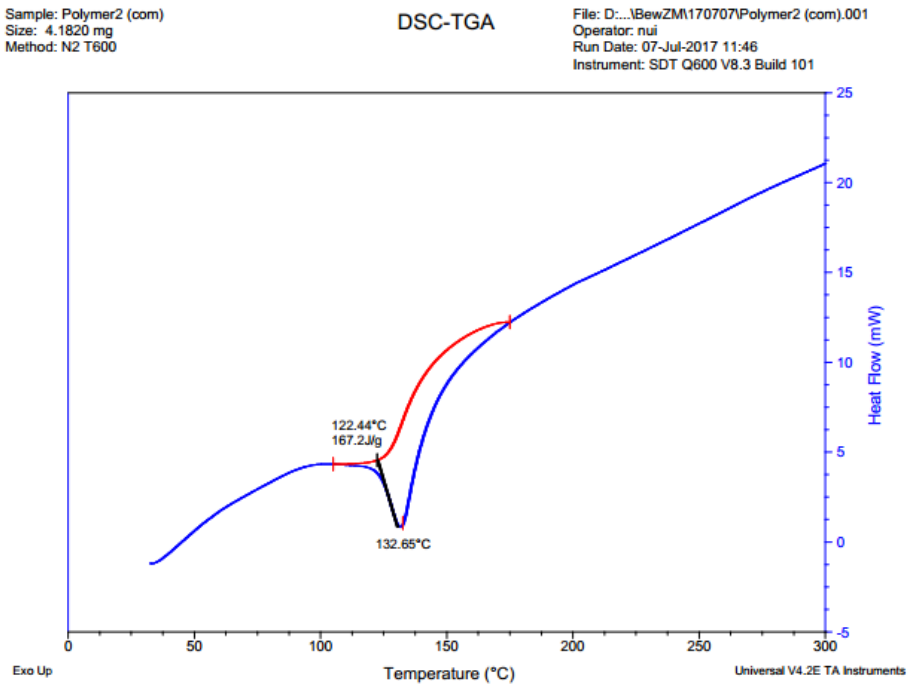

Figure C-2 DSC of Polyethylene using MCC as support

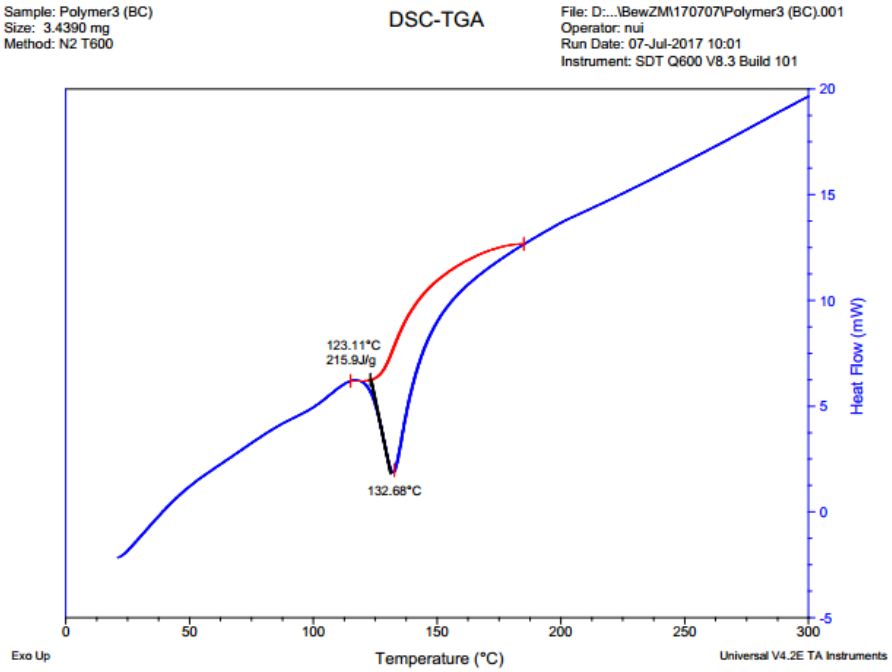

Figure C-3 DSC of Polyethylene using BAC-P as support

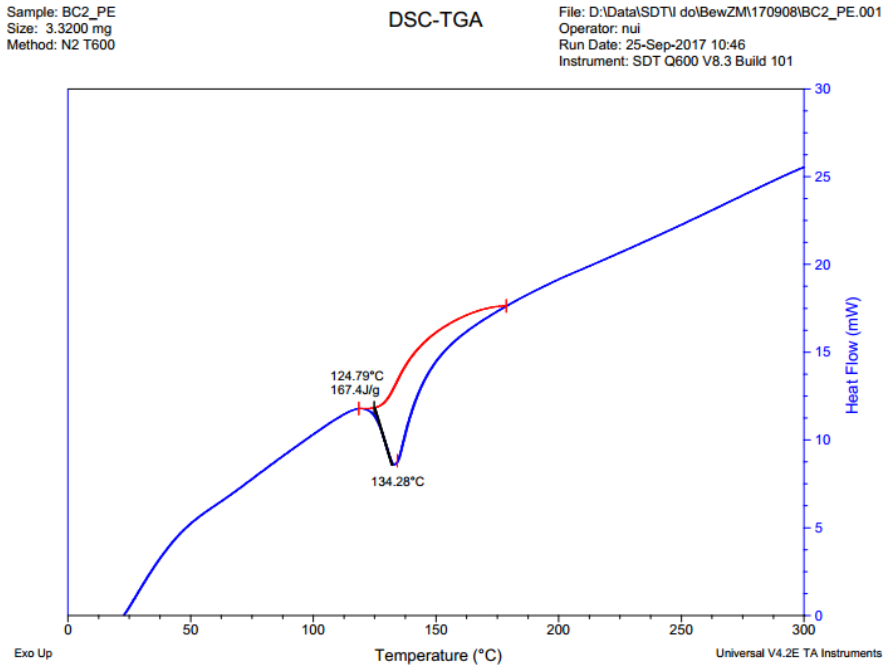

Figure C-4 DSC of Polyethylene using BAC-C as support

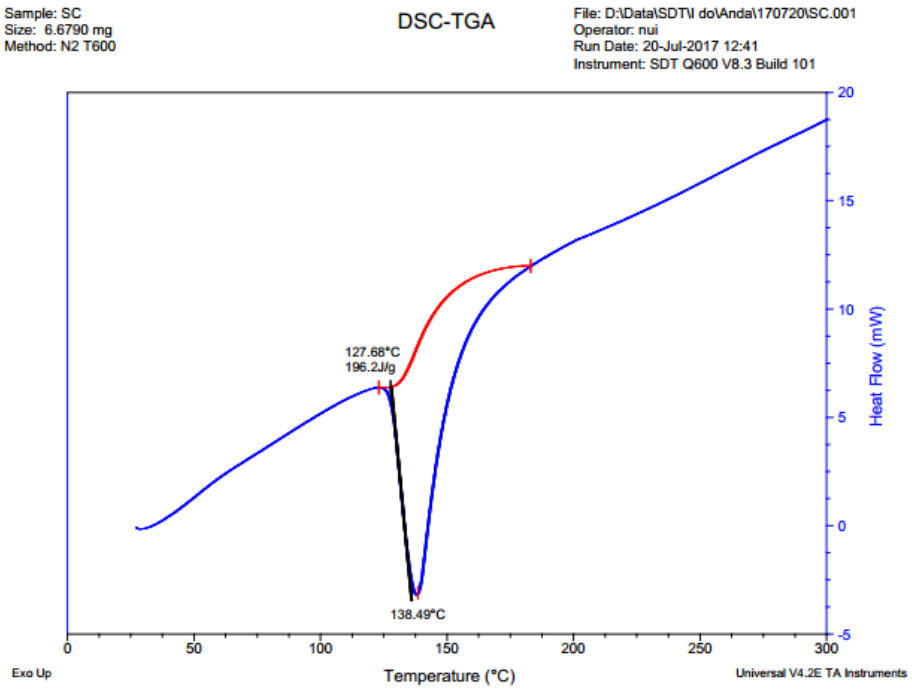

Figure C-5 DSC of Polyethylene using SC as support

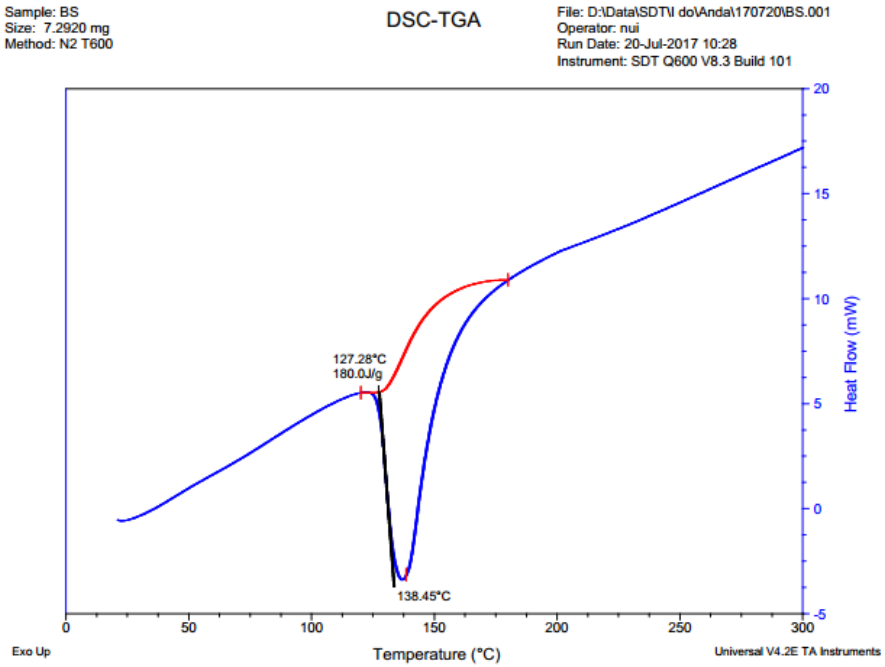

Figure C-6 DSC of Polyethylene using BS as support

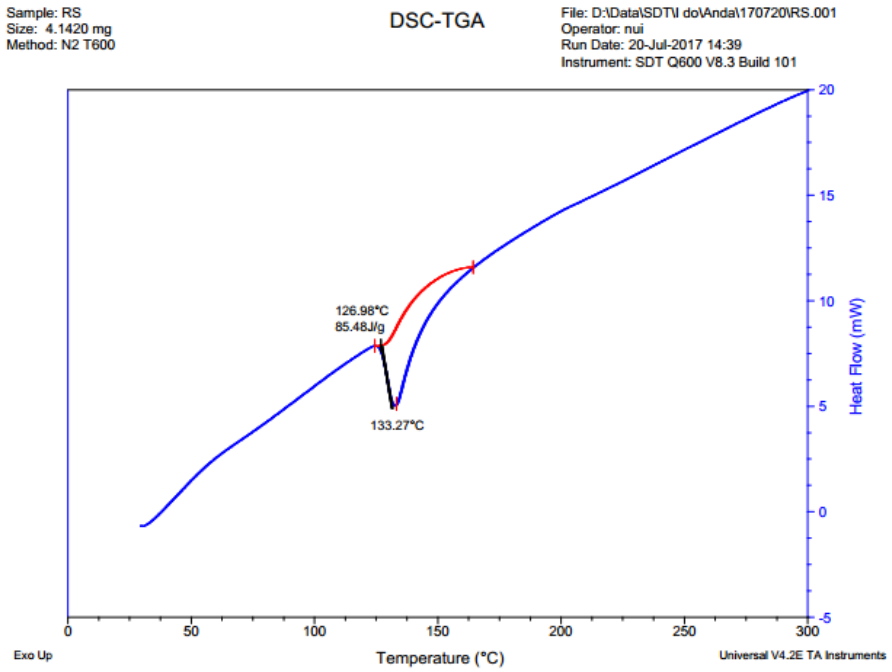

Figure C-7 DSC of Polyethylene using RS as support

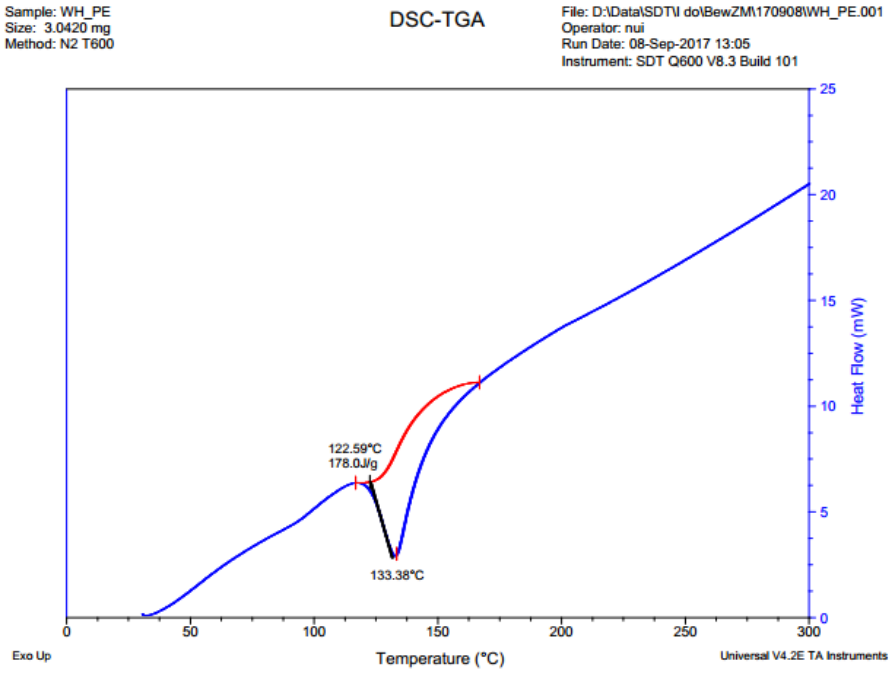

Figure C-8 DSC of Polyethylene using WH as support

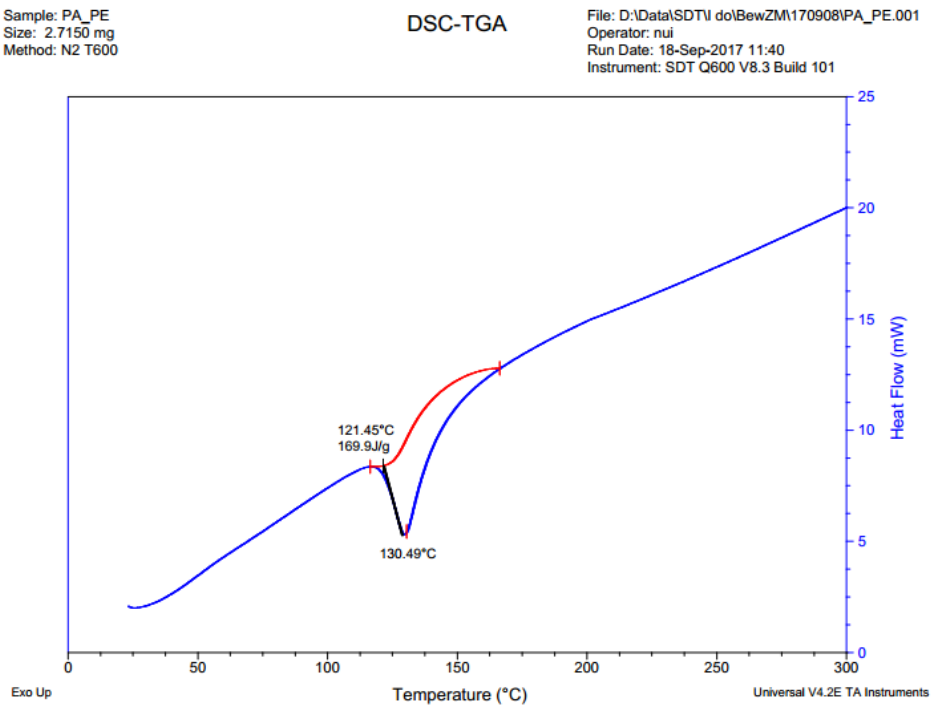

Figure C-9 DSC of Polyethylene using PA as support

APPENDIX D : TABLE OF CELLULOSE PERCENTAGE IN POLYETHYLENE

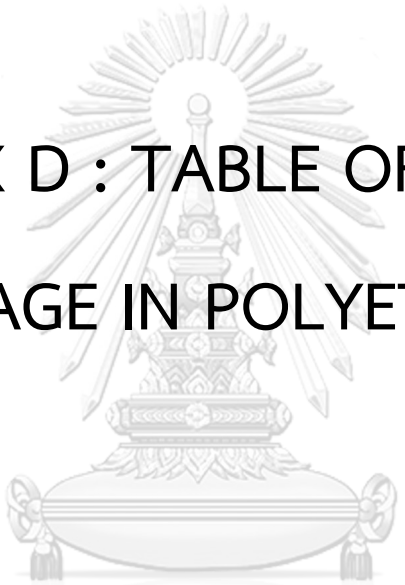

Table D.1 briefly recorded percentage of cellulose in polyethylene

Polyethylene-Cellulose	Polymer weight (g)	Polyethylene weight (g)	Cellulose weight (g)	% cellulose in polyethylene[a]
PE-HOMO	0.7894	0.7894	0	0
PE-MCC	0.6915	0.4943	0.1972	28.52
PE-BAC-P	0.6545	0.4291	0.2254	34.44
PE-BAC-C	0.6559	0.4196	0.2363	**36.03**
PE-SC	0.7956	0.598	0.1976	24.84
PE-BS	0.7892	0.5487	0.2405	30.47
PE-RS	0.8746	0.729	0.1456	16.65
PE-WH	1.2464	0.9054	0.3410	27.36
PE-PA	1.2980	1.0406	0.2574	19.83

% cellulose in polyethylene = (weight of cellulose/weight of polymer)x100%

APPENDIX E : LIST OF PUBLICATION

Thanarattanasap N. et al. “PRODUCTION OF POLYETHYLENE-CELLULOSE COMPOSITE USING ZIRCONOCENE/MMAO CATALYST” (The proceeding of 7th International Thai Institute of Chemical Engineering and Applied Chemistry Conference, ITIChE 2017, Bangkok, Thailand)

VITA

Miss Natthadabhorn Thanarattanasap was born on October 5, 1992 in Chiangmai Thailand. She graduated a high school from Rangsee Vittaya School, Chiangmai in March 2011. In May 2015, she completed the Bachelor's Degree in Industrial Chemistry from Department of Chemistry, Faculty of Science, Kasetsart University. Thereafter, she continued her Master's Degree in Chemical Engineering, Chulalongkorn University and joined Catalysis and Catalytic Reaction Engineering research group under the supervision of Prof. Dr. Bunjerd Jongsomjit in August, 2016.